Physical Oceanographic Conditions on the Newfoundland and Labrador Shelf during 2023

Frédéric Cyr, Jonathan Coyne, Steve Snook, Charlie Bishop, Peter S. Galbraith, Nancy Chen and Guoqi Han

Northwest Atlantic Fisheries Centre
Fisheries and Oceans Canada
80 East White Hills Road
St. John's, NL
A1C 5X1, Canada

2024

Canadian Technical Report of Hydrography and Ocean Sciences 382

Fisheries and Oceans Canada | Pêches et Océans Canada

Canada

Canadian Technical Report of Hydrography and Ocean Sciences

Technical reports contain scientific and technical information of a type that represents a contribution to existing knowledge but which is not normally found in the primary literature. The subject matter is generally related to programs and interests of the Oceans and Science sectors of Fisheries and Oceans Canada.

Technical reports may be cited as full publications. The correct citation appears above the abstract of each report. Each report is abstracted in the data base *Aquatic Sciences and Fisheries Abstracts.*

Technical reports are produced regionally but are numbered nationally. Requests for individual reports will be filled by the issuing establishment listed on the front cover and title page.

Regional and headquarters establishments of Ocean Science and Surveys ceased publication of their various report series as of December 1981. A complete listing of these publications and the last number issued under each title are published in the *Canadian Journal of Fisheries and Aquatic Sciences*, Volume 38: Index to Publications 1981. The current series began with Report Number 1 in January 1982.

Rapport technique canadien sur l'hydrographie et les sciences océaniques

Les rapports techniques contiennent des renseignements scientifiques et techniques qui constituent une contribution aux connaissances actuelles mais que l'on ne trouve pas normalement dans les revues scientifiques. Le sujet est généralement rattaché aux programmes et intérêts des secteurs des Océans et des Sciences de Pêches et Océans Canada.

Les rapports techniques peuvent être cités comme des publications à part entière. Le titre exact figure au-dessus du résumé de chaque rapport. Les rapports techniques sont résumés dans la base de données *Résumés des sciences aquatiques et halieutiques*.

Les rapports techniques sont produits à l'échelon régional, mais numérotés à l'échelon national. Les demandes de rapports seront satisfaites par l'établissement auteur dont le nom figure sur la couverture et la page de titre.

Les établissements de l’ancien secteur des Sciences et Levés océaniques dans les régions et à l'administration centrale ont cessé de publier leurs diverses séries de rapports en décembre 1981. Vous trouverez dans l'index des publications du volume 38 du *Journal canadien des sciences halieutiques et aquatiques*, la liste de ces publications ainsi que le dernier numéro paru dans chaque catégorie. La nouvelle série a commencé avec la publication du rapport numéro 1 en janvier 1982.

Canadian Technical Report

of Hydrography and Ocean Sciences 382

2024

Physical Oceanographic Conditions on the Newfoundland and Labrador Shelf during 2023

Frédéric Cyr[1], Jonathan Coyne[1], Steve Snook[1], Charlie Bishop[1], Peter S. Galbraith[2], Nancy Chen[3], and Guoqi Han[3]

[1] Northwest Atlantic Fisheries Centre
Fisheries and Oceans Canada
80 East White Hills Road
St. John's, NL
A1C 5X1, Canada

[2] Maurice-Lamontagne Institute
Fisheries and Oceans Canada
850 Rte de la Mer
Mont-Joli, QC
G5H 3Z4, Canada

[3] Institute of Ocean Sciences
Fisheries and Oceans Canada
9860 West Saanich Road
Sidney, BC
V8L 4B2, Canada

© His Majesty the King in Right of Canada, as represented by the Minister of the Department of Fisheries and Oceans, 2024

Cat. No. Fs97-18/382E-PDF ISBN 978-0-660-72810-0 ISSN 1488-5417

Correct citation for this publication:

Cyr, F., Coyne, J., Snook, S., Bishop, C., Galbraith, P.S., Chen, N., Han, G. 2024. Physical Oceanographic Conditions on the Newfoundland and Labrador Shelf during 2023. Can. Tech. Rep. Hydrogr. Ocean Sci. 382: iv + 54 p.

Contents

ABSTRACT

Cyr, F., Coyne, J., Snook, S., Bishop, C., Galbraith, P.S., Chen, N., Han, G. 2024. Physical Oceanographic Conditions on the Newfoundland and Labrador Shelf during 2023. Can. Tech. Rep. Hydrogr. Ocean Sci. 382: iv + 54 p.

An overview of physical oceanographic conditions in the Newfoundland and Labrador (NL) Region during 2023 is presented in support of the Atlantic Zone Monitoring Program (AZMP). The winter North Atlantic Oscillation (NAO) index, a key indicator of the direction and intensity of the winter wind field patterns over the Northwest (NW) Atlantic was near neutral (+0.2) in 2023. Since 2014, all years except 2021 were positive (normally indicative of colder conditions). About half of the environmental parameters presented in this report were above normal in 2023 (normal being defined as the average over the 1991–2020 climatological period), except for sea ice, Station 27 temperature, bottom temperature and the cold intermediate layer area which were normal. Sea surface temperatures were at their second warmest on record (after 2022), establishing new monthly and seasonal records among most NAFO divisions. The last three years registered the warmest annual SST on record. While the transport on the Scotian Slope was above normal for the first time in a decade (+1.4 SD), the transport on the Labrador and northeastern Newfoundland Slope was also above normal (+1.1 SD). It is the first time since 1996 that the transport in both regions was more than one standard deviation above normal. The NL Climate index was at +0.7, making 2023 the 7th warmest year since 1951.

RÉSUMÉ

Cyr, F., Coyne, J., Snook, S., Bishop, C., Galbraith, P.S., Chen, N., Han, G. 2024. Physical Oceanographic Conditions on the Newfoundland and Labrador Shelf during 2023. Can. Tech. Rep. Hydrogr. Ocean Sci. 382: iv + 54 p.

Un sommaire des conditions océanographiques physiques pour la région de Terre-Neuve et Labrador (TNL) en 2023 est présenté dans le cadre du Programme de Monitorage de la Zone Atlantique (PMZA). L'Oscillation Nord-Atlantique (ONA), un indicateur clé pour la direction et l'intensité des champs de vents hivernaux au-dessus de l'Atlantique nord-ouest, était près de la normale 2023 (+0.2). Depuis 2014, toutes les années sauf 2021 étaient positives (normalement indicatif de conditions froides). À peu près la moitié des indices climatiques rapportées dans ce rapport étaient au-dessus de la normale en 2023 (la normale étant définie comme la moyenne sur la période climatologique 1991-2021), à l'exception de la glace de mer, la température à la Station 27, la température au fond et de l'aire de la couche intermédiaire froide qui étaient normales. Les températures de surface de la mer étaient à leur deuxième plus chaud niveau enregistrés (après 2022), incluant de nombreux records mensuels et saisonniers pour les différentes divisions de l'OPANO analysées. Les trois dernières années ont été les trois plus chaudes enregistrées pour la température de surface de la mer. Alors que le transport le long du talus néo-écossais était au-dessus de la normale (+1.4 É-T) pour la première fois en une décennie, le transport sur le talus de TNL était également au-dessus de la normale (+1.1 É-T). L'indice du climat de TNL était à +0.7, faisant de 2023 la septième année la plus chaude depuis 1951.

1 Introduction

This manuscript presents an overview of the 2023 environmental and physical oceanographic conditions in the Newfoundland and Labrador (NL) Region (Figure 1), in support of the Fisheries and Oceans Canada (DFO) Atlantic Zone Monitoring Program (AZMP; Therriault et al., 1998). This report complements similar reviews of the environmental conditions in the Gulf of St. Lawrence (Galbraith et al., 2024) and the Scotian Shelf and Gulf of Maine (Hebert et al., 2024). Physical oceanographic conditions for the NL region in 2022 were presented in Cyr et al. (2024).

The information presented in this report is derived from various sources:

1. Ice data from the Canadian Ice Service, while meteorological data are from Environment and Climate Change (ECCC) Canada and other sources cited in the text;
2. Sea Surface Temperatures (SSTs) (Galbraith et al., 2021). These correspond to a blend of Advanced Very High Resolution Radiometer (AVHRR) data from Pathfinder version 5.3 (1982–2014), the Maurice Lamontagne Institute (1985–2013) and the GHRSST NOAA/STAR L3S-LEO-Daily (2007–present). See Galbraith et al., (2021, 2023) for a description;
3. Observations made throughout the year at monitoring Station 27 near St. John's, NL;
4. Measurements made along standard AZMP cross-shelf sections (see map Figure 1);
5. Oceanographic observations made during spring and fall multi-species resource assessment surveys;
6. Other multi-source historical data (ships of opportunity, international campaigns, surveys from other DFO regions, the Argo program, etc.).

All vertical profiles of temperature and salinity used in this report (e.g. points 3-6 above) are available at https://doi.org/10.20383/102.0739 [consulted 2024-05-30] (Coyne et al., 2023).

Time series of temperature and salinity anomalies, as well as other climate indices were constructed by subtracting the average computed over a standard climatological period from 1991 to 2020. When a variable is measured throughout the seasonal cycle (e.g. air temperature, station 27 observations), the annual anomaly is calculated as the average of monthly anomalies. Unless otherwise specified, annual or seasonal anomalies were normalized by dividing the values by the standard deviation (SD) of the data time series over the climatological period. A value of 2, for example, indicates that the index was 2 SD higher than its long-term average. As a general guide, anomalies within ±0.5 SD are considered to be normal.

The normalized values of water properties and derived climate indices are presented as “scorecards”, which are color-coded gradations of 0.5 SD (Figure 2). Shades of blue represent cold environmental conditions and red represent warm conditions. In some instances, such as for the North Atlantic Oscillation (NAO), or for ice and cold intermediate layer (CIL) properties, negative anomalies indicate warm conditions, and are therefore colored red. Most of the colormaps used in this report are taken from the *cmocean* colormaps package for oceanography (Thyng et al., 2016).

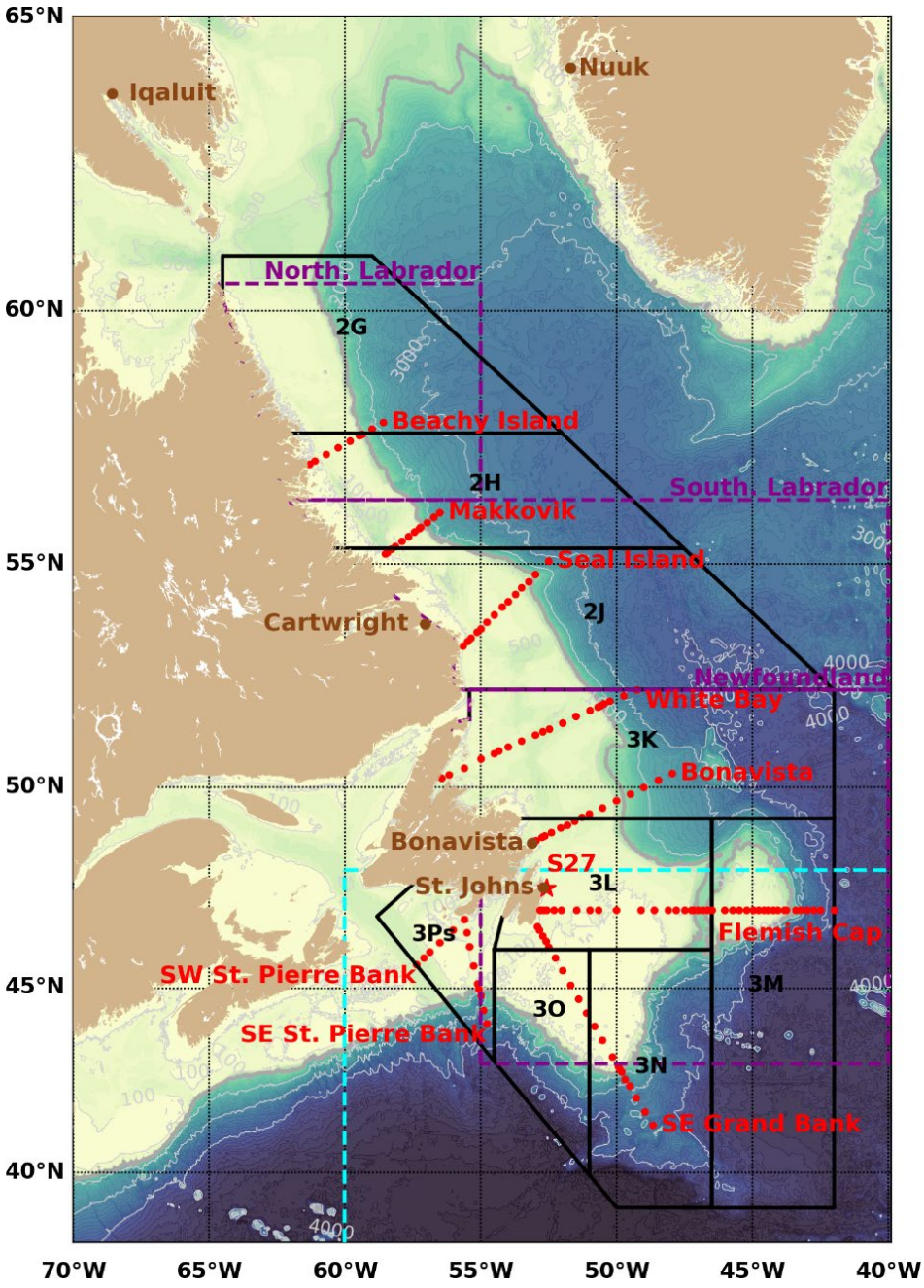

Figure 1: Map of the Northwest Atlantic Ocean, including important bathymetric features (the gray isobaths are identified on the figure). NAFO Divisions (sub-areas 2 and 3) on the Newfoundland and Labrador (NL) shelf are drawn. (black boxes) The AZMP hydrographic sections are shown with red dots, and their names labeled in red text on the figure. Long-term AZMP hydrographic Station 27 is highlighted with a red star. The five stations used for the air temperature time series are shown in brown. The three regions used for sea ice calculations (Northern Labrador shelf, Southern Labrador shelf and Newfoundland shelf) are drawn with dashed magenta lines. The region used by the International Ice Patrol for iceberg sightings south of 48°N is drawn in dashed cyan. The shelf break is delimited by a thicker and darker gray contour corresponding to the isobath 1,000 m (used to clip the SST and bottom temperature).

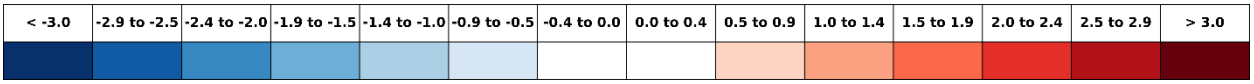

Figure 2: Color scale used for the presentation of normalized anomalies. Color levels are incremented by 0.5 standard deviations (SD), where blue is below normal and red above normal. Values between 0 and ±0.5 SD remain white indicating normal conditions. Anomalies are rounded to the nearest tenth.

2 Meteorological conditions

The North Atlantic Oscillation (NAO; see Figure 3 for time series since 1951 and Figure 4 for tabulated values since 1980) refers to the anomaly in the sea-level pressure (SLP) difference between the sub-tropical high (average location near the Azores) and the subpolar low (average location near Iceland). Several definitions of the NAO exist, though the one used here is from the National Center for Environmental Information of the National Oceanic and Atmospheric Administration (NOAA) available online. The winter NAO (defined here as the average of monthly values from December to March) is considered a measure of the strength of the winter westerly and northwesterly winds over the Northwest Atlantic. A high NAO index (positive phase) occurs during an intensification of the Icelandic Low and Azores High. Except for some years for which the SLP patterns are spatially shifted (e.g., 1999, 2000, and 2018), positive winter NAO years favor strong northwesterly winds, cold air and sea surface temperatures (SSTs), and heavy ice conditions on the NL shelves (Colbourne et al., 1994; Drinkwater et al., 1994; Petrie et al., 2007). The winter NAO was neutral in 2023 (+0.2; first row in Figure 4) for the second time in 3 years (2021 was also neutral). While the lowest winter NAO index value was reached in 2010, all years between 2012 and 2020 (except 2013) were positive, including the record high of +1.6 in 2015.

The Arctic Oscillation (AO) is a larger scale index intimately linked with the NAO. During a positive phase, the Arctic air outflow to the Northwest Atlantic increases, resulting in colder winter air temperatures over much of NL and adjacent shelf regions. The AO was neutral in 2022 at 0.0 (Figure 4). In 2015, the AO was at its highest value since 1990 at +0.6. A record low was reached in 2010 when it was below normal at -1.5 (warm air temperatures).

The Atlantic Multidecadal Oscillation (AMO) is also provided in Figure 4. This index, based on the Sea Surface Temperature of the Atlantic Ocean, evolves as part of a 65–80 year cycle that influences the regional climate and has consequences on the ocean circulation in the North Atlantic (e.g., Kerr, 2000). The AMO has been in a positive phase since the late 1990s.

Air temperature anomalies (winter and annual values) from five coastal communities around the Northwest Atlantic (Nuuk, Greenland; Iqaluit on Baffin Island, Nunavut; Cartwright, Labrador; Bonavista and St. John's in Newfoundland; see Figure 1) are shown in Figure 4 as normalized anomalies between 1980 and 2023, and in Figure 5 and Figure 6 as monthly and annual (cumulative for all stations) anomalies, respectively. Except for Nuuk for which data are obtained from the Danish Meteorological Institute, the air temperature data from Canadian sites are from the second generation of Adjusted and Homogenized Canadian Climate Data (AHCCD), which accounts for shifts in station location and changes in observation methods (Vincent et al., 2012). Because the AHCCD product was not ready for the year 2023, historical data from the Government of Canada Monthly Climate Summaries have been used for that year.

In 2023, the air temperature exhibited large intra-annual fluctuations that were generally coherent between all sites (Figure 4). Temperatures were especially cold in February and warm in March, July and during the late fall. Averaged over the year, the air temperatures were above normal, making 2023 the 9th warmest year since 1950 at +0.6 SD (Figure 5). 2010 was the warmest year at +2.1 SD, and all of the warmest 5 years have happened since 2005.

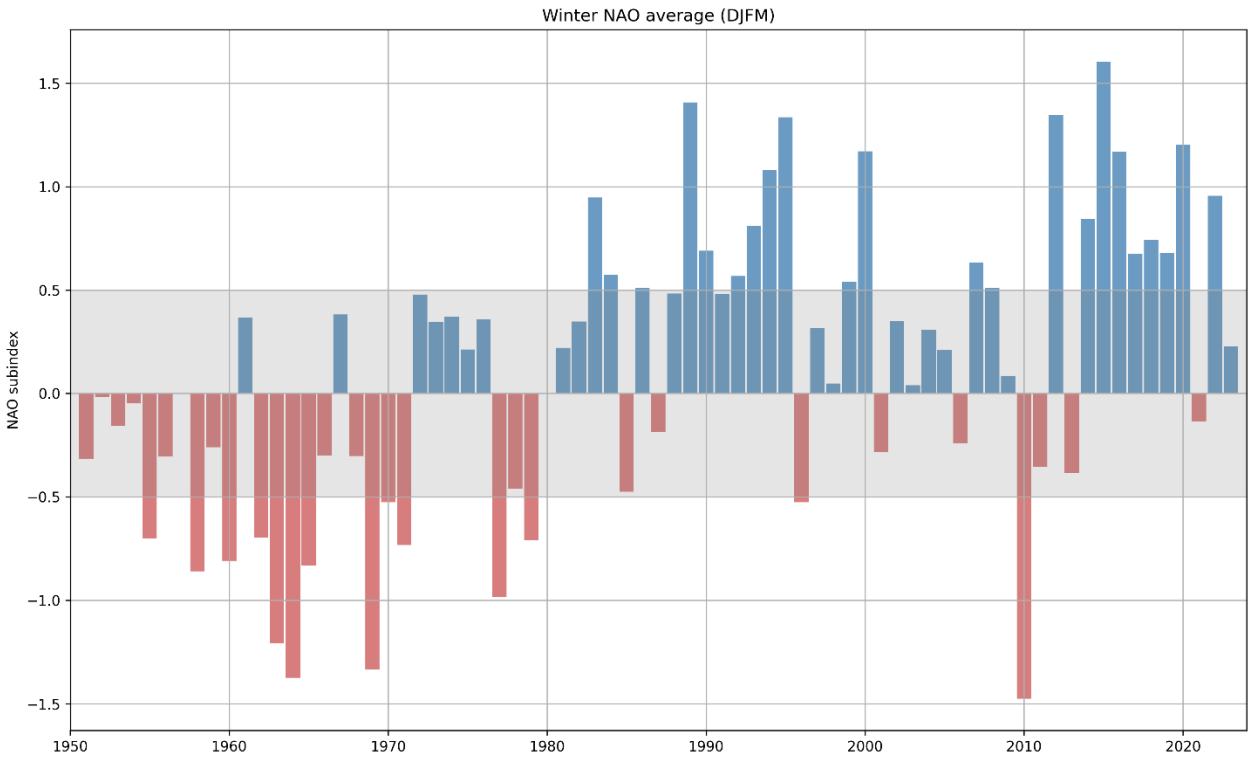

Figure 3: Winter North Atlantic Oscillation (NAO) Index calculated by averaging the December to March values since 1951 (which correspond to the average of December 1950 and January-March 1951). The NAO Index used here is from the National Center for Environmental Information of the NOAA. This index is used as part of the NL climate index mentioned in the summary (Figure 39).

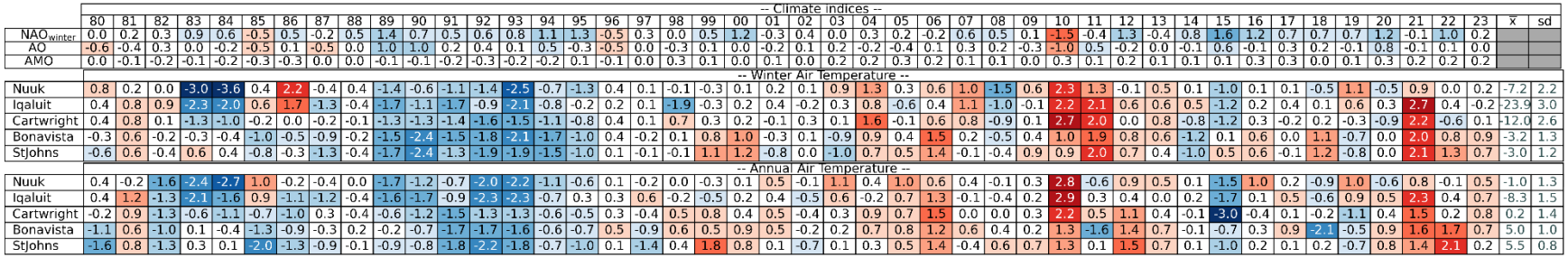

	-- Climate indices --																																												
	80	81	82	83	84	85	86	87	88	89	90	91	92	93	94	95	96	97	98	99	00	01	02	03	04	05	06	07	08	09	10	11	12	13	14	15	16	17	18	19	20	21	22	23	$\bar{x}$	sd
NAO_{winter}	0.0	0.2	0.3	0.9	0.6	-0.5	0.5	-0.2	0.5	1.4	0.7	0.5	0.6	0.8	1.1	1.3	-0.5	0.3	0.0	0.5	1.2	-0.3	0.4	0.0	0.3	0.2	-0.2	0.6	0.5	0.1	-1.5	-0.4	1.3	-0.4	0.8	1.6	1.2	0.7	0.7	0.7	1.2	-0.1	1.0	0.2		
AO	-0.6	-0.4	0.3	0.0	-0.2	-0.5	0.1	-0.5	0.0	1.0	1.0	0.2	0.4	0.1	0.5	-0.3	-0.5	0.0	-0.3	0.1	0.0	-0.2	0.1	0.2	-0.2	-0.4	0.1	0.3	0.2	-0.3	-1.0	0.5	-0.2	0.0	-0.1	0.6	-0.1	0.3	0.2	-0.1	0.8	-0.1	0.1	0.0		
AMO	0.0	-0.1	-0.2	-0.1	-0.2	-0.3	-0.3	0.0	0.0	-0.1	-0.1	-0.2	-0.3	-0.2	-0.2	0.1	-0.1	0.0	0.3	0.1	0.0	0.1	0.0	0.2	0.2	0.3	0.2	0.1	0.1	0.0	0.3	0.1	0.2	0.1	0.1	0.1	0.3	0.3	0.0	0.1	0.3	0.2	0.2	0.2		
	-- Winter Air Temperature --																																												
Nuuk	0.8	0.2	0.0	-3.0	-3.6	0.4	2.2	-0.4	0.4	-1.4	-0.6	-1.1	-1.4	-2.5	-0.7	-1.3	0.4	0.1	-0.1	-0.3	0.1	0.2	0.1	0.9	1.3	0.3	0.6	1.0	-1.5	0.6	2.3	1.3	-0.1	0.5	0.1	-1.0	0.1	0.1	-0.5	1.1	-0.5	0.9	0.0	0.2	-7.2	2.2
Iqaluit	0.4	0.8	0.9	-2.3	-2.0	0.6	1.7	-1.3	-0.4	-1.7	-1.1	-1.7	-0.9	-2.1	-0.8	-0.2	0.2	0.1	-1.9	-0.3	0.2	0.4	-0.2	0.3	0.8	-0.6	0.4	1.1	-1.0	-0.1	2.2	2.1	0.6	0.6	0.5	-1.2	0.2	0.4	0.1	0.6	0.3	2.7	0.4	-0.2	-23.9	3.0
Cartwright	0.4	0.8	0.1	-1.3	-1.0	-0.2	0.0	-0.2	-0.1	-1.3	-1.3	-1.4	-1.6	-1.5	-1.1	-0.8	0.4	0.1	0.7	0.3	0.2	-0.1	0.3	0.1	1.6	-0.1	0.6	0.8	-0.9	0.1	2.7	2.0	0.0	0.8	-0.8	-1.2	0.3	-0.2	0.2	-0.3	-0.9	2.2	-0.6	0.1	-12.0	2.6
Bonavista	-0.3	0.6	-0.2	-0.3	-0.4	-1.0	-0.5	-0.9	-0.2	-1.5	-2.4	-1.5	-1.8	-2.1	-1.7	-1.0	0.4	-0.2	0.1	0.8	1.0	-0.3	0.1	-0.9	0.9	0.4	1.5	0.2	-0.5	0.4	1.0	1.9	0.8	0.6	-1.2	0.1	0.6	0.0	1.1	-0.7	0.0	2.0	0.8	0.9	-3.2	1.3
StJohns	-0.6	0.6	-0.4	0.6	0.4	-0.8	-0.3	-1.3	-0.4	-1.7	-2.4	-1.3	-1.9	-1.9	-1.5	-1.0	0.1	-0.1	-0.1	1.1	1.2	-0.8	0.0	-1.0	0.7	0.5	1.4	-0.1	-0.4	0.9	0.9	2.0	0.7	0.4	-1.0	0.5	0.6	-0.1	1.2	-0.8	0.0	2.1	1.3	0.7	-3.0	1.2
	-- Annual Air Temperature --																																												
Nuuk	0.4	-0.2	-1.6	-2.4	-2.7	1.0	-0.2	-0.4	0.0	-1.7	-1.2	-0.7	-2.0	-2.2	-1.1	-0.6	0.1	-0.2	0.0	-0.3	0.1	0.5	-0.1	1.1	0.4	1.0	0.6	0.4	-0.1	0.3	2.8	-0.6	0.9	0.5	0.1	-1.5	1.0	0.2	-0.9	1.0	-0.6	0.8	-0.1	0.5	-1.0	1.3
Iqaluit	0.4	1.2	-1.3	-2.1	-1.6	0.9	-1.1	-1.2	-0.4	-1.6	-1.7	-0.9	-2.3	-2.3	-0.7	0.3	0.3	0.6	-0.2	-0.5	0.2	0.4	-0.5	0.6	-0.2	0.7	1.3	-0.1	-0.4	0.2	2.9	0.3	0.4	0.0	0.2	-1.7	0.1	0.5	-0.6	0.9	0.5	2.3	0.4	0.7	-8.3	1.5
Cartwright	-0.2	0.9	-1.3	-0.6	-1.1	-0.7	-1.0	0.3	-0.4	-0.6	-1.2	-1.5	-1.3	-1.3	-0.6	-0.5	0.3	-0.4	0.5	0.8	0.4	0.5	-0.4	0.3	0.9	0.7	1.5	0.0	0.0	0.3	2.2	0.5	1.1	0.4	-0.1	-3.0	-0.4	0.1	-0.2	-1.1	0.4	1.5	0.2	0.8	0.2	1.4
Bonavista	-1.1	0.6	-1.0	0.1	-0.4	-1.3	-0.9	-0.3	0.2	-0.2	-0.7	-1.7	-1.7	-1.6	-0.6	-0.7	0.5	-0.9	0.6	0.5	0.9	0.5	-0.2	0.2	0.7	0.8	1.2	0.6	0.4	0.2	1.3	-1.6	1.4	0.7	-0.1	-0.7	0.3	0.9	-2.1	-0.5	0.9	1.6	1.7	0.7	5.0	1.0
StJohns	-1.6	0.8	-1.3	0.3	0.1	-2.0	-1.3	-0.9	-0.1	-0.9	-0.8	-1.8	-2.2	-1.8	-0.7	-1.0	0.1	-1.4	0.4	1.8	0.8	0.1	-0.7	0.1	0.3	0.5	1.4	-0.4	0.6	0.7	1.3	0.1	1.5	0.7	0.1	-1.0	0.2	0.1	0.2	-0.7	0.8	1.4	2.1	0.2	5.5	0.8

Figure 4: Scorecard of large-scale indices (winter NAO, AO and AMO) and normalized air temperature anomalies (winter and annual) for five cities between 1980 and 2023. Means and standard deviations for the air temperatures during the 1991–2020 period are provided in the last column (in °C). No means or standard deviations are provided for the large-scale indices (grayed boxes).

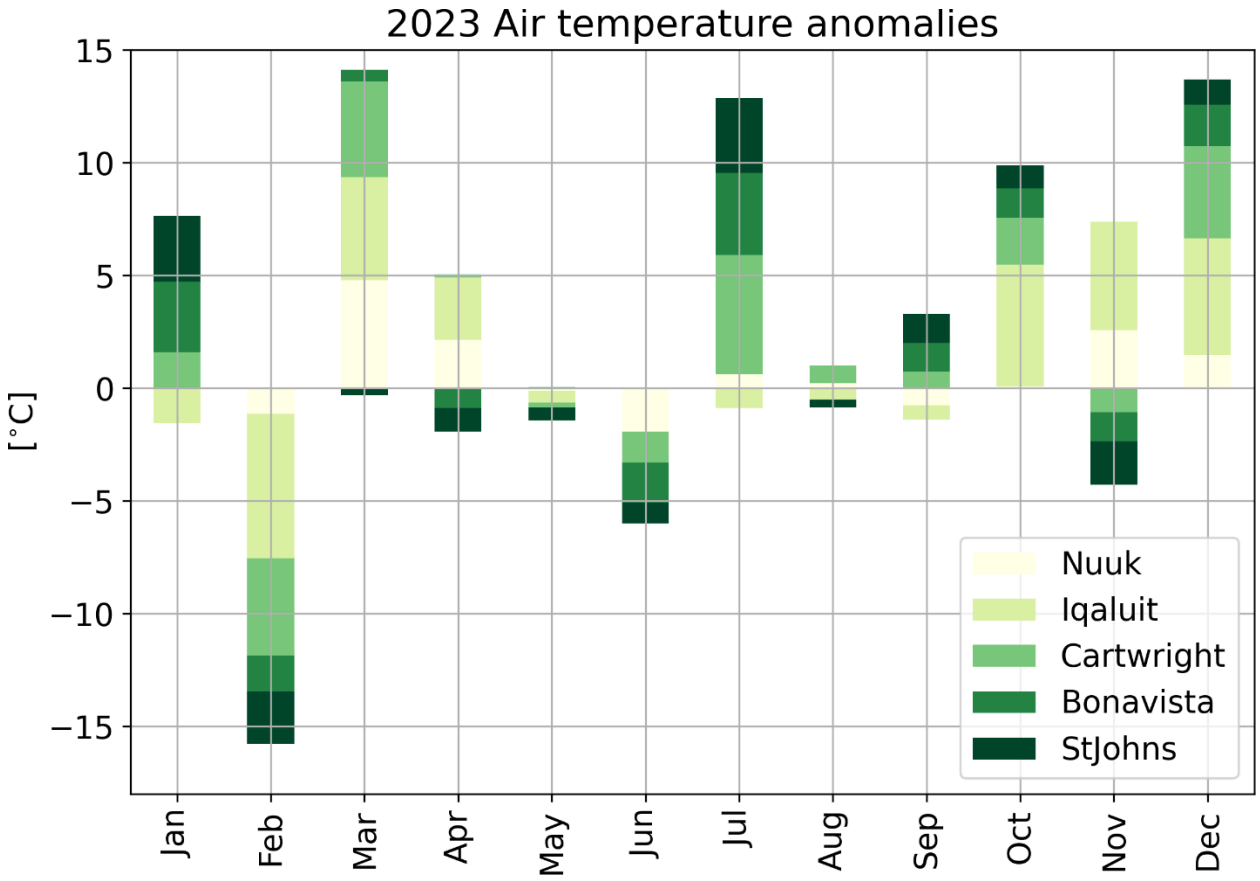

Figure 5: Cumulative monthly air temperature anomalies at Nuuk, Iqaluit, Cartwright, Bonavista and St. John's for 2023.

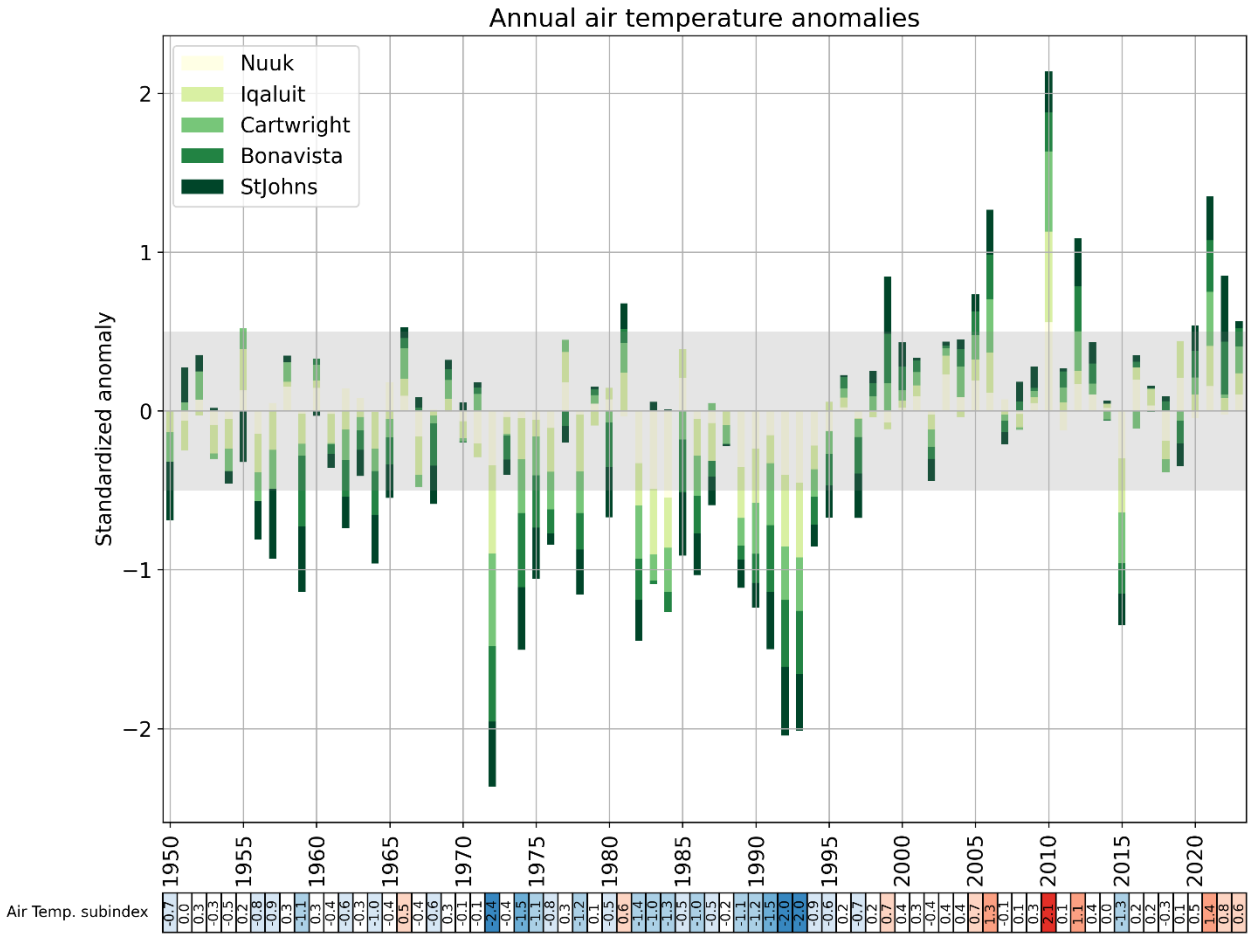

Figure 6: Normalized annual air temperature anomalies for Nuuk, Iqaluit, Cartwright, Bonavista and St. John's. This figure shows the average of the five stations, in which the length of each bar corresponds to the relative contribution of the individual station to the average. The shaded area corresponds to the 1991–2020 average ±0.5 SD, a range considered normal. The numerical values of this time series are reported in a color-coded scorecard at the bottom of the figure. The bottom scorecard is the average of these five time series, and is used to construct the NL climate index presented in the summary (Figure 39).

3 Sea ice conditions

Ice cover area, volume and seasonal duration are estimated from ice cover products obtained from the Canadian Ice Service (CIS). These products consist of Geographic Information System (GIS) charts covering the East Coast and Hudson Bay system, the latter providing coverage of the Northern Labrador Shelf. The East Coast region has weekly charts available for 1969–2023 and daily charts for 2009–2023 while only weekly charts are available for the Hudson Bay system for 1980–2023. All vector charts were further converted into regular 0.01° latitude by 0.015° longitude grids (approximately 1 km resolution), with ice concentrations and growth stages attributed to each grid point. Average thicknesses (and therefore regional volumes) are estimated from standard thicknesses associated with each stage of ice growth from new ice and nilas (5 cm), grey ice (12.5 cm), grey-white ice (22.5 cm), thin first year ice (50 cm), medium first year ice (95 cm) and thick first year ice (160 cm). Prior to 1983, the CIS reported ice categories with fewer classifications, where a single category of first year ice (≥30 cm) was used with a suggested average thickness of 65 cm. We have found this value leads to underestimates of the seasonal maximum thickness and volume based on high interannual correlations between the estimated volume of the weekly seasonal maximums and its area or sea ice season duration. The comparisons of the slope of these correlations pre- and post-1983 provided estimates of first-year ice thickness of 85 cm in the Gulf of St. Lawrence and 95 cm on the Newfoundland and Labrador Shelf for this single first year ice category, which were used instead of the suggested 65 cm.

Several products were computed to describe the sea ice cover inter-annual variability. The day of first and last occurrence, ice season duration (Figure 7) and the distribution of ice thickness during the week of maximum volume (Figure 8) are presented as maps. These two figures combine information from the East Coast sea ice charts and Hudson Bay system charts, leading to a slight jump in the climatology maps of first occurrence and duration. This occurs because there are often missing weeks in the Hudson Bay charts around the period of first occurrence on the northern Labrador Shelf. Therefore, anomalies of these two parameters have more uncertainty than the rest. Regional scorecards of anomalies for the first and last day of ice, duration of the sea ice season and maximum ice volume are presented in Figure 9 for the Labrador and Newfoundland shelves. Here, the areas defined as the Northern and Southern Labrador shelves and the Newfoundland Shelf are depicted in Figure 1, with the Newfoundland Shelf and Gulf of St. Lawrence delimited at the Eastern end of the Strait of Belle Isle. Evolution of the ice volume during the 2023 ice season is presented in Figure 9 for the three regions in relation to the climatology and historical extremes. The Northern Labrador Shelf progression is shown using weekly data extracted from Hudson Bay charts, while the others are shown using daily data extracted from East Coast charts. Time series of seasonal maximum ice volume, area (excluding thin new ice) and ice season duration are presented for the Northern (top) and Southern (middle) Labrador Shelf and for the Newfoundland Shelf (bottom) in Figure 10. The December-to-April air temperature anomaly at Cartwright showed the best correlation with sea ice properties and is included with reversed scale in the Newfoundland Shelf panel. The durations shown in Figure 9 and Figure 11 are different products. The first corresponds to the number of weeks where the volume of ice anywhere within the region exceeded 5% of the climatological maximum, while the second is the average duration at every pixel of Figure 7, which is much shorter than the first.

Ice typically starts forming in December along the Labrador coast and only by late February at the southernmost extent of sea ice presence (Figure 7).The last occurrence is usually in late June to early July on the Labrador coast, leading to sea ice season durations of 23 weeks or more. There has been a declining trend in ice cover severity since the early 1990s, reaching the lowest values in 2010 and 2011, with a rebound in 2014 and third lowest value in 2021 (Figure 9 and Figure 11). On the Newfoundland Shelf, the sea ice metrics of annual maximum ice area, volume, and ice cover duration are all well-correlated with each other (R^2 = 0.70 to 0.74; Figure 11). The strongest correlation with air temperature

was found between the December-April air temperature anomaly at Cartwright and the sea ice metrics of the Newfoundland Shelf (R^2 = 0.62–0.78), indicative of the advective nature of the Newfoundland shelf sea ice; i.e. strong ice cover is associated with cold air temperatures in the source area. Sensitivity of the Newfoundland Shelf ice cover to increases in air temperature (e.g. through climate change) can thus be estimated using 1969–2023 co-variations between winter air temperature at Cartwright and sea ice parameters, which indicate losses of 14 km^3, 26,000 km^2 and eight days of sea ice season for each 1°C increase in winter air temperature.

In 2023, the sea ice cover first appeared at generally later than normal dates (Figure 7), leading to regional thresholds marking the beginning and end of the season that were crossed later than normal (Figure 9). The last occurrence on the northern Labrador Shelf was a mix of earlier than normal inshore and later than normal offshore, with the opposite on the Newfoundland and southern Labrador shelves (Figure 7). Sea ice volumes progressed below normal on the Labrador Shelf until April, closer to normal in May and well above normal in June before ending very abruptly (Figure 10). The progression on the Newfoundland Shelf was well below normal with three pulse events of advection from the Labrador Shelf; the volume was only above normal during May (Figure 10). The maximum ice volumes reached during the season were near normal on the Labrador Shelf, at 106 km^3 (-0.1 SD) and 83 km^3 (-0.45 SD) on the northern and southern parts respectively, but below normal on the Newfoundland Shelf at 44 km^3 (-0.7 SD). The December-to-June seasonal averages followed the same pattern of near normal at 51 km^3 (-0.2 SD) and 33 km^3 (-0.48 SD) on the Northern and Southern Labrador Shelves and below normal at 9 km^3 (-0.8 SD) on the Newfoundland Shelf (Figure 9). From North to South, the pixel average durations were below normal at 113 (-0.7 SD), 83 (-0.6 SD) and 29 days (-0.8 SD), respectively (Figure 7 and Figure 11). The maximum area reached within each region (excluding ice less than 15 cm thick) was near normal at 97 000 km^2 (-0.2 SD), 113 000 km^2 (-0.35 SD) and 120 000 km^2, -0.05 SD). An overview of sea ice conditions (area and season duration) for NL since 1969 is presented in Figure 12 as the average of normalized anomalies. In 2023, this index was near normal at
-0.5 SD.

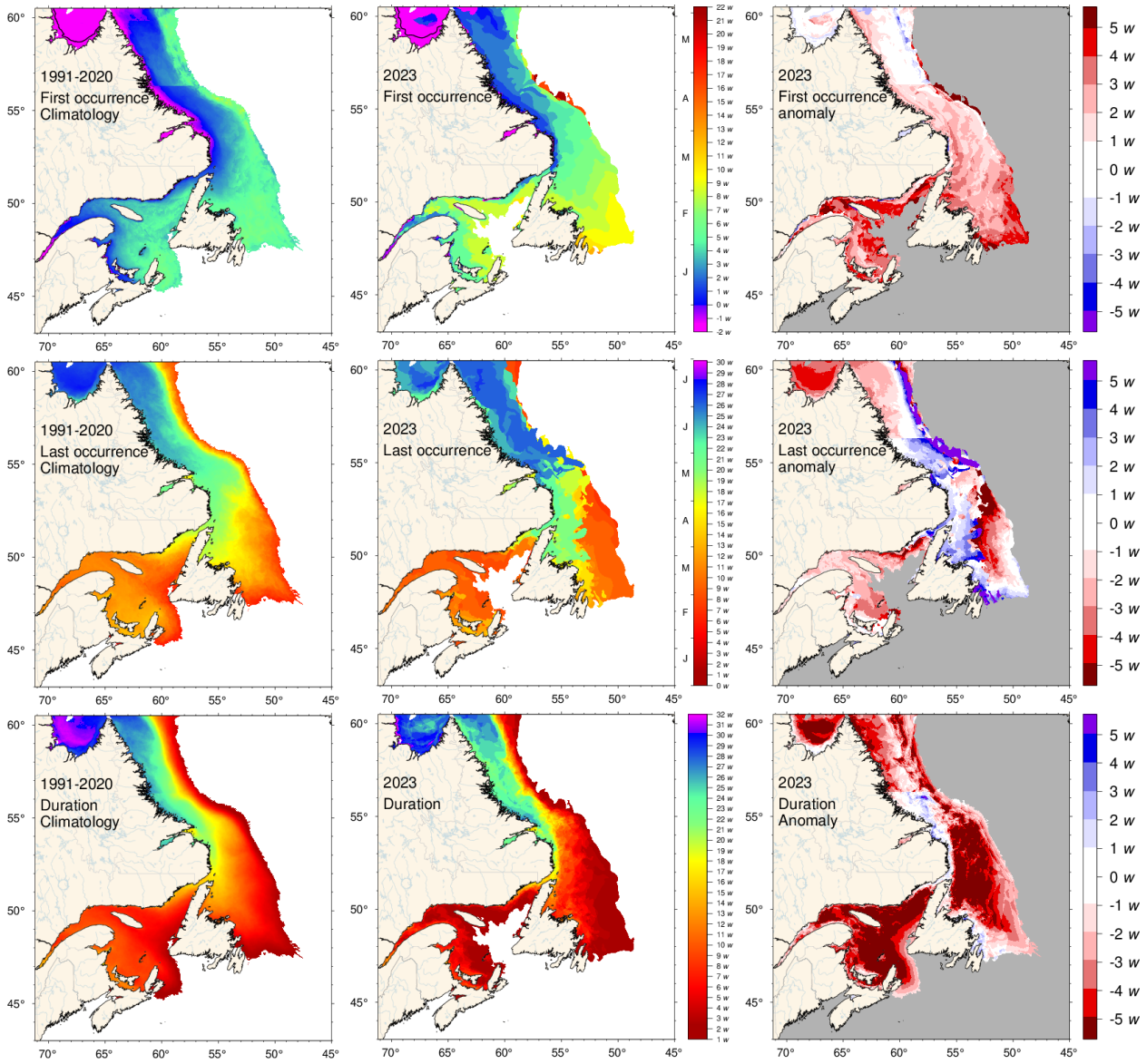

Figure 7: First (top) and last (middle) occurrence of ice and ice season duration (bottom) based on weekly data. The 1991–2020 climatologies are shown (left) as well as the 2023 values (middle) and anomalies (right). First and last occurrences are defined here as the first and last weekly chart in which any amount of ice is recorded for each pixel and are illustrated as day-of-year. Ice duration sums the number of weeks with ice cover for each pixel. Climatologies are shown for pixels that had at least 15 years out of 30 with occurrence of sea ice, and therefore also show the area with 50% likelihood of having some sea ice at any time during any given year. The duration anomaly map includes pixels with no ice cover where some was expected based on the climatology.

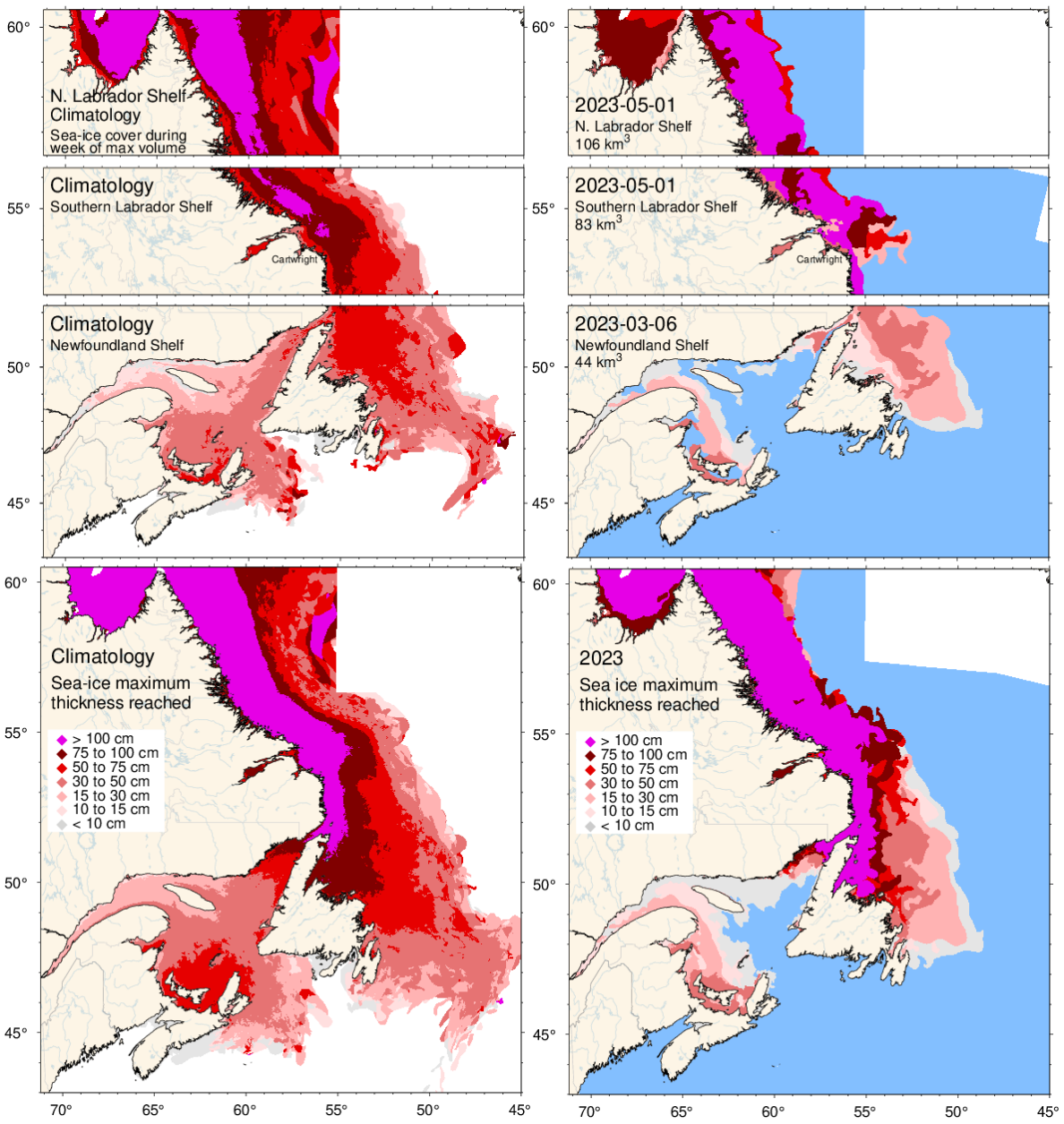

Figure 8: Ice thickness map for 2023 for the week with the maximum annual volume on the Newfoundland and Labrador Shelf (three upper right panels) and similarly for the 1991–2020 climatology of the weekly maximum (three upper left panels). Note that these maps reflect the ice thickness distribution on that week. The maximum ice thickness observed at any given location during the year is presented in the lower panels, showing the 1991–2020 climatology and 2023 distribution of the thickest ice recorded during the season at any location.

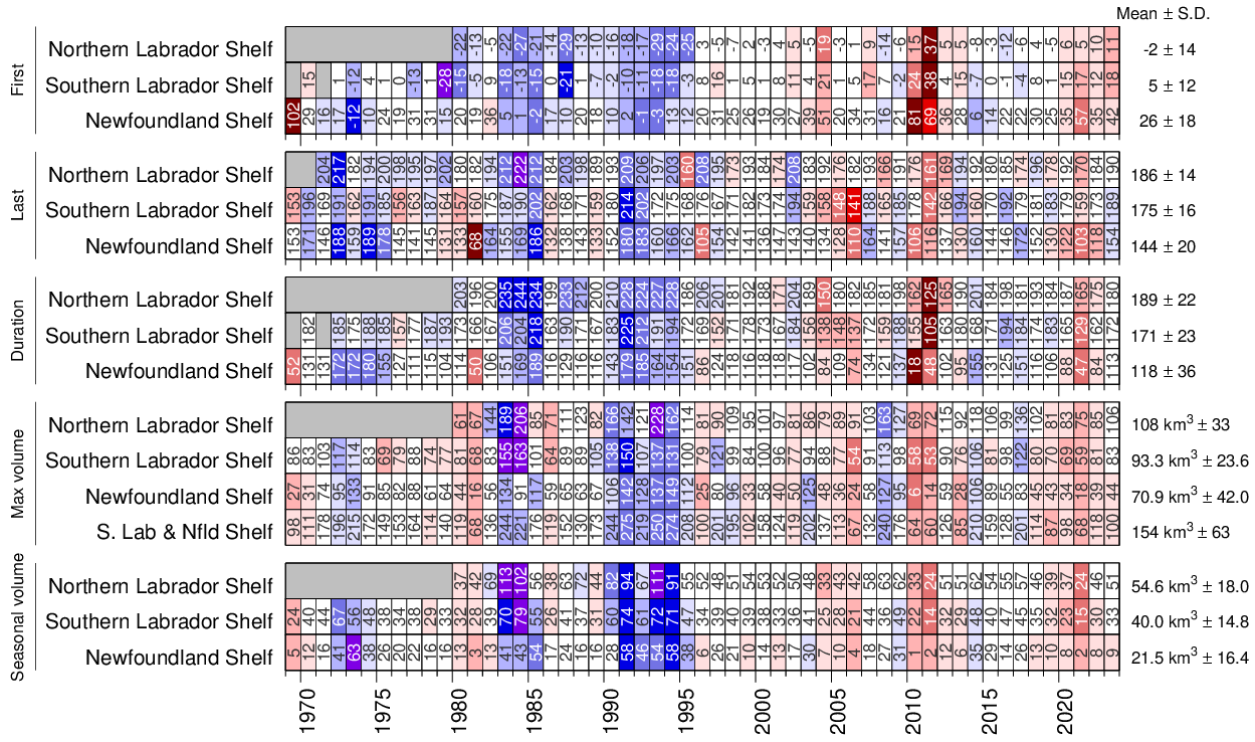

Figure 9: First and last day of ice occurrence, ice duration, maximum seasonal ice volume and average seasonal (DJFMAMJ) ice volume by region. The moment when ice was first and last observed in days from the beginning of each year is indicated for each region, and the color code expresses the anomaly based on the 1991–2020 climatology, with blue (cold) representing earlier first occurrence and later last occurrence. The threshold is 5% of the climatological average of the seasonal maximum ice volume. Numbers in the table are the actual day of the year or volume, but the color coding is according to normalized anomalies based on the climatology of each region. Duration is the numbers of days that the threshold was exceeded. Seasonal average volumes (lowermost scorecard) are reported in the ICES Report on Ocean Climate (Cyr & Galbraith, 2023).

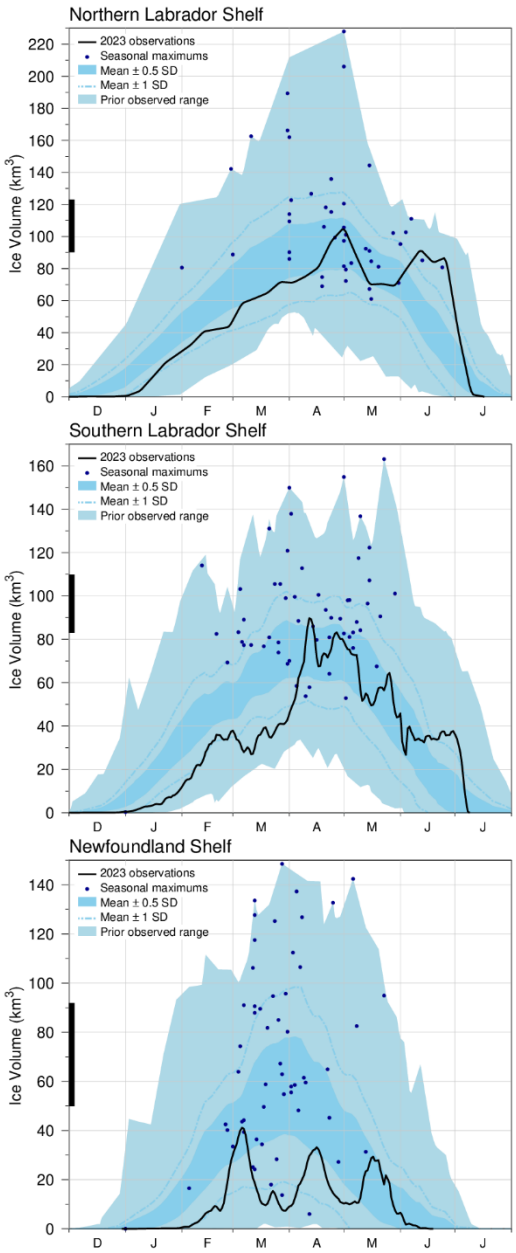

Figure 10: Time series of the 2022–23 mean ice volume (black lines) for the Northern Labrador Shelf (top), Southern Labrador Shelf (middle), and Newfoundland Shelf (bottom), the 1991–2020 climatological mean volume ±0.5 and ±1 SD (dark blue area and dashed line respectively), the minimum and maximum span of 1969–2021 observations (light blue), and the date and volumes of 1969–2021 seasonal maximums (blue dots). The black thick line on the left indicates the mean volume ±0.5 SD of the annual maximum ice volume, which is higher than the peak of the mean daily ice volume distribution.

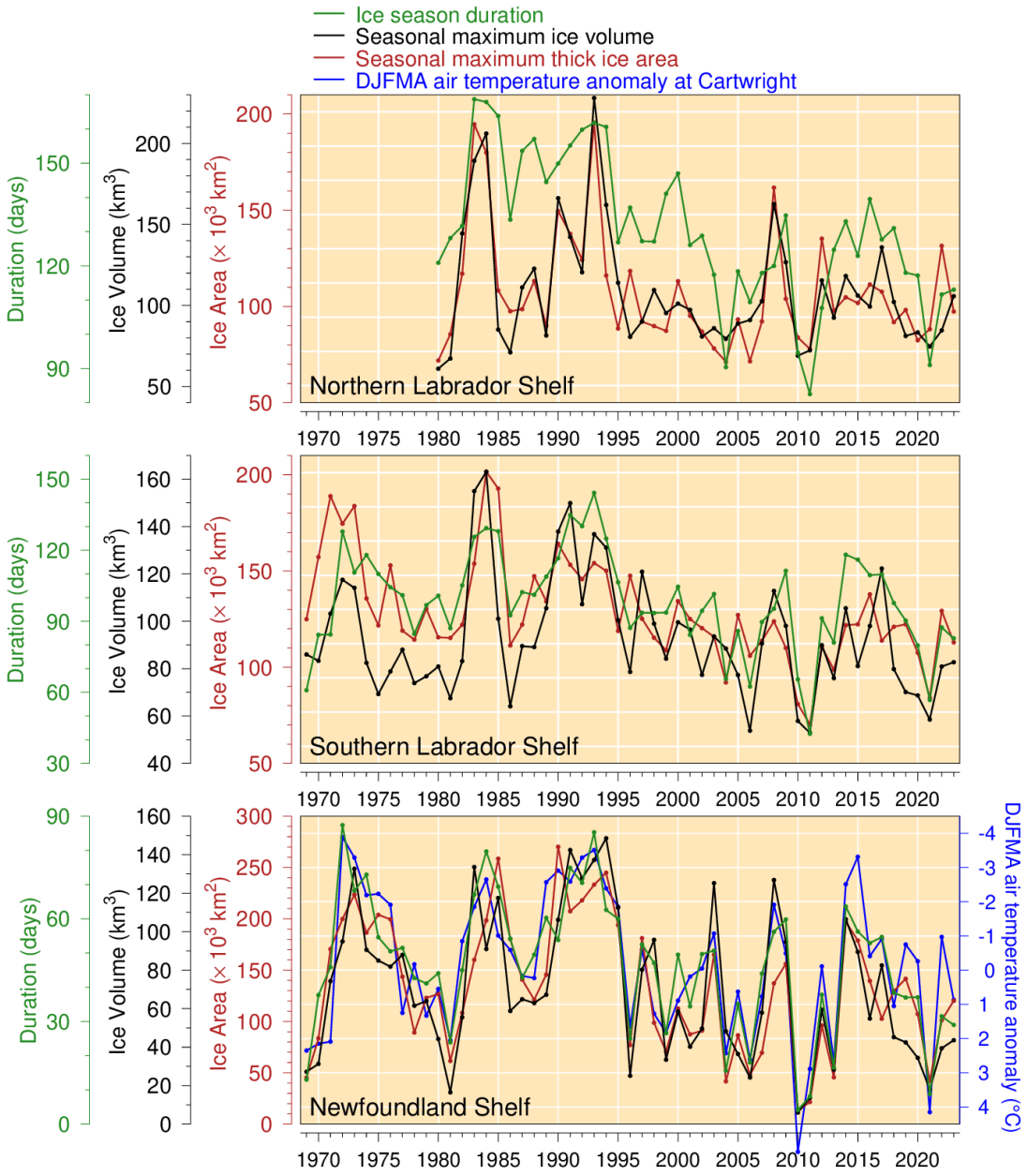

Figure 11. Regional average sea ice metrics and NL sea ice index. Seasonal maximum ice volume (black lines) and area (excluding ice less than 15 cm thick; red lines), and ice season duration (green lines) for the Northern and Southern Labrador Shelf (first and second panels, respectively) and the Newfoundland Shelf (third), and December-to-April air temperature anomaly at Cartwright (blue line).

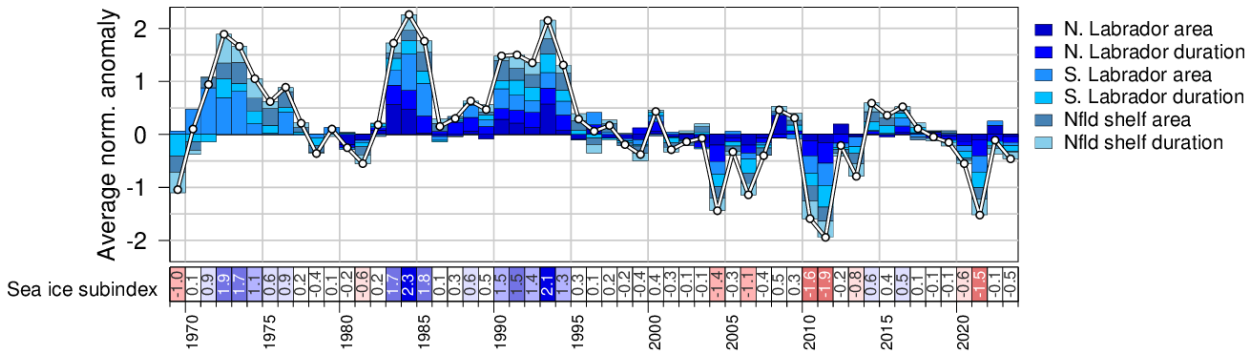

Figure 12. Newfoundland and Labrador sea ice index established by averaging the normalized anomalies of volume and duration of sea ice for Newfoundland and Labrador shelves (black and green time series in Figure 11). This sea ice index contributes to the NL climate index described in the summary (Figure 39).

4 Icebergs

Iceberg counts obtained from the International Ice Patrol of the US Coast Guard indicate that 385 icebergs drifted south of 48ºN onto the Northern Grand Banks during 2023 (Figure 13). This number is lower than the climatological (1991–2020) average of 771. Some years have seen even lower numbers. For example, only one iceberg was observed in 2010 and 2021, two in 2011 and 13 in 2013. Only two years (1966 and 2006) in the 120-year time series have reported no icebergs south of 48ºN. More than 1,500 icebergs have been observed in some years during the cold periods of the early 1980s and 1990s, including the all-time record of 2,202 in 1984, along with a recent high number of 1,515 in 2019. Years with low iceberg numbers on the Grand Banks generally correspond to higher-than-normal air temperatures, lighter-than-normal sea ice conditions, and warmer-than-normal ocean temperatures on the NL Shelf. As such, the normalized anomaly of the number of icebergs (scorecard at the bottom of Figure 13) is used as one component of the NL climate index presented in the summary.

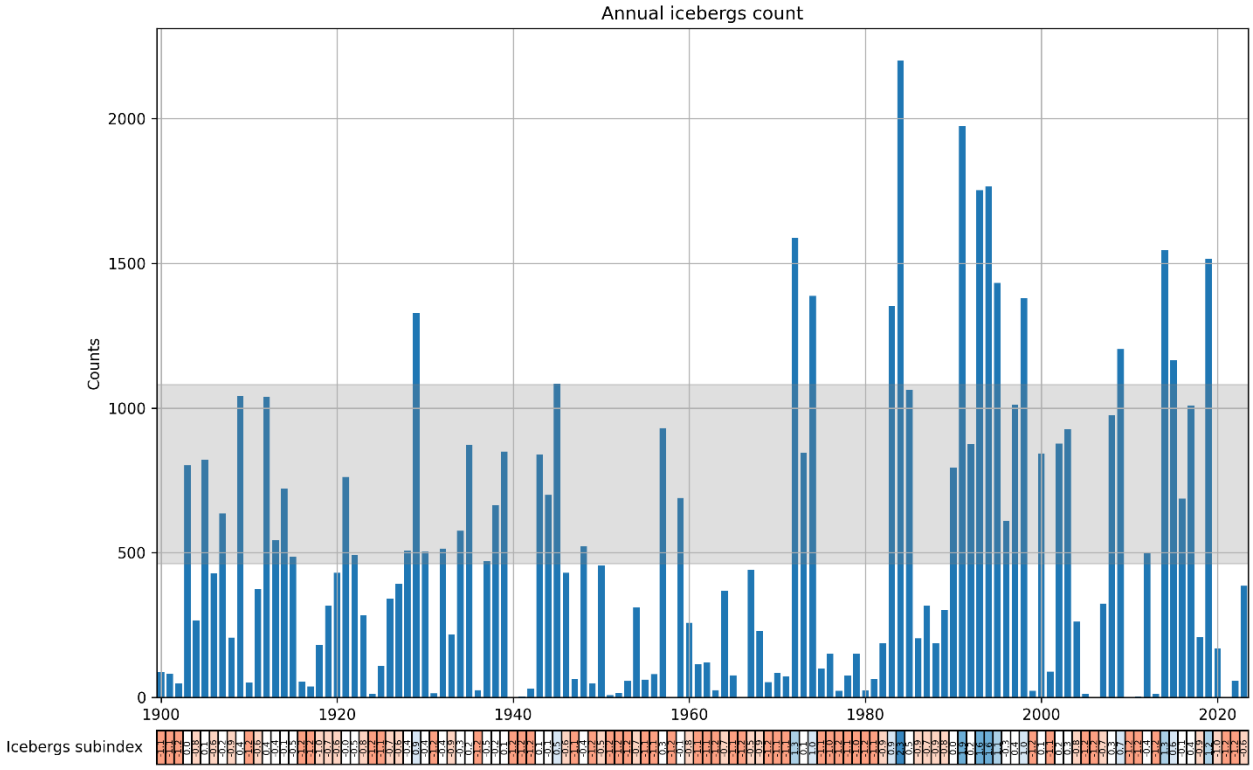

Figure 13: Annual iceberg count crossing south of 48°N on the northern Grand Bank. The shaded area corresponds to the 1991–2020 average ±0.5 SD. The data are from the International Ice Patrol (International Ice Patrol, 2020). *The normalized anomaly of this time series is color-coded in the bottom scorecard. This iceberg sub-index contributes to the NL climate index described in the summary (Figure 39).*

5 Satellite sea-surface temperature

The satellite-based sea surface temperature product used in the previous two years' reports blends data from Pathfinder version 5.3 (4 km resolution for 1982–2020; Casey et al. 2010), Maurice Lamontagne Institute (MLI; 1.1 km resolution for 1985–2013) and Bedford Institute of Oceanography (BIO; 1.5 km resolution for 1997–2022) as detailed in Galbraith et al. (2021). The process selects the products with the best percent coverage for every averaging area and period (week or month). Monthly (and weekly) temperature composites are calculated from averaged available daily anomalies to which monthly (or weekly) climatological average temperatures are added.

The BIO data stopped being produced in June 2022 and so two NOAA operational products were investigated to continue our operational coverage of the Atlantic Zone. The GHRSST NOAA/STAR L3S-LEO-Daily "super-collated" product was retained (0.02° resolution for 2007 to present; NOAA/STAR 2021). Day and night composites for each day are used to create a daily composite as the average of both values if available for a pixel, or using the available day or night pixel value minus or plus half of the average diurnal variation in the Atlantic Zone (0.22°C). Daily pixel values were then compared against the daily range of observations at four offshore thermograph stations (Mont-Louis, Havre-Saint-Pierre, Beaugé, La Romaine) as well as at all oceanographic Viking buoys. From the initial 10165 days of observations, we excluded all thermograph and buoy daily data that had diurnal temperature variations greater than the mean diurnal range, leaving 6691 days of observations available for comparison. This filtering is done because the difference between in-situ and satellite observations is greater when the diurnal range is high and may bias the calibration. A linear regression was performed of the average daily temperature at thermographs against the NOAA/LEO daily composite values at corresponding pixels and used as a calibration (SST = 1.01 LEO – 0.41). This calibration cools the NOAA/LEO daily composite values by 0.41°C at 0°C and by 0.19°C at 20°C. Before calibration, 69% of NOAA/LEO observations were within the 10165 thermograph/buoy diurnal ranges. After calibration, this increased to 95.4%. The calibrated NOAA/LEO daily composites were added to our blend method (Galbraith et al. 2021) and the BIO product was removed. The new blend was introduced last year (Cyr et al. 2024).

Figure 14 shows the 2023 weekly evolution of the SSTs (black lines in each panel) for NAFO divisions 2GHJ3KLMNOP cropped at the shelf break (see Figure 1) in relation to the 1991–2020 climatology (blue shades). The color-coded anomalies are shown below each panel as weekly, monthly and seasonal scorecards. Only SST measurements during the ice-free periods of the year are considered. These range from as short as June to September on the northern Labrador Shelf (NAFO division 2H), to as long as March to November on the south coast of Newfoundland (NAFO division 3P).

In 2023, monthly average SSTs were largely above normal in ice-free areas across the region with the warmest anomalies found between July and October (Figure 14, middle scorecards at the bottom of panels). Several new monthly warm records were established across the different NAFO divisions and for the different months. The largest departures from the average temperature were reached on the northern Newfoundland shelf (Division 3K) and Flemish Cap (Division 3M) in July (+5.1°C and +5.0°C above average, respectively).

Seasonal SSTs averaged over the ice-free months were also significantly above normal across the NL Shelf (between +0.7 to +2.0 SD above average for the different NAFO divisions; Figure 14, bottom scorecards at the bottom of panel). It is thus not surprising that the spatially weighted average over the NL region was also warm at +2.0 SD above average making 2023 the second warmest year on average after 2021 (Figure 15). Note that the last three years are the three warmest on record.

Note that air temperature has been found to be a good proxy of sea surface temperature. The warming trend observed in air temperature since the 1870s of about 1°C per century is also expected to have occurred in surface water temperatures across Atlantic Canada (Galbraith et al. 2021).

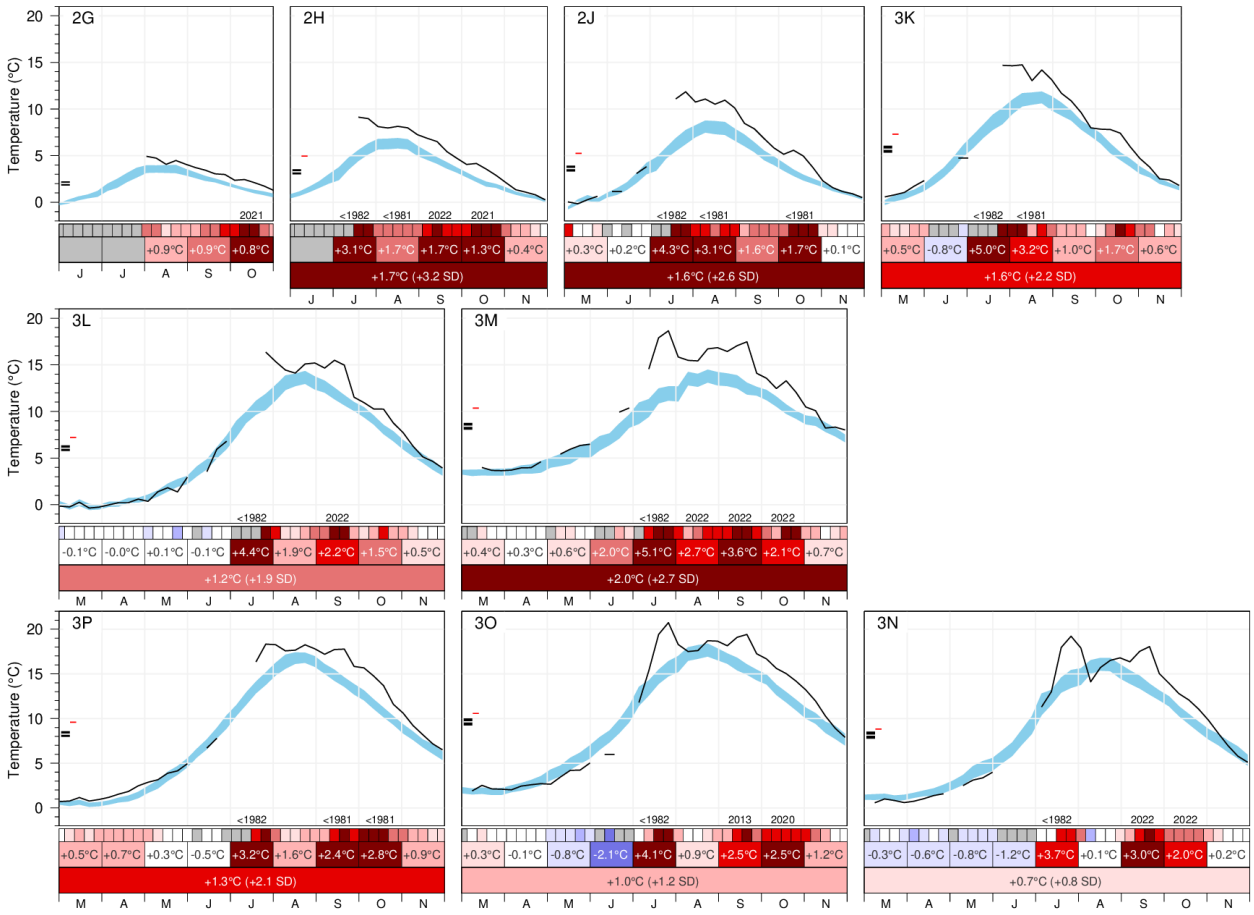

Figure 14: Weekly evolution of AVHRR Sea surface temperature evolution in 2023 for NAFO divisions 2GHJ3KLMNOP (black lines) during the ice-free season (season-length variable). Broken lines indicate that the threshold for the number of good pixels was not reached during these weeks (no data). The blue area represents the 1991–2020 climatological weekly mean ±0.5 SD. Scorecards representing the weekly, monthly and seasonal averages (in °C) appear at the bottom of each panel and are color-coded according to the normalized anomalies (top, middle and bottom row, respectively), with data gaps in grey. The two black ticks along the y-axis correspond to the seasonal climatological average ±0.5 SD, while the red tick represents the 2023 seasonal average.

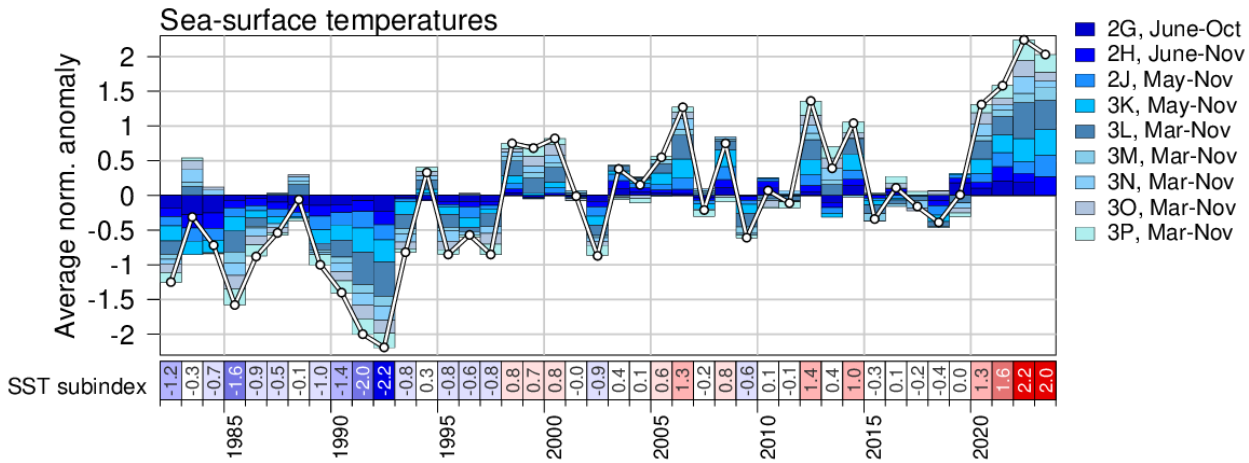

Figure 15: Northwest Atlantic SST index built from the average of the seasonal anomalies for all NAFO divisions (bottom rows of panels in Figure 14). This index contributes to the NL climate index described in the summary (Figure 39).

6 Ocean conditions on the Newfoundland and Labrador shelf

The following section presents observations of various ocean parameters at long-term monitoring Station 27, along standard hydrographic sections, and over the ocean bottom.

6.1 Long-term observations at Station 27

Station 27 (47°32.8'N, 52°35.2'W), is located in the Avalon Channel off Cape Spear, NL (Figure 1). It is one of longest hydrographic time series in Canada with frequent, near-monthly, occupations since 1948. In 2023, the station was occupied 36 times including 16 Conductivity-Temperature-Depth (CTD)-only casts, 18 full AZMP physical-biogeochemical samplings and 2 Expendable Bathythermograph (XBT) measurements.

Since 2017, an automatic profiling system installed on a surface buoy (type Viking) usually provides extended temporal coverage of temperature (T) and salinity (S) at Station 27. The buoy was deployed in June 2023, but unfortunately the mini-winch used to collect CTD profile data was non-operational. Multiple attempts were made to repair the mini-winch at sea but they proved unsuccessful. No CTD profiles were collected in 2023 by the buoy, but all other surface instruments were operational and collected data until late September, after which data collection was impacted by the reduced sunlight affecting the power generation by the solar panels. The buoy was recovered in December.

Station occupations were used to obtain the annual evolution of temperature and salinity at Station 27, as well as the anomaly compared to the 1991–2020 climatology, shown in Figure 16 and Figure 17. These figures demonstrate the seasonal warming of the top layer (~20 m), with temperature peaking in August before being mixed during the fall. The CIL (Petrie et al., 1988), a remnant of the previous winter cold layer and defined by temperatures below 0°C (thick black line in Figure 16) is also evident below 100 m throughout the summer. Interestingly, the coldest water body within the CIL (darkest shades of blue in the middle panel of Figure 16) is generally found in the summer between mid-June and mid-August, suggesting advection of cold waters from the Labrador Shelf and the Arctic to the Newfoundland Shelf. The surface layer is generally freshest between early-September and mid-October, with salinities below 31 (Figure 17). These low near-surface salinities are a prominent feature of the salinity cycle on the Newfoundland Shelf and are largely due to the melting of coastal sea ice. The presence of such a large volume of freshwater late in the summer season also points to advection from northern areas (Labrador and the Arctic).

The water column was warmer and fresher than average during the early months of 2023 (Figure 16 and Figure 17, top and bottom panels). While the fresh conditions continued through the spring and the summer, a cold anomaly developed in the surface in the spring and in the subsurface in the summer (Figure 16, bottom panel). As a warm anomaly developed in a very thin layer at the surface in July and August (see also Section 6.2), the cold anomaly was significant in August-September, reaching more than 5°C below average between about 20-30 m. This cold anomaly is likely driven by the advection of a thick CIL from the north and coherent with the cold month of February on the Labrador shelf (e.g. Figure 5). At depth, the rest of the year was relatively normal. Except for a salty anomaly in August-September coinciding with the cold anomaly observed, the water column at Station 27 was fresher than average for most of the year and at all depths (Figure 17).

Over 2023, the annual temperature anomaly (defined as the average of monthly anomalies) for the vertically averaged (0–176 m) temperature was normal (+0.4 SD), while the vertically-averaged salinity was slightly fresh at -1.1 SD (Figure 18 and Figure 19). The fresh anomaly of the early 1970s (Figure 18, bottom panel), commonly referred to as the Great Salinity Anomaly in the North Atlantic (Dickson et al., 1988), now looks very minor compared to the freshening happening at Station 27 since the late 2010s. This is partly due to a change in the mean state towards a freshening of the NL shelf. Normalized anomalies of temperature and salinity for all years since 1980 and for different depth ranges (0–176 m, 0–50 m and 150–176 m) are reported in scorecards in Figure 19.

The summer (May-July) CIL statistics at Station 27 since 1951 are presented in Figure 20. Here the CIL mean temperature corresponds to the average of all temperatures below 0°C. The CIL thickness as well as the CIL core temperature (the minimum temperature of the CIL) and its depth are also presented in Figure 20. In last year's report (Cyr et al., 2024), the discovery in our internal database of a set of problematic casts associated with Mechanical Bathythermographs (MBTs) collected in the 1960s and 1970s, where the negative temperatures were converted into positive values, has slightly reduced the warm anomalies during these decades. This year, we have found and removed more of these problematic data. The new time series suggest that the warm early 1960s to the mid-1970s for the CIL mean and core temperatures remain (top and middle panels, respectively), but that the magnitudes of these anomalies have decreased compared to the assessment prior to the discovery of the problematic MBTs (Cyr et al., 2022). After the prevalence of a warm CIL in the early 2010s (with some of the warmest years since the mid-1970s), there was a cooler period between about 2014 and 2017. The CIL was warmer than normal between 2018 and 2023, except in 2020 when it was normal. The SD of these metrics are reported in a scorecard in Figure 19.

The monthly mean mixed layer depth (MLD) at Station 27 was also estimated from the density profiles as the depth of maximum buoyancy frequency (N) calculated from the monthly averaged density profiles ($\rho(z)$):

$$N^2 = \frac{-g}{\rho_0} \frac{\Delta\rho(z)}{\Delta z},$$

with $g = 9.8$ ms^{-2} as the gravitational acceleration, z the depth and ρ_0 the mean density. Here N^2 is calculated using the Gibbs-SeaWater (GSW) Oceanographic Toolbox (McDougall & Barker, 2011).

Climatological monthly MLD values, as well as monthly MLDs during 2023, are presented in Figure 21. The climatological annual cycle shows a gradual decrease of the MLD between late fall and summer (the mixed layer is thickest in December-January and shallowest in July-August). Overall, the MLD was deeper than average in the winter (Jan-Feb; no data for March), close to normal in spring and fall, and shallower than average in June, July and September. The MLD was especially thin in September with values of ~15m, which are as shallow as in July and much shallower than the climatological values of ~35m for this month. Annual mean values of the MLD and its 5-year moving average are shown in Figure 22 (solid gray line and dashed-black line, respectively). In general, there is a strong interannual and decadal oscillation in MLD, but the striking feature is a step-like increase in the 1990s. A scorecard of annual and seasonal MLD anomalies since 1980 can be found in Figure 19.

Stratification is an important characteristic of the water column, since it influences, for example, the transfer of solar heat to deeper layers and the vertical exchange of biogeochemical tracers between the deeper layers and the surface. The seasonal development of stratification is also an important process influencing the formation and evolution of the CIL on the shelf regions of Atlantic Canada. It insulates the lower water column from the upper layers, thus slowing the vertical heat flux from the seasonally heated surface layer.

Stratification at Station 27 is calculated from monthly average density profiles using discrete differences between two averaged depth ranges. Two definitions of the stratification indices are calculated for Station

27. The first one uses density differences (i.e. $\Delta\rho/\Delta z$) between 0-5 m and 48-53 m (labelled 0-50 m definition) and the second one between 8-13 m and 148-153 m (labelled 10-150 m definition). See bottom two scorecards in Figure 19. Measurements taken from non-bottle instrument types were discarded in the top two depth levels to mitigate the influence of problem surface measurements. The reason for these two definitions is that historical near-surface measurements in the 1950s and 1960s were made at discrete depths of z=0, 25, and 50 m. In the 1970s and 1980s, these discrete depths were changed to z=0, 10, 20, 30, 50 m. Finally, since the widespread use of electronic measurements using CTDs mounted on rosettes started in the 1980s, near-surface (z=0) measurements of density are usually discarded, and each high-resolution cast usually starts between 2-5 m depth to avoid electronic noise contamination or damage to the rosette by surface waves or ship motion. There is thus no simple definition that can ensure continuity of the metric from the 1950s to present. Here the definition 0-50 m will mostly focus on the 1950-1990 period, while the definition 10-150 m will be representative of the period 1960-present. Note that the 0-50 m definition is also calculated until present, but it considers the average over 0-5 m as the surface measurement, making it difficult to directly compare with historical data. When reporting annual averages, yearly stratification values are omitted if there is less than 3 months of data available. When reporting seasonal averages, only one measurement must be present.

The 2023 and climatological evolution of the 0-50 m stratification throughout the year are shown in Figure 23. The stratification is generally weakest between December and April, before rapidly increasing at the onset of spring until it peaks in August. While the stratification was close to normal for most of the year, a notable observation is the high stratification in September 2023 (Figure 23). This anomalously high stratification value is coherent with the shallow MLD observed that month (Figure 21).

The interannual evolution of the stratification anomaly since 1950 is shown in Figure 24. Strong decadal variations exist in the two different definitions of stratification. For the 0-50m range, an increase in stratification from the 1950s to about 2000 is observed, followed by a slight decrease since then. For the 10-150m definition, no real trends are discernible, but a step-wise increase seems to occur in the early 1990s, especially in the 0-50 definition. We have shown this increase by averaging the stratification between 1950-1990 and 1990-present (Figure 24). In 2023 the annual stratification was about normal relative to the 1991-2020 climatology. A scorecard of annual and seasonal stratification anomalies since 1980 can be found in Figure 19.

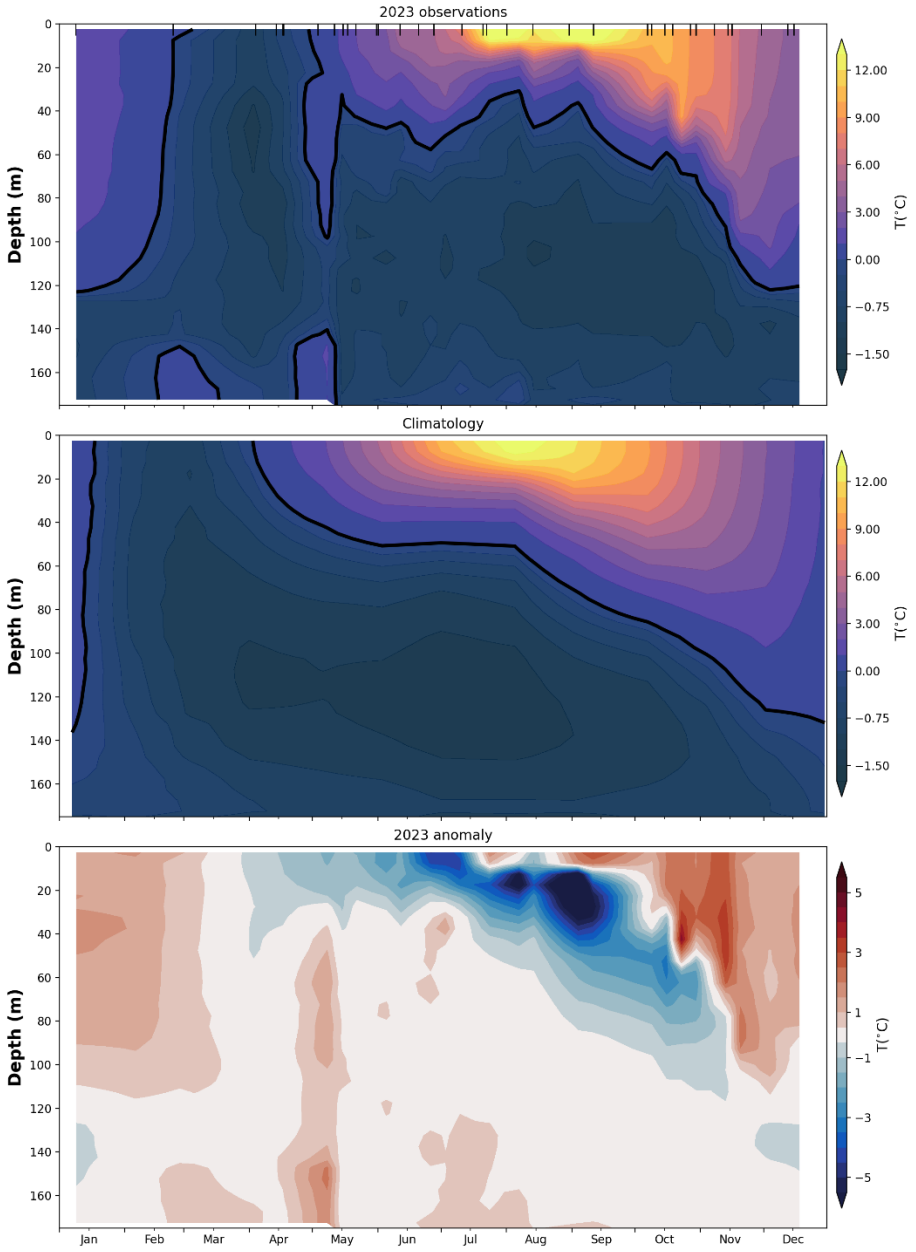

Figure 16: Annual evolution of temperature at Station 27. The 2023 contour plot (top panel) is generated from weekly averaged profiles from all available data, including station occupations and Viking buoy casts (indicated by black tick marks on top of panel). The solid black contour delineates the cold intermediate layer (CIL), defined as water below 0°C. The 1991–2020 weekly climatology is plotted in the middle panel. Note the uneven colorbar used in the two first panels: below 0°C, 0.25°C increments are used, while 1°C increments are used above 0°C. The anomaly (bottom panel) is the difference between the 2023 field and the climatology.

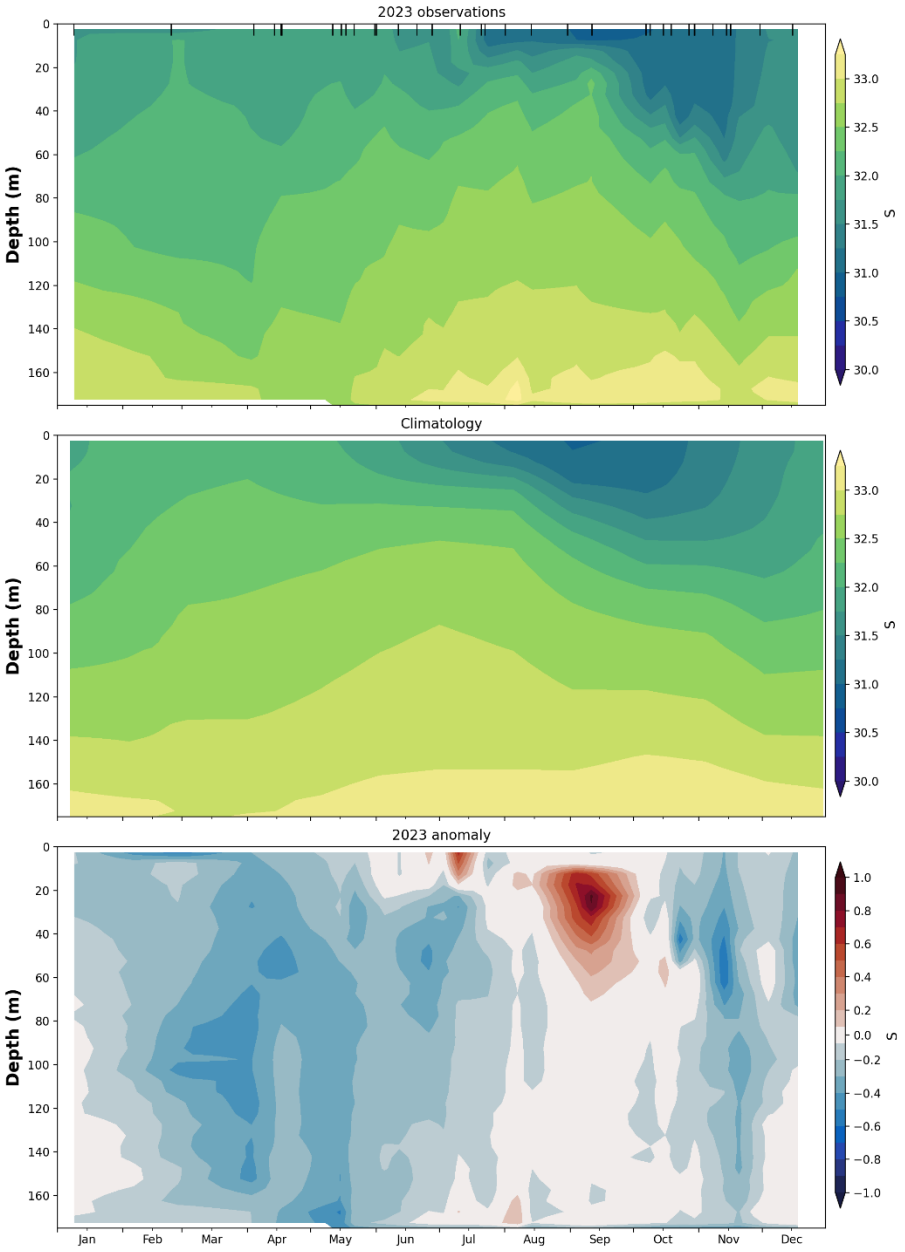

Figure 17: Same as in Figure 16, but for salinity.

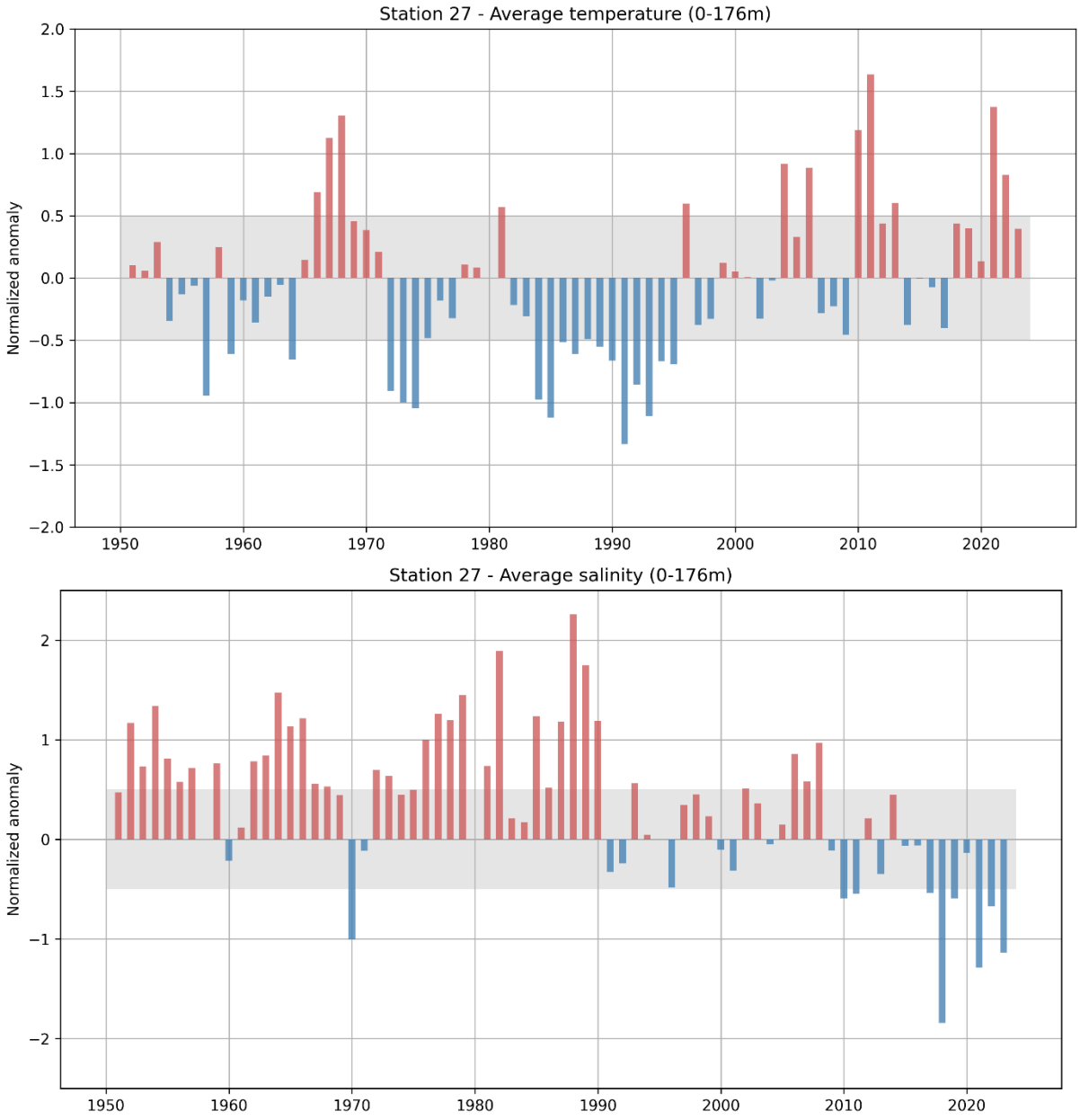

Figure 18: Annual normalized anomaly of vertically averaged (0–176 m) temperature (top) and salinity (bottom) at Station 27 calculated from all occupations since 1951. Only years where at least 8 months of the year are sampled are presented. Shaded gray areas represent the climatological (1991–2020) average ±0.5 SD range considered "normal". These two time series contribute to the NL climate index described in the summary (Figure 39).

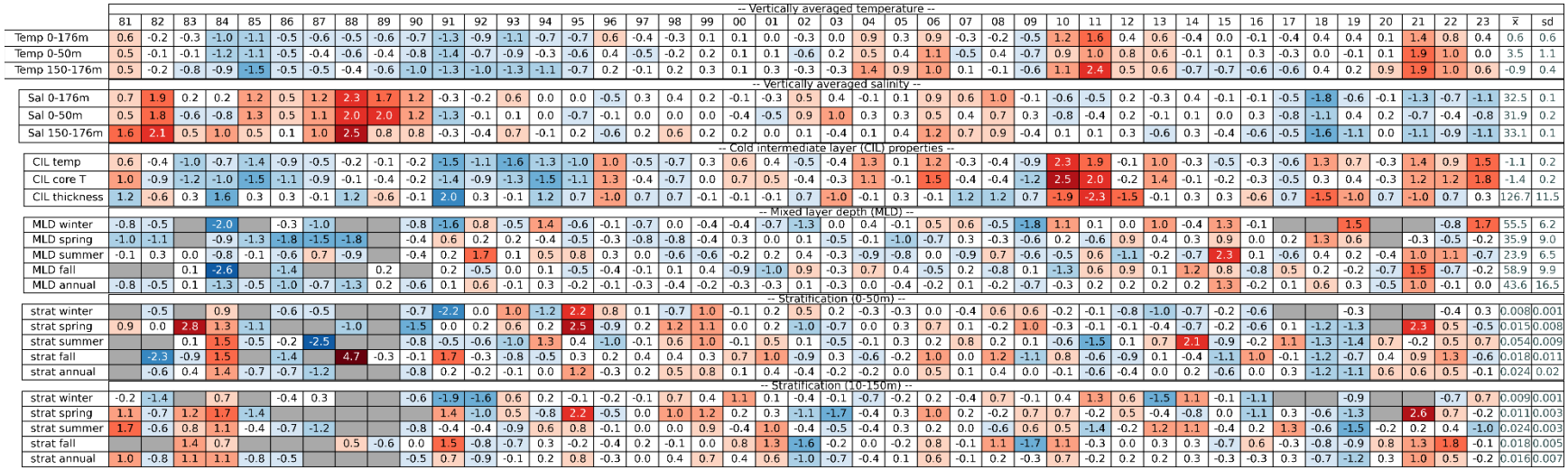

	81	82	83	84	85	86	87	88	89	90	91	92	93	94	95	96	97	98	99	00	01	02	03	04	05	06	07	08	09	10	11	12	13	14	15	16	17	18	19	20	21	22	23	$\bar{x}$	sd
-- Vertically averaged temperature --																																													
Temp 0-176m	0.6	-0.2	-0.3	-1.0	-1.1	-0.5	-0.6	-0.5	-0.6	-0.7	-1.3	-0.9	-1.1	-0.7	-0.7	0.6	-0.4	-0.3	0.1	0.1	0.0	-0.3	0.0	0.9	0.3	0.9	-0.3	-0.2	-0.5	1.2	1.6	0.4	0.6	-0.4	0.0	-0.1	-0.4	0.4	0.4	0.1	1.4	0.8	0.4	0.6	0.6
Temp 0-50m	0.5	-0.1	-0.1	-1.2	-1.1	-0.5	-0.4	-0.6	-0.4	-0.8	-1.4	-0.7	-0.9	-0.3	-0.6	0.4	-0.5	-0.2	0.2	0.1	0.1	-0.6	0.2	0.5	0.4	1.1	-0.5	0.4	-0.7	0.9	1.0	0.8	0.6	-0.1	0.1	0.3	-0.3	0.0	-0.1	0.1	1.9	1.0	0.0	3.5	1.1
Temp 150-176m	0.5	-0.2	-0.8	-0.9	-1.5	-0.5	-0.5	-0.4	-0.6	-1.0	-1.3	-1.0	-1.3	-1.1	-0.7	0.2	-0.1	0.2	0.3	0.1	0.3	-0.3	-0.3	1.4	0.9	1.0	0.1	-0.1	-0.6	1.1	2.4	0.5	0.6	-0.7	-0.7	-0.6	-0.6	0.4	0.2	0.9	1.9	1.0	0.6	-0.9	0.4
-- Vertically averaged salinity --																																												
Sal 0-176m	0.7	1.9	0.2	0.2	1.2	0.5	1.2	2.3	1.7	1.2	-0.3	-0.2	0.6	0.0	0.0	-0.5	0.3	0.4	0.2	-0.1	-0.3	0.5	0.4	-0.1	0.1	0.9	0.6	1.0	-0.1	-0.6	-0.5	0.2	-0.3	0.4	-0.1	-0.1	-0.5	-1.8	-0.6	-0.1	-1.3	-0.7	-1.1	32.5	0.1
Sal 0-50m	0.5	1.8	-0.6	-0.8	1.3	0.5	1.1	2.0	2.0	1.2	-1.3	-0.1	0.1	0.0	-0.7	-0.1	0.0	0.0	0.0	-0.4	-0.5	0.9	1.0	0.3	0.3	0.5	0.4	0.7	0.3	-0.8	-0.4	0.2	-0.1	0.1	0.0	0.3	-0.8	-1.1	0.4	0.2	-0.7	-0.4	-0.8	31.9	0.2
Sal 150-176m	1.6	2.1	0.5	1.0	0.5	0.1	1.0	2.5	0.8	0.8	-0.3	-0.4	0.7	-0.1	0.2	-0.6	0.2	0.6	0.2	0.2	0.0	0.1	-0.4	0.1	0.4	1.2	0.7	0.9	-0.4	0.1	0.1	0.3	-0.6	0.3	-0.4	-0.6	-0.5	-1.6	-1.1	0.0	-1.1	-0.9	-1.1	33.1	0.1
-- Cold intermediate layer (CIL) properties --																																												
CIL temp	0.6	-0.4	-1.0	-0.7	-1.4	-0.9	-0.5	-0.2	-0.1	-0.2	-1.5	-1.1	-1.6	-1.3	-1.0	1.0	-0.5	-0.7	0.3	0.6	0.4	-0.5	-0.4	1.3	0.1	1.2	-0.3	-0.4	-0.9	2.3	1.9	-0.1	1.0	-0.3	-0.5	-0.3	-0.6	1.3	0.7	-0.3	1.4	0.9	1.5	-1.1	0.2
CIL core T	1.0	-0.9	-1.2	-1.0	-1.5	-1.1	-0.9	-0.1	-0.4	-0.2	-1.4	-0.9	-1.3	-1.5	-1.1	1.3	-0.4	-0.7	0.0	0.7	0.5	-0.4	-0.3	1.1	-0.1	1.5	-0.4	-0.4	-1.2	2.5	2.0	-0.2	1.4	-0.1	-0.2	-0.3	-0.5	0.3	0.4	-0.3	1.2	1.2	1.8	-1.4	0.2
CIL thickness	1.2	-0.6	0.3	1.6	0.3	0.3	-0.1	1.2	-0.6	-0.1	2.0	0.3	-0.1	1.2	0.7	-1.0	0.7	0.7	-0.1	-0.1	-0.1	0.7	-1.0	-0.1	0.3	-0.1	1.2	1.2	0.7	-1.9	-2.3	-1.5	-0.1	0.3	0.3	-0.6	0.7	-1.5	-1.0	0.7	-1.0	0.7	0.3	126.7	11.5
-- Mixed layer depth (MLD) --																																												
MLD winter	-0.8	-0.5		-2.0		-0.3	-1.0			-0.8	-1.6	0.8	-0.5	1.4	-0.6	-0.1	-0.7	0.0	-0.4	-0.4	-0.7	-1.3	0.0	0.4	-0.1	0.5	0.6	-0.5	-1.8	1.1	0.1	0.0	1.0	-0.4	1.3	-0.1			1.5			-0.8	1.7	55.5	6.2
MLD spring	-1.0	-1.1		-0.9	-1.3	-1.8	-1.5	-1.8		-0.4	0.6	0.2	0.2	-0.4	-0.5	-0.3	-0.8	-0.8	-0.4	0.3	0.0	0.1	-0.5	-0.1	-1.0	-0.7	0.3	-0.3	-0.6	0.2	-0.6	0.9	0.4	0.3	0.9	0.0	0.2	1.3	0.6		-0.3	-0.5	-0.2	35.9	9.0
MLD summer	-0.1	0.3	0.0	-0.8	-0.1	-0.6	0.7	-0.9		-0.4	0.2	1.7	0.1	0.5	0.8	0.3	0.0	-0.6	-0.6	-0.2	0.2	0.4	-0.3	-0.9	-0.8	0.0	-0.9	0.7	-0.6	-0.5	0.6	-1.1	-0.2	-0.7	2.3	0.1	-0.6	0.4	0.2	-0.4	1.0	1.1	-0.7	23.9	6.5
MLD fall			0.1	-2.6		-1.4			0.2		0.2	-0.5	0.0	0.1	-0.5	-0.4	-0.1	0.1	0.4	-0.9	-1.0	0.9	-0.3	0.7	0.4	-0.5	0.2	-0.8	0.1	-1.3	0.6	0.9	0.1	1.2	0.8	-0.8	0.5	0.2	-0.2	-0.7	1.5	-0.7	-0.2	58.9	9.9
MLD annual	-0.8	-0.5	0.1	-1.3	-0.5	-1.0	-0.7	-1.3	0.2	-0.6	0.1	0.6	-0.1	0.3	-0.2	-0.1	-0.3	-0.4	-0.2	-0.3	-0.3	0.1	-0.3	0.0	-0.4	-0.2	0.1	-0.2	-0.7	-0.3	0.2	0.2	0.2	0.2	1.3	-0.2	0.1	0.6	0.3	-0.5	1.0	-0.1	0.0	43.6	16.5
-- Stratification (0-50m) --																																												
strat winter		-0.5		0.9		-0.6	-0.5			-0.7	-2.2	0.0	1.0	-1.2	2.2	0.8	0.1	-0.7	1.0	-0.1	0.2	0.5	0.2	-0.3	-0.3	0.0	-0.4	0.6	0.6	-0.2	-0.1	-0.8	-1.0	-0.7	-0.2	-0.6			-0.3			-0.4	0.3	0.008	0.001
strat spring	0.9	0.0	2.8	1.3	-1.1			-1.0		-1.5	0.0	0.2	0.6	0.2	2.5	-0.9	0.2	1.2	1.1	0.0	0.2	-1.0	-0.7	0.0	0.3	0.7	0.1	-0.2	1.0	-0.3	-0.1	-0.1	-0.4	-0.7	-0.2	-0.6	0.1	-1.2	-1.3		2.3	0.5	-0.5	0.015	0.008
strat summer			0.1	1.5	-0.5	-0.2	-2.5			-0.8	-0.5	-0.6	-1.0	1.3	0.4	-1.0	-0.1	0.6	1.0	-0.1	0.5	0.1	-0.5	-0.1	0.3	0.2	0.8	0.2	0.1	-0.6	-1.5	0.1	0.7	2.1	-0.9	-0.2	1.1	-1.3	-1.4	0.7	-0.2	0.5	0.7	0.054	0.009
strat fall		-2.3	-0.9	1.5		-1.4		4.7	-0.3	-0.1	1.7	-0.3	-0.8	-0.5	0.3	0.2	0.4	0.4	0.3	0.7	1.0	-0.9	0.3	-0.6	-0.2	1.0	0.0	1.2	-1.1	0.8	-0.6	-0.9	0.1	-0.4	-1.1	1.0	-0.1	-1.2	-0.7	0.4	0.9	1.3	-0.6	0.018	0.011
strat annual		-0.6	0.4	1.4	-0.7	-0.7	-1.2			-0.8	0.2	-0.2	-0.1	0.0	1.2	-0.3	0.2	0.5	0.8	0.1	0.4	-0.4	-0.2	-0.2	0.0	0.5	0.1	0.4	0.0	-0.1	-0.6	-0.4	0.0	0.2	-0.6	0.0	0.3	-1.2	-1.1	0.6	0.6	0.5	-0.1	0.024	0.02
-- Stratification (10-150m) --																																												
strat winter	-0.2	-1.4		0.7		-0.4	0.3			-0.6	-1.9	-1.6	0.6	0.2	-0.1	-0.2	-0.1	0.7	0.4	1.1	0.1	-0.4	-0.1	-0.7	-0.2	0.2	-0.4	0.7	-0.1	0.4	1.3	0.6	-1.5	1.1	-0.1	-1.1			-0.9			-0.7	0.7	0.009	0.001
strat spring	1.1	-0.7	1.2	1.7	-1.4						1.4	-1.0	0.5	-0.8	2.2	-0.5	0.0	1.0	1.2	0.2	0.3	-1.1	-1.7	-0.4	0.3	1.0	0.2	-0.2	0.7	0.7	-0.2	0.5	-0.4	-0.8	0.0	-1.1	0.3	-0.6	-1.3		2.6	0.7	-0.2	0.011	0.003
strat summer	1.7	-0.6	0.8	1.1	-0.4	-0.7	-1.2			-0.8	-0.4	-0.4	-0.9	0.6	0.8	-0.1	0.0	0.0	0.9	-0.4	1.0	-0.4	-0.5	-0.4	0.3	0.2	0.0	-0.6	0.6	0.5	-1.4	-0.2	1.2	1.1	-0.4	0.2	1.3	-0.6	-1.5	-0.2	0.2	0.4	-1.0	0.024	0.003
strat fall			1.4	0.7				0.5	-0.6	0.0	1.5	-0.8	-0.7	0.3	-0.2	-0.4	0.2	-0.1	0.0	0.8	1.3	-1.6	-0.2	0.0	-0.2	0.8	-0.1	1.1	-1.7	1.1	-0.3	0.0	0.3	0.3	-0.7	0.6	-0.3	-0.8	-0.9	0.8	1.3	1.8	-0.1	0.018	0.005
strat annual	1.0	-0.8	1.1	1.1	-0.8	-0.5				-0.5	0.7	-0.9	-0.1	0.2	0.8	-0.3	0.0	0.4	0.7	0.4	0.6	-1.0	-0.7	-0.4	0.1	0.6	-0.1	0.2	-0.3	0.7	-0.2	0.2	0.2	0.3	-0.3	-0.3	0.3	-0.7	-1.2	0.3	1.0	0.5	-0.2	0.016	0.007

Figure 19: Annual normalized anomalies of hydrographic parameters for Station 27. The different boxes from top to bottom are: vertically averaged temperature and salinity for different depth ranges, cold intermediate layer (CIL) properties, mixed layer depth (MLD), stratification between 0 and 50m, and stratification between 10 and 150m for the 4 seasons and annual average. The cells are color-coded according to Figure 2. Gray cells indicate an absence of data.

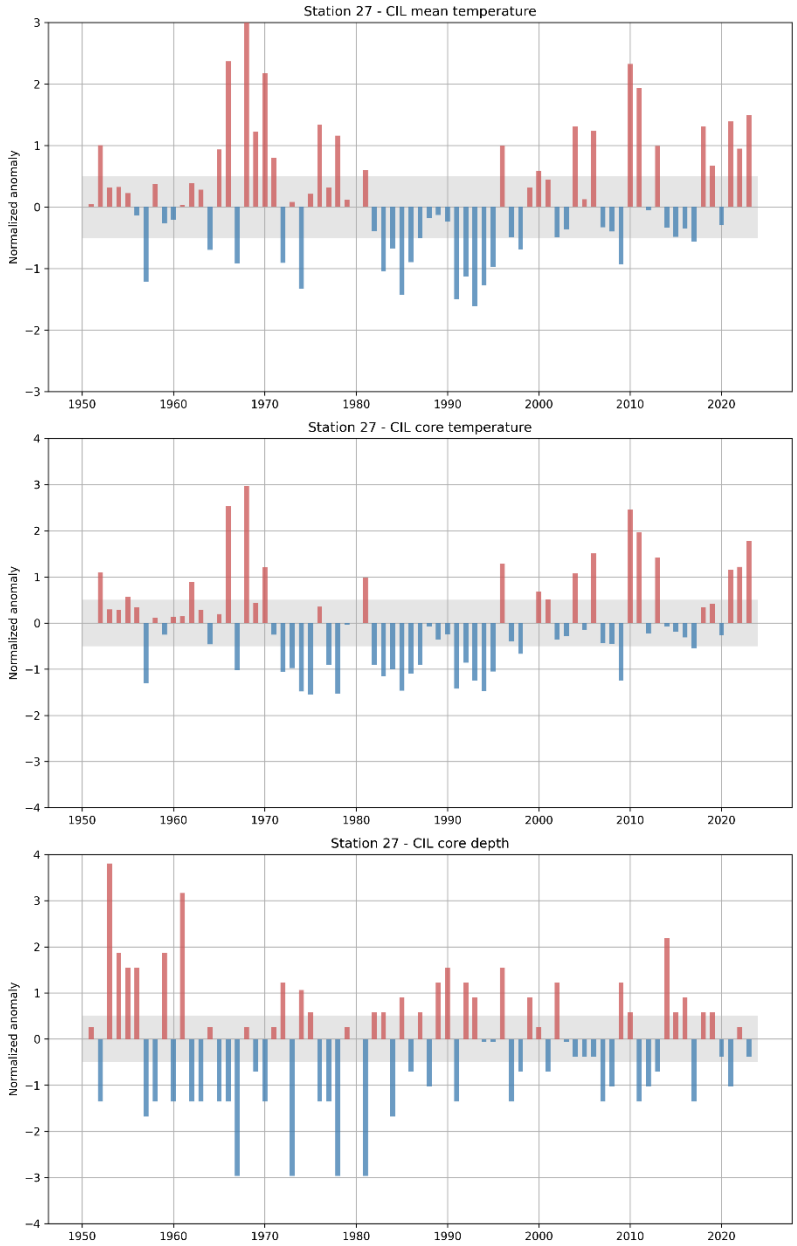

Figure 20: Normalized anomalies of summer (May-July) cold intermediate layer (CIL) statistics at Station 27 since 1951. Only years where at least 8 months of the years are sampled are presented. The top panel shows the CIL mean temperature, the middle the CIL core temperature (minimum temperature of the CIL) and the bottom panel the depth of the CIL core. Shaded gray areas represent the climatological (1991–2020) average ±0.5 SD range considered "normal". The CIL core temperature anomalies (middle panel) contribute to the NL climate index described in the summary (Figure 39).

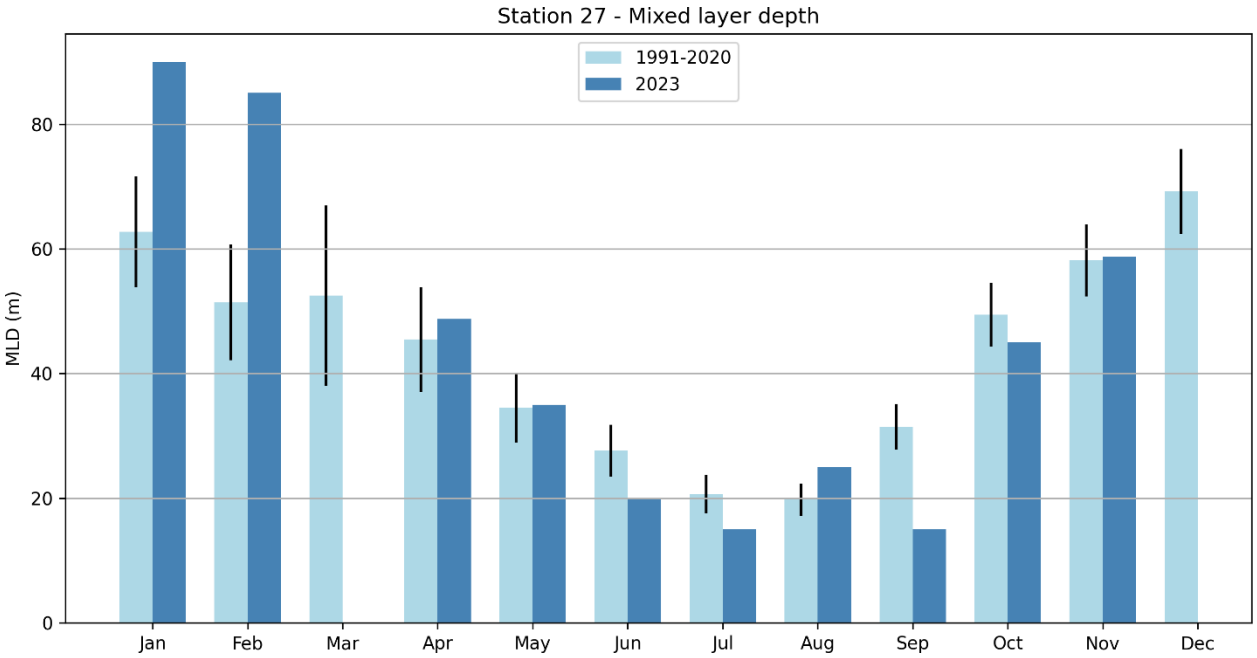

Figure 21: Bar plot of the monthly averaged mixed layer depth (MLD) at Station 27. The 1991–2020 climatology is shown in light blue while the update for 2023 is shown in dark blue. The black lines represent 0.5 SD above and below the climatology. No observations were made in March and in December.

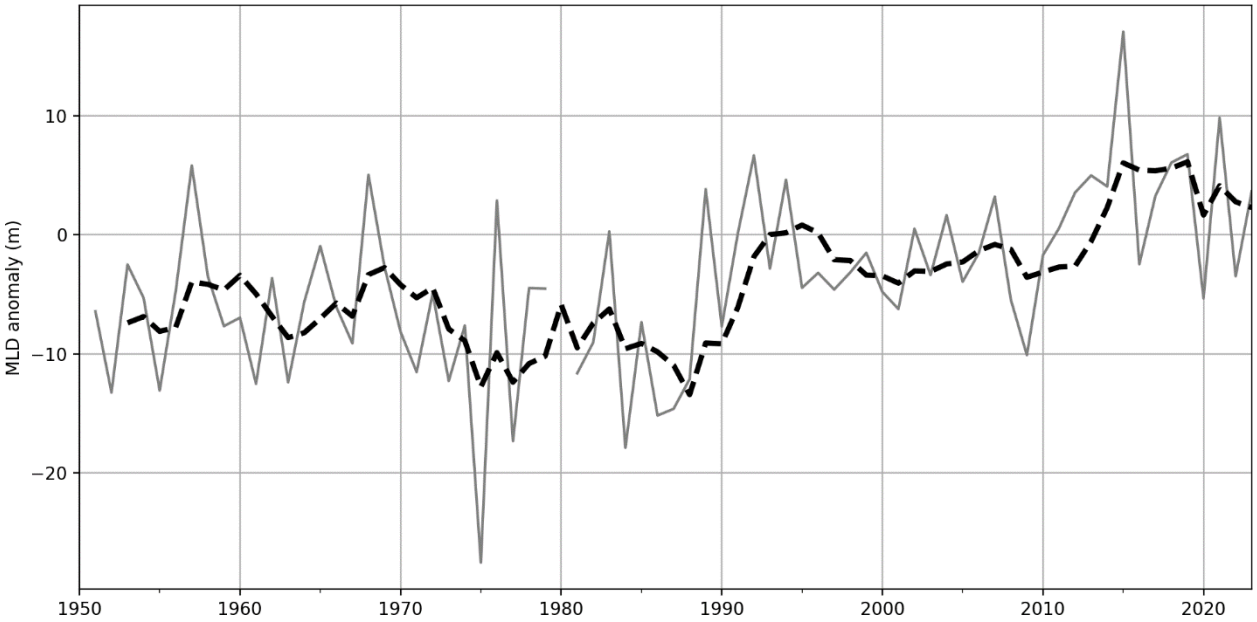

Figure 22: Time series of the annual mixed layer depth (MLD) average at Station 27 since 1950 (gray solid line) and its 5-year running mean (dashed-black line).

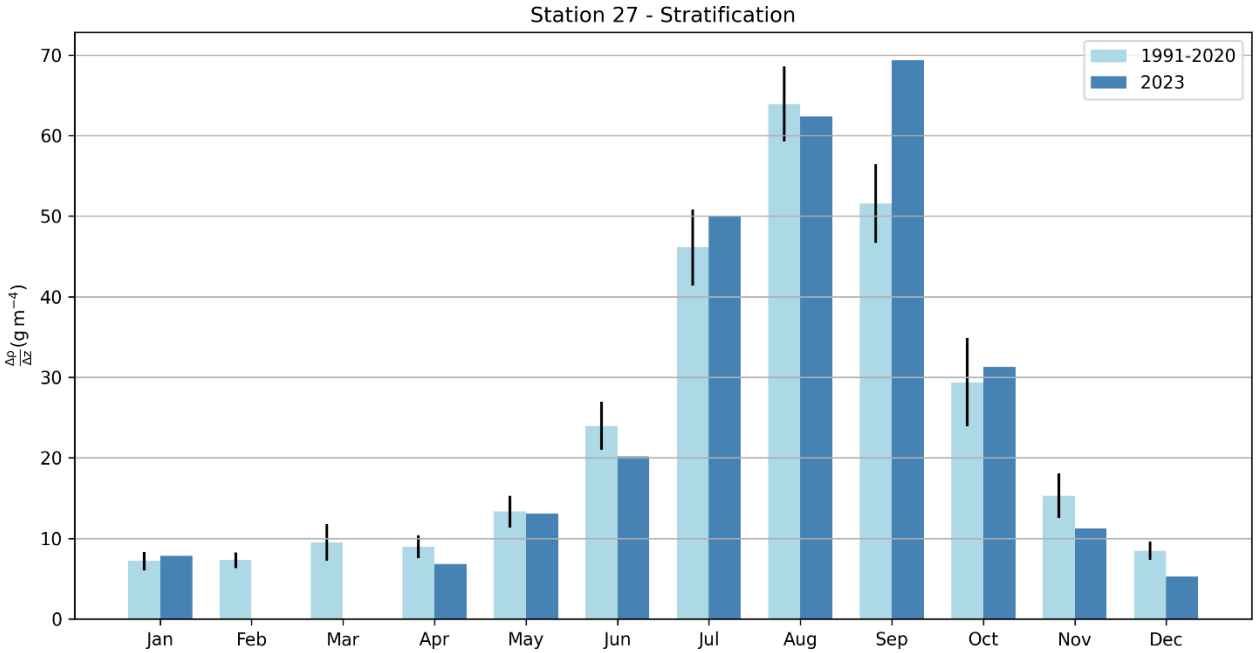

Figure 23: Bar plot of the monthly average stratification (defined as the density difference between 0 and 50 m) at Station 27. The 1991–2020 climatology is shown in light blue while the update for 2023 is shown in dark blue. The black lines represent 0.5 SD above and below the climatology. No observations were made in February and in March.

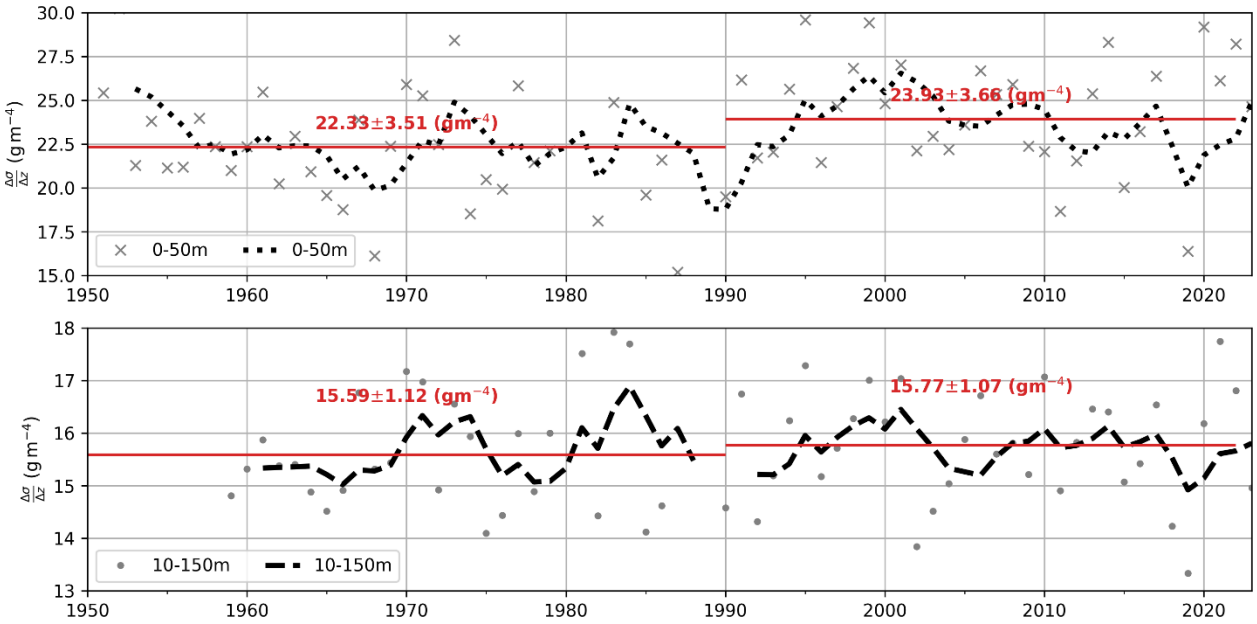

Figure 24. Time series of the annual average stratification at Station 27 between 0 and 50m (gray crosses; top) and 10 and 150m (gray dots; bottom) since 1950. For each panel, the 5-year running mean is shown as a dotted/dashed black line. Note the different vertical axis for the two panels. The average annual stratification from 1950 to 1990 and 1990 to 2023 is shown in red.

6.2 Standard hydrographic sections

In the early 1950s, several countries under the auspices of the International Commission for the Northwest Atlantic Fisheries (ICNAF) carried out systematic monitoring along hydrographic sections in NL waters. In 1976, ICNAF normalized a suite of oceanographic monitoring stations along sections in the Northwest Atlantic Ocean from Cape Cod (USA) to Egedesminde (West Greenland) (ICNAF, 1978). In 1998 under the AZMP, the Seal Island (SI), Bonavista Bay (BB), Flemish Cap (47°N) (FC) and Southeast Grand Bank (SEGB) historical stations were selected as core monitoring sections. The White Bay section (WB) continued to be sampled during the summer as a long time series ICNAF/NAFO section (see Figure 1).

Two ICNAF sections on the mid-Labrador Shelf, the Beachy Island (BI) and the Makkovik Bank (MB) sections, were selected to be sampled during the summer if survey time permitted. Starting in the spring of 2009, a section crossing south-west over St. Pierre Bank (SWSPB) and one crossing south-east over St. Pierre Bank (SESPB) were added to the AZMP surveys.

During the spring 2023 survey (April 3-17 onboard the CCGS Capt. Jacques Cartier), sections SWSPB, SEGB and FC were sampled. The summer 2023 survey (July 20 – August 1 onboard the CCGS John Cabot) sampled sections FC, BB and SI, while the fall 2023 survey (October 6-27 onboard the RRS Discovery) sampled sections SWSPB, SEGB, FC, BB and SI. In this manuscript we present the summer cross-sections of temperature and salinity and their anomalies along the SI, BB and FC sections to represent the vertical temperature and salinity structure across the NL Shelf during 2023.

6.2.1 Temperature and Salinity Variability

The water mass characteristics observed along the standard sections crossing the NL Shelf are typical of Arctic-origin waters with a subsurface temperature range of -1.5°C to 2°C and salinities from 31.5 to 33.5. Labrador Slope water flows southward along the shelf edge and into the Flemish Pass and Flemish Cap regions. With temperatures in the range of 3°C to 4°C and salinities in the range of 34 to 34.75, this water mass is generally warmer and saltier than the shelf waters. Surface temperatures normally warm to between 10°C and 12°C during late summer, while bottom temperatures remain <0°C over much of the Grand Banks, increasing to between 1°C and 3.5°C near the shelf edge below 200 m and in the deep troughs between the banks. In the deeper (>1,000 m) waters of the Flemish Pass and across the Flemish Cap, bottom temperatures generally range from 3°C to 4°C. In general, the near-surface water mass characteristics along the standard sections undergo seasonal modification from annual cycles of air-sea heat flux, wind-forced mixing, and the formation and melting of sea ice. These mechanisms cause intense vertical and horizontal temperature and salinity gradients, particularly along the frontal boundaries separating the shelf and slope water masses. The seasonal changes in the temperature and salinity fields along the Bonavista section are presented in Colbourne et al. (2015).

Summer temperature and salinity structures along the SI, BB and FC (47°N) are presented in Figure 25 to Figure 27. The dominant thermal feature along these sections is associated with the cold and relatively fresh CIL overlying the shelf. This water mass is separated from the warmer and denser water of the continental slope region by strong temperature and salinity fronts. The cross-sectional area of the CIL is bounded by the 0°C isotherm and highlighted as a thick black contour in the temperature panels. The CIL parameters are regarded as robust indicators of ocean climate conditions on the eastern Canadian Continental Shelf. While the CIL area undergoes significant seasonal variability, the changes are highly coherent from the Labrador Shelf to the Grand Banks. The CIL remains present throughout most of the summer until it gradually decays during the fall as increasing winds and storm episodes deepen the surface mixed layer.

The analysis of summer section observations gives an interesting perspective on the warm SSTs observed in 2023. All sections show the presence of a very thin (<15m) surface layer with temperature anomalies reaching +3.5°C above normal. Below this thin surface layer, a negative anomaly indicates that the top of the CIL was shallower than normal. While the temperature of the CIL was approximately normal, the CIL extended further offshore on the SI section (indicated by a negative anomaly at the shelf break in Figure 25, bottom left). The CIL remained closer to the shore on the BB section (indicated by a positive anomaly on the offshore part of the shelf in Figure 26, bottom left). The latter anomaly resembles the intrusion of warm and salty slope water on the shelf.

The corresponding salinity cross sections show a relatively fresh (<33) upper water layer over the shelf with sources from Arctic outflow on the Labrador Shelf, in contrast to the saltier Labrador Slope water further offshore with values >34 (Figure 25 to Figure 27, right panels). In 2023, salinities were mostly fresh across all sections, except for a thin surface near-shore lens in the nearshore area of SI section and for the warmer intrusion on the shelf at BB section.

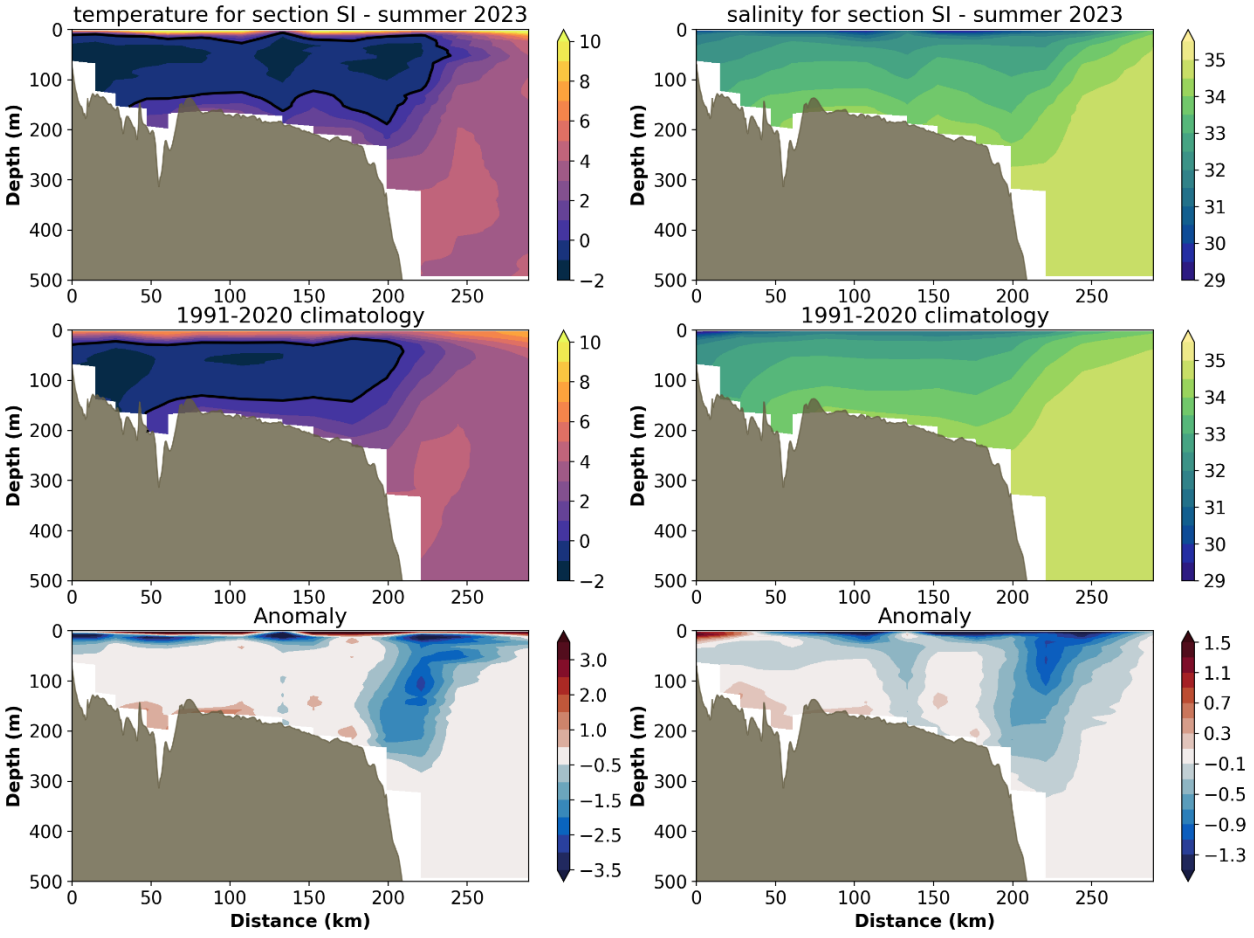

Figure 25: Contours of temperature (°C), left column, and salinity, right column, during summer 2023 (top row), with climatological averages (middle row) for the Seal Island (SI) hydrographic section (see map Figure 1 for location). Their respective anomalies for 2023 are plotted in the bottom panels.

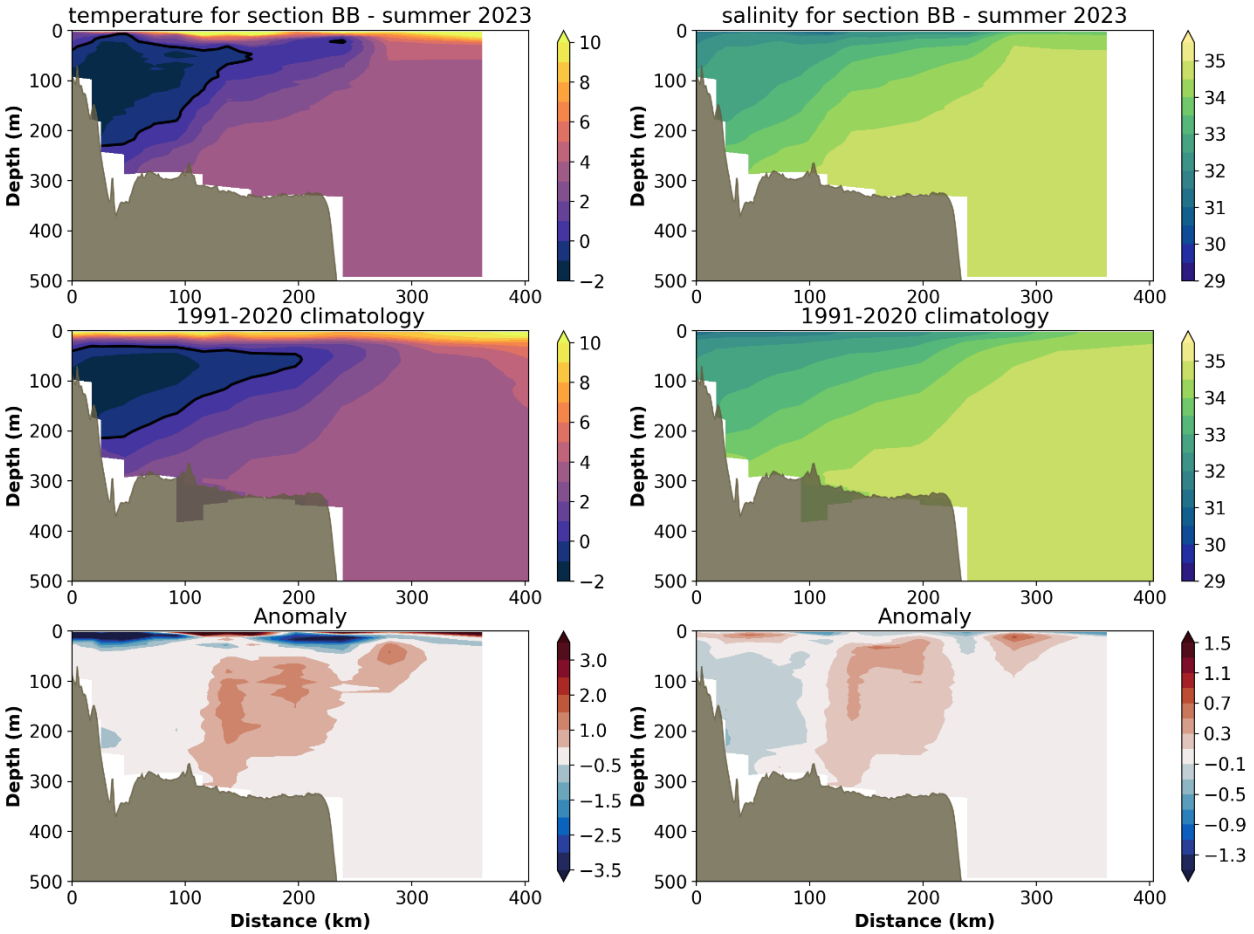

Figure 26: Same as in Figure 25, but for the Bonavista (BB) hydrographic section (see map Figure 1 for location).

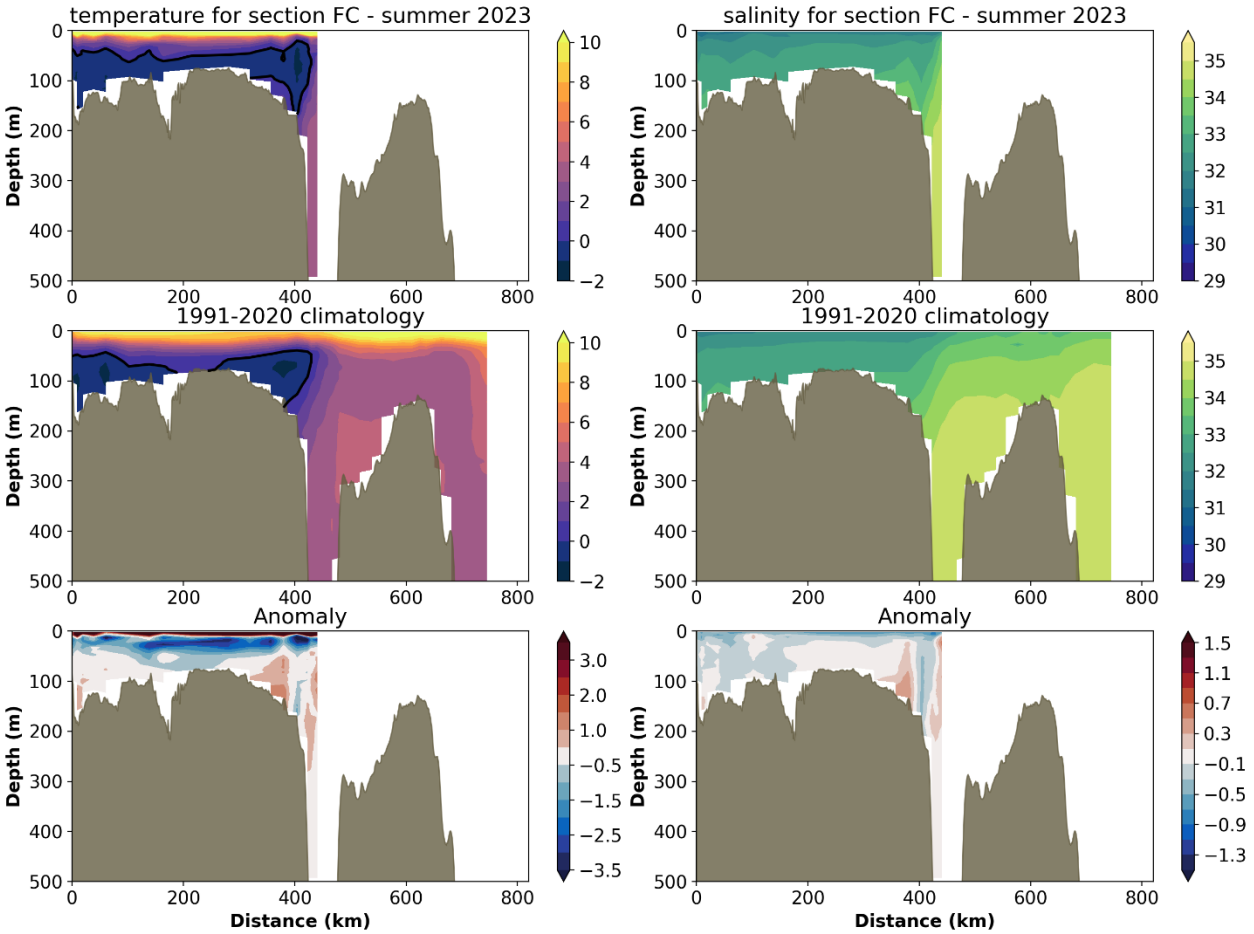

Figure 27: Same as in Figure 25, but for the Flemish Cap (FC) hydrographic section (see map Figure 1 for location).

6.2.2 Cold Intermediate Layer Variability

New for this year, two different methodologies were used to select temperature profiles used to determine the summer CIL area and core temperature. First, for years when AZMP trips were successfully completed (typically after 1995), profiles associated with the trip were isolated using the "STATION_NAME" variable from CASTS. Second, for years when no AZMP trip was completed or properly labeled in the metadata (prior to 1995, and during 2022 for example), a 0.25° radius circle surrounding the nominal position of each standardized station on the section was used to isolate all temperature profiles from CASTS taken between June and August. Each of the profiles was then vertically interpolated to fill any vertical gap and averaged into a single profile per station. After these profiles were identified (i.e., based on station names or by a search in a radius around the nominal location of the station), the procedure for calculating the CIL metrics remains the same.

The climatology of each section was determined by averaging all annual summer temperature profile for each station between 1991 and 2020. Then, for each individual year where the CIL metrics are derived, any missing profile from a station in a given year was filled with the climatological profile from that station. After visual inspection, and based on expert judgement, yearly CIL area and core temperature were set to NaNs if the sampling did not properly resolve the CIL (e.g. if too many stations are missing in the inshore part of the section). If the sampling was deemed sufficient, temperature measurements between stations were then horizontally interpolated to a constant 1km grid cell size and depth-averaged into 5m bins. The number of grid cells below 0°C was then multiplied by the now-constant grid size to determine the CIL area. This was repeated between 1980 and 2023.

Statistics of summer CIL anomalies (CIL area, CIL core temperature and CIL core depth) for the three sections discussed above (SI, BB and FC) are presented in a scorecard in Figure 28. The years where data are re-constructed using profiles collected between June and August are identified in the bottom row of the scorecards with small black dots. Because this method uses the average between June and August, the core CIL temperature is not derived. The climatological average cross-sectional areas of the summer CIL along these sections are 24±6 km^2, 24±7 km^2 and 20±5 km^2, respectively. The averaged anomalies of the CIL cross-sectional area for these three sections are summarized in Figure 29 as a time series going back to 1950. In general, the summer CIL has been predominantly warmer and smaller than average since the mid-1990s, with a cold phase extending from about 2012 or 2014 to 2017. However, the most striking aspect of this long time series is the warm conditions that prevailed in the mid-1960s and mid-1970s, followed by a cold period that lasted from the mid-1980s to the mid-1990s.

In 2023, the CIL area was near-normal (+0.6 SD for SI and FC, and -0.6 SD for BB). Averaged together, this leads to a normal CIL subindex of +0.2 SD for 2023 (Figure 29). The normal CIL is likely the result of the relatively cold winter that occurred in Labrador and in the Eastern Arctic in 2023 and contrasts with near-record warm SSTs. This is because the summer CIL is a remnant of the previous winter's conditions that are advected from the north during the rest of the year, and its properties are isolated from the summer atmospheric warming.

	80	81	82	83	84	85	86	87	88	89	90	91	92	93	94	95	96	97	98	99
-- Seal Island section --																				
CIL area (km^2)	0.6	-0.4	0.9	0.6	2.0	1.6	-0.3	1.1	-0.3		2.3	1.9	0.9			-0.5	0.3	-0.6		-0.3
CIL core (°C)																1.1	-0.7	-1.0		0.7
June-Aug. ave.	•	•	•	•	•	•	•	•	•	•	•	•	•							
-- Bonavista section --																				
CIL area (km^2)	-0.6	-0.5	0.3	1.8	3.1	2.2	-0.3	-0.7	0.7	0.0	2.4	2.2	0.7			-0.4	0.1	-0.5	0.1	-0.4
CIL core (°C)																0.7	-0.1			
June-Aug. ave.	•	•	•	•	•	•	•	•	•	•	•	•	•					•	•	•
-- Flemish Cap section --																				
CIL area (km^2)	-0.2	-1.2	0.3	1.3	2.4	1.7	1.3	0.2	0.7	0.7	0.7	2.1	1.1			0.1	-0.2	0.9	0.1	-0.5
CIL core (°C)																1.0	0.5			1.0
June-Aug. ave.	•	•	•	•	•	•	•	•	•	•	•	•	•					•	•	

	00	01	02	03	04	05	06	07	08	09	10	11	12	13	14	15	16	17	18	19	20	21	22	23	$\overline{x}$	sd
-- Seal Island section --																										
CIL area (km^2)	0.9	-0.4	-0.2	0.1	-1.0	-0.4	-0.3	-0.3	0.2	1.2	-0.8	-1.2	0.1	-0.4	0.9	1.1	-0.6	1.4	-1.6	-0.8	-1.7	-2.0		0.6	24.1	5.8
CIL core (°C)		0.7	-1.0			0.8	0.7	0.0	-1.1	-0.7	1.1	1.5	-0.9	1.0	-1.5	-0.2	-0.9	-1.1	1.1	-1.0	1.5	1.5		-0.3	-1.5	0.1
June-Aug. ave.	•			•	•																					
-- Bonavista section --																										
CIL area (km^2)	0.5	-0.9	-0.1	-0.2	0.0	-0.6	-0.8	-0.1	-0.8	0.5	-0.2	-2.2	-0.2	-0.6	1.9	1.0	0.7	0.5	-0.4	-1.0	-1.2	-1.5	-0.5	-0.6	23.4	7.1
CIL core (°C)				-0.6	0.7	0.8	1.0	0.7	-0.5	-1.0	0.6	2.3	-1.1	0.1	-1.3	-1.4	-1.0	-1.2	0.5	0.1	0.9	1.3		1.4	-1.5	0.1
June-Aug. ave.	•	•	•																				•			
-- Flemish Cap section --																										
CIL area (km^2)	-0.5	0.3	0.1	-0.2	-0.8	0.2	-1.3	0.5	-0.4	1.4	-2.3	-1.9	1.0	-1.0	1.4	0.6	0.5	0.3	-0.9	-0.3	-1.2	-2.6	-0.7	0.6	20.0	4.8
CIL core (°C)				0.0	1.1	-0.2			-0.3	-1.1	1.7	1.3	-1.3	1.6	-1.1	-1.3	-0.6	-0.2	-0.7	-0.2	-1.0	-0.6		0.5	-1.4	0.2
June-Aug. ave.	•	•	•				•	•															•			

Figure 28: Scorecards of the cold intermediate layer (CIL) summer statistics along the Seal Island, Bonavista and Flemish Cap hydrographic sections. The CIL area is defined as all water below 0°C (see black contours in Figure 25 to Figure 27) and the CIL core temperature as the minimum temperature of the CIL. Color codes for the CIL area have been reversed (positive is blue and negative is red) because a large CIL represents cold conditions, and vice-versa. Grayed cells indicate an absence of data. When possible, the AZMP station labeled in the data files are used, but in some instances (indicated here by black dots in the last row of each table) the average June-August profile of all available casts in at 0.25°x0.25° (lat x lon) box around the nominal station locations are used to reconstruct the section.

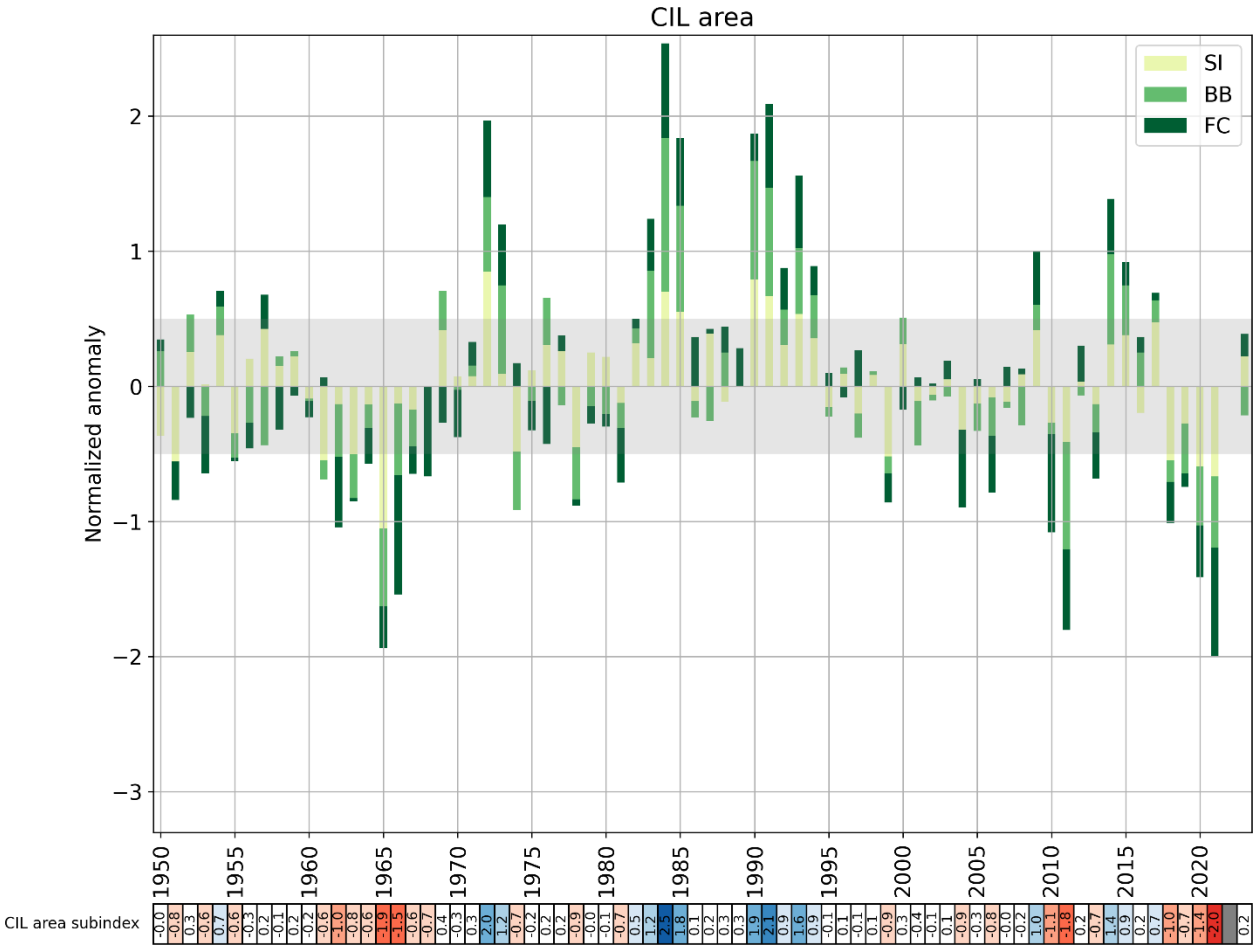

Figure 29: Normalized anomalies of the mean CIL area for hydrographic sections Seal Island (SI), Bonavista Bay (BB) and Flemish Cap (FC). This time series corresponds to the average of the three sections, in which the contribution of each section is represented (values for each separate section since 1980 can be found in Figure 28). The shaded area corresponds to the 1991–2020 average ±0.5 SD, a range considered "normal". The numerical values of this time series are reported in a color-coded scorecard at the bottom of the figure. Here negative anomalies (generally corresponding to warmer conditions) are colored red and positive anomalies blue. Years with no data present are colored grey. This time series is one component of the NL climate index (Figure 39).

6.3 Bottom observations in NAFO sub-areas

Canada has been conducting stratified random bottom trawl surveys in NAFO Sub-areas 2 and 3 on the NL Shelf since 1971. Areas within each division, with a selected depth range, were divided into strata, and the number of fishing stations in an individual stratum was based on an area-weighted proportional allocation (Doubleday, 1981). Temperature profiles (and since 1990, salinity profiles) are available for most fishing sets in each stratum. These surveys provide large spatial-scale oceanographic data sets for the Newfoundland and Labrador Shelf. NAFO Subdivision 3Ps on the Newfoundland south coast and Divisions 3LNO on the Grand Banks are surveyed in the spring, and Divisions 2HJ off Labrador in the north, 3KL off eastern Newfoundland, and 3NO on the southern Grand Bank are surveyed in the fall. The hydrographic data collected on these surveys are routinely used to assess the spatial and temporal variability in the thermal habitat of several fish and invertebrate species. Many products based on the data are used to characterize the oceanographic bottom habitat. Among these are contour maps of the bottom temperatures and their anomalies, the area of the bottom covered by water in various temperature ranges, etc. In addition, species-specific 'thermal habitat' indices are often used in marine resource assessments for snow crab and northern shrimp.

Maps and statistics of bottom temperature and salinity observations, originally introduced by Cyr et al. (2019), are now taken from the Canadian Atlantic Bottom Observations of Temperature-Salinity (CABOTS) data product (Coyne & Cyr, 2024). This methodology is recalled here. First, all available seasonal (April-June for spring, July-September for summer – not shown in this report –, and October-December for fall) temperature and salinity profiles are taken from the CASTS dataset (Coyne et al., 2023). A 0.05° latitude by 0.05° longitude grid is defined using GEBCO_2023 gridded bathymetry (GEBCO Compilation Group, 2023). Cycling over each grid cell, all profile measurements taken within 25m of the recorded depth and less than 2° distance from the point of interpolation were isolated. Profile measurements with land barriers between them and the point of interpolation were not considered. If three or more profile measurements met all of these requirements, inverse distance-weighted interpolation with adaptive power determination (Lu & Wong, 2008) was then used to determine the associated grid cell value. Lastly, bottom observations were restricted between 10m and 1,000m, that is below the surface and shallower than down the continental slope where the data coverage is much lower. This procedure was performed for all years and all seasons between 1980 and 2023, from which the climatological seasonal averages (averages over 1991-2020) were derived.

Before calculating statistics on bottom observations (e.g. mean temperature or salinity, area of the sea floor covered by a certain temperature range, etc.), missing observations on the annual maps (for example when no observations are available for a specific year) are filled with the climatology. This allows us to calculate these metrics on the same seafloor area (especially important for areas covered by a certain temperature range). We note that this method is conservative as it will tend to pull anomalies towards zero. As part of CABOTS, we provide the percentage area of each NAFO division covered so users can assess the confidence of the observations for a certain year and season. Annual anomalies are calculated as the difference between annual observations and climatology.

6.3.1 Spring Conditions

Maps of spring climatological temperature and salinity, together with 2023 observations and anomalies for NAFO divisions 3LNOPs, are presented in Figure 30 and Figure 31, respectively (with the center panel showing also the station occupation coverage). In 2023, the coverage in 3Ps was not sufficient to derive further statistics. Since 2019, we were only capable of deriving spring bottom observations for the entire region in 2022. Due to the COVID-19 pandemic, the area was not surveyed during the spring of 2020, while in 2021 only the division 3Ps was properly sampled.

Bottom temperatures are generally colder in the northern part of the Grand Banks (3L) and warmer in the shallower southern part of the Grand Banks (3NO) and along the slopes (Figure 30, left panel). In 2023, bottom temperatures were slightly warmer than average in 3L and in the eastern part of 3Ps, and colder than average in 3NO. Spring bottom salinities in 3LNO generally range from 32 to 33 over the central Grand Bank, and from 33 to 35 closer to the shelf edge (Figure 31, left panel). In 3Ps, salinities are between 32 and 33 over shallower areas and above 34.5 in the Laurentian Channel. In 2023, salinities were close to normal in most of the Grand Banks, except slightly salty in the northeast part of 3L and slightly fresh in 3Ps and in the southwest part of 3O.

Climate indices based on normalized spring bottom temperature anomalies (mean temperature and temperature in areas shallower than 200 m), as well as the area of the sea floor covered by water above 2°C and below 0°C between 1980 and 2023 are shown in a color-coded scorecard in Figure 32. Overall, the colors visually highlight two contrasting periods of this time series: the cold period of the late 1980s / early 1990s (mostly blue cells) and the warm period of the early 2010s (mostly red cells). This warm period lasted between 2010 and 2013 (2011 being the warmest at 2.2 SD above normal in 3LNO) before returning towards to normal values between 2015 and 2019 (2014 was slightly cold). Between 2015 and 2019 the bottom area that was covered by <0°C water was also normal. While no information was available for 2020, 2021 and 2022 were the third and second warmest years in 3LNO, respectively. Bottom temperatures were however back to normal in 3LNO in 2023.

Division 3Ps bottom temperatures exhibit some similarities to those from 3LNO, with two periods of warm years, 1999–2000 and 2005–06, separated by a colder period (2003 is the coldest year on record since 1991 at -2.1 SD). With the exception of 2017 (which was normal) and 2020 (no data), all years between 2010 and 2022 were warmer than normal. 2021 and 2022 are the warmest years on record since 1980 at +2.5 SD and +2.6 SD, respectively. 2022 also established a new record for the area of the seafloor covered with water >2°C at +2.9 SD, beating the 2021 record of +2.3 SD. While spatial data suggest that the anomalies for 2023 were not as warm (Figure 30), bottom statistics were omitted for 3Ps because the coverage was very sparse in the deeper portion of the Division (Figure 32).

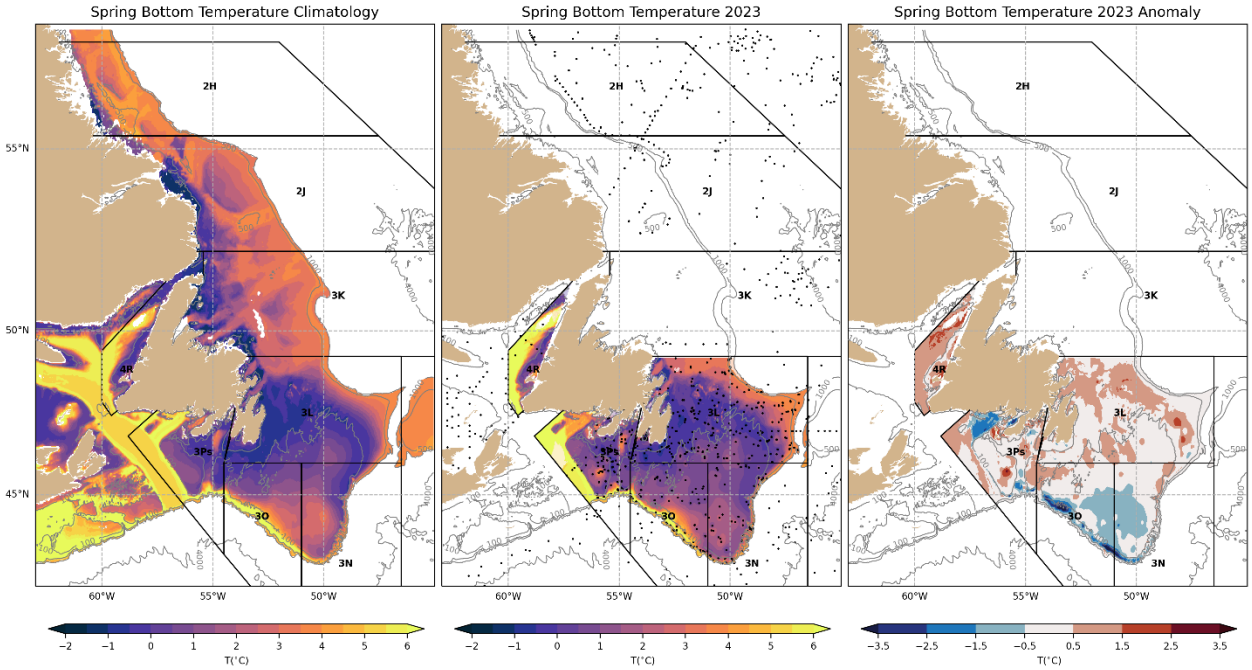

Figure 30: Maps of the climatological (1991–2020) mean spring bottom temperature (left), and spring 2023 bottom temperature (center) and anomalies (right) for NAFO Divisions 3LNOPs only. The location of observations used to derive the temperature field is shown as black dots in the center panel. When applicable, the portions of the shelf missing bottom temperatures were filled with the climatology (see methodology) and are left semi-transparent.

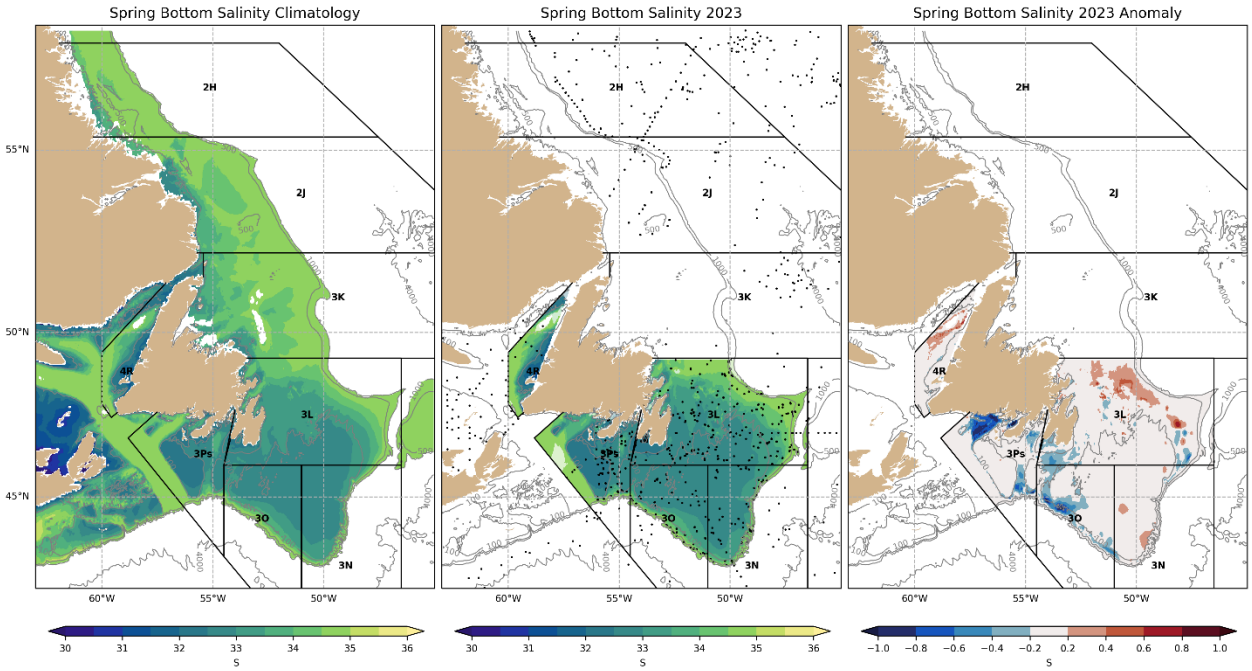

Figure 31: Maps of the climatological (1991–2020) mean spring bottom salinity (left), and spring 2023 bottom salinity (center) and anomalies (right) for NAFO Divisions 3LNOPs only. The location of observations used to derive the salinity field is shown as black dots in the center panel. When applicable, the portions of the shelf where missing bottom salinities were filled with the climatology (see methodology) are left semi-transparent.

-- NAFO division 3LNO --

	80	81	82	83	84	85	86	87	88	89	90	91	92	93	94	95	96	97	98	99	00	01
T_{bot}	-0.2	1.1	-0.9	1.2	-1.0	-2.0	-1.6	-0.7	-0.5	-1.6	-2.1	-2.1	-1.8	-1.4	-1.6	-0.7	-0.2	-0.9	0.5	1.2	0.5	-0.1
$T_{bot<200m}$	-0.1	1.4	-0.6	1.8	-0.7	-1.7	-1.6	-0.5	-0.2	-1.2	-2.1	-2.0	-1.7	-1.2	-1.5	-0.8	-0.1	-1.0	0.6	1.4	0.5	-0.2
Area $_{>2°C}$	0.0	1.0	-1.7	1.1	-0.7	-2.2	-1.6	-0.7	-0.9	-2.1	-2.1	-1.7	-1.9	-1.3	-1.2	-0.4	-0.5	-0.9	0.8	1.2	0.1	-0.6
Area $_{<0°C}$	-0.1	-0.8	0.1	0.0	1.0	1.5	1.4	0.6	0.5	1.2	1.7	2.1	1.5	1.4	1.3	0.8	0.0	1.0	-0.5	-1.0	-0.1	0.1
% Cov	96	96	95	95	93	95	96	95	94	93	97	98	98	97	97	99	99	98	98	97	98	98

	02	03	04	05	06	07	08	09	10	11	12	13	14	15	16	17	18	19	20	21	22	23	$\bar{x}$	sd
T_{bot}	-0.3	-1.1	1.3	0.6	0.4	0.2	0.1	0.4	0.8	2.2	1.3	0.9	-0.5	-0.1	-0.1	-0.1	0.3	0.2		1.4	1.5	0.3	1.1	0.5
$T_{bot<200m}$	-0.2	-1.3	1.3	0.6	0.3	0.2	-0.1	0.4	0.8	2.2	1.4	0.9	-0.6	-0.1	-0.1	-0.2	0.3	0.1		1.4	1.5	0.1	0.7	0.6
Area $_{>2°C}$	-0.4	-1.2	1.8	0.6	0.0	0.1	0.4	0.5	0.2	2.6	1.2	0.6	-0.4	0.1	0.1	-0.3	0.1	0.3		0.6	1.0	-0.3	76.5	22.5
Area $_{<0°C}$	0.2	1.0	-1.5	-0.6	-1.5	-0.1	0.1	0.3	-1.5	-2.1	-0.8	-0.9	0.7	0.3	0.1	0.1	-0.2	-0.1		-2.5	-1.3	-0.8	87.3	34.2
% Cov	98	99	99	97	96	98	99	99	98	98	99	99	99	98	98	99	97	99	42	88	98	98		

-- NAFO division 3Ps --

	80	81	82	83	84	85	86	87	88	89	90	91	92	93	94	95	96	97	98	99	00	01
T_{bot}	1.0		-0.8	0.1	1.5									-0.9	-1.4	-0.9	-0.3	-1.2	-0.5	0.5	0.9	-1.2
$T_{bot<200m}$	0.7		-0.8	0.4	1.6									-1.6	-1.6	-1.0	-0.2	-1.2	0.1	0.9	1.1	-0.9
Area $_{>2°C}$	-0.1		-0.5	0.2	1.1									-1.4	-0.8	-1.3	-0.4	-1.3	-0.3	1.0	1.1	-1.1
Area $_{<0°C}$	-0.8		0.3	-0.4	-0.9									1.1	1.4	1.0	-0.4	1.2	0.0	-0.5	-0.7	0.9
% Cov	80	79	93	94	87	60	63	58	70	51	57	58	72	96	97	97	97	98	97	98	98	97

	02	03	04	05	06	07	08	09	10	11	12	13	14	15	16	17	18	19	20	21	22	23	$\bar{x}$	sd
T_{bot}	-0.7	-2.1	-0.2	0.6	0.5	-1.4	-0.6	0.1	0.5	1.2	1.3	1.1	0.5	0.5	1.8	0.1	1.2	0.7		2.5	2.6		2.6	0.5
$T_{bot<200m}$	-0.6	-2.1	0.0	1.0	0.9	-0.9	-0.4	0.3	0.4	1.5	1.1	1.2	0.1	0.2	1.3	-0.5	0.8	0.0		1.9	2.0		1.7	0.6
Area $_{>2°C}$	-0.7	-1.9	0.0	0.9	0.5	-1.3	-0.2	0.1	0.1	1.5	1.5	1.0	0.5	0.3	1.5	-0.4	1.0	0.0		2.3	2.9		36.7	5.9
Area $_{<0°C}$	0.6	2.8	-0.8	-1.0	-1.0	0.7	0.5	0.1	-0.8	-1.5	-1.1	-1.4	0.0	-0.3	-0.8	0.1	-0.5	0.3		-1.5	-1.4		9.3	5.4
% Cov	97	97	97	97	91	98	97	99	98	98	99	98	98	98	98	98	97	98	0	98	98	93		

Figure 32: Scorecards of normalized spring bottom temperature anomalies (mean temperature, mean temperature for area shallower than 200 m, and area of sea floor covered by water above 2°C and below 0°C, respectively) for 3LNO and 3Ps.

6.3.2 Fall Conditions

Maps of fall climatological temperature and salinity, together with 2023 observations and anomalies for NAFO Divisions 2HJ3KLNO, are presented in Figure 33 and Figure 34 respectively (see center panel for station occupation coverage). Bottom temperatures are generally cold (<0°C) in shallow areas of 2HJ3KLNO and warmer on the slopes and the different troughs, and on the southern areas of the Grand Banks that lie at depths shallower than the CIL (e.g. <50m). In 2023, anomalies are generally cold along the Labrador coast where the CIL hugs the seafloor, as well as near the tail of the Grand Banks (Division 3N). Scattered areas of warmer anomalies are found near the NL shelf break and in Division 3O of the Grand Banks.

Bottom salinities in divisions 2HJ and 3K generally display an inshore-offshore gradient between <33 close to the coast and 34 to 35 at the shelf edge (Figure 34, left panel). The Grand Banks (3LNO) bottom salinities range from <33 to 35, with the lowest values on the southeast shoal. In 2023 the bottom salinities were close to normal in most of the region, although they followed similar patterns to the temperature with some fresh anomalies near the coast and salty anomalies near the shelf break. There is a large positive temperature and salinity anomaly in the north of 2H, but it will not be emphasized in this report because it seems driven by one or two data points only and it may be an artefact of the interpolation method.

Normalized bottom temperature anomalies (mean temperature and temperature in areas shallower than 200 m), as well as area of the sea floor covered by water above 2°C and below 1°C between 1980 and 2022 are shown in a color-coded scorecard in Figure 35. A clear cold period is visible from the early 1980s to the mid-1990s, with the coldest anomalies reached in NAFO Divisions 2J and 3K. This was followed by a warmer period peaking in 2010 and 2011, the warmest years on records for these divisions. After a slight return to normal-to-cold anomalies between 2012 and 2017, bottom temperatures have been generally above or close to normal since. In 2023, bottom temperatures were above average in 2H with the third warmest anomaly (+1.7 SD) after 2010 and 2011 (tied at +1.8 SD). While slightly above normal in 3K (+0.7 SD), bottom temperatures were normal in 2J and 3LNO.

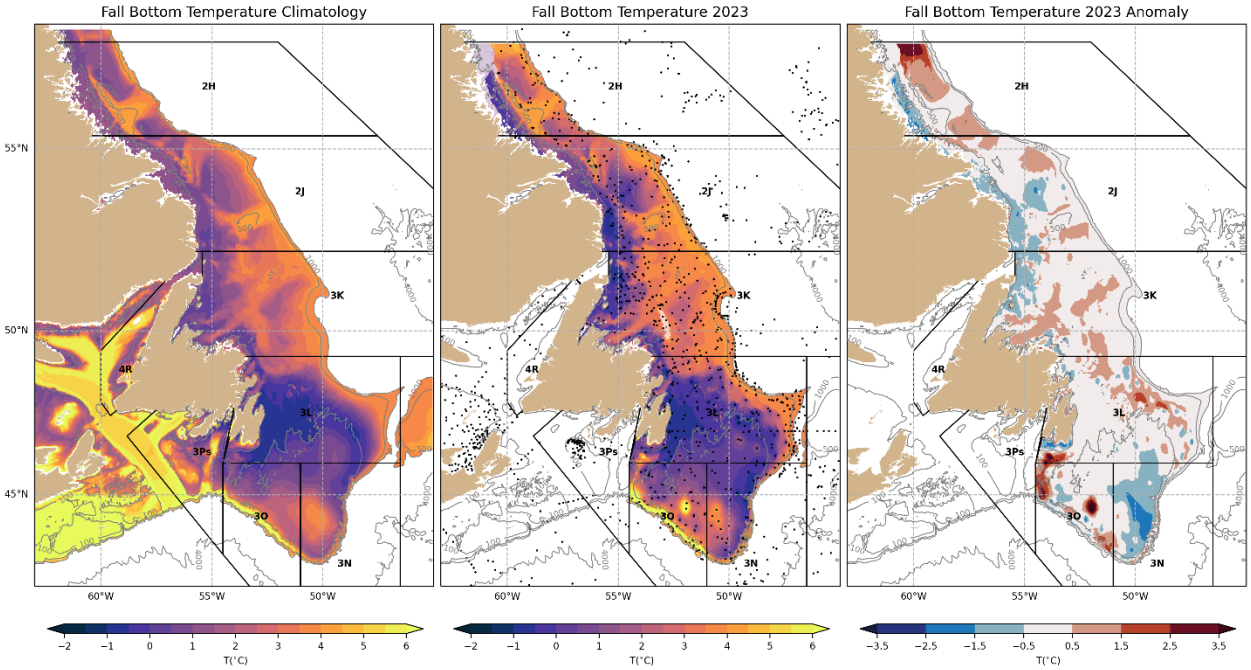

Figure 33: Maps of the climatological (1991–2020) mean fall bottom temperature (left), and fall 2023 bottom temperature (center) and anomalies (right) for NAFO Divisions 2HJ3KLNO only. The location of observations used to derive the temperature field is shown as black dots in the center panel. When applicable, the portions of the shelf where missing bottom temperatures were filled with the climatology (see methodology) are left semi-transparent.

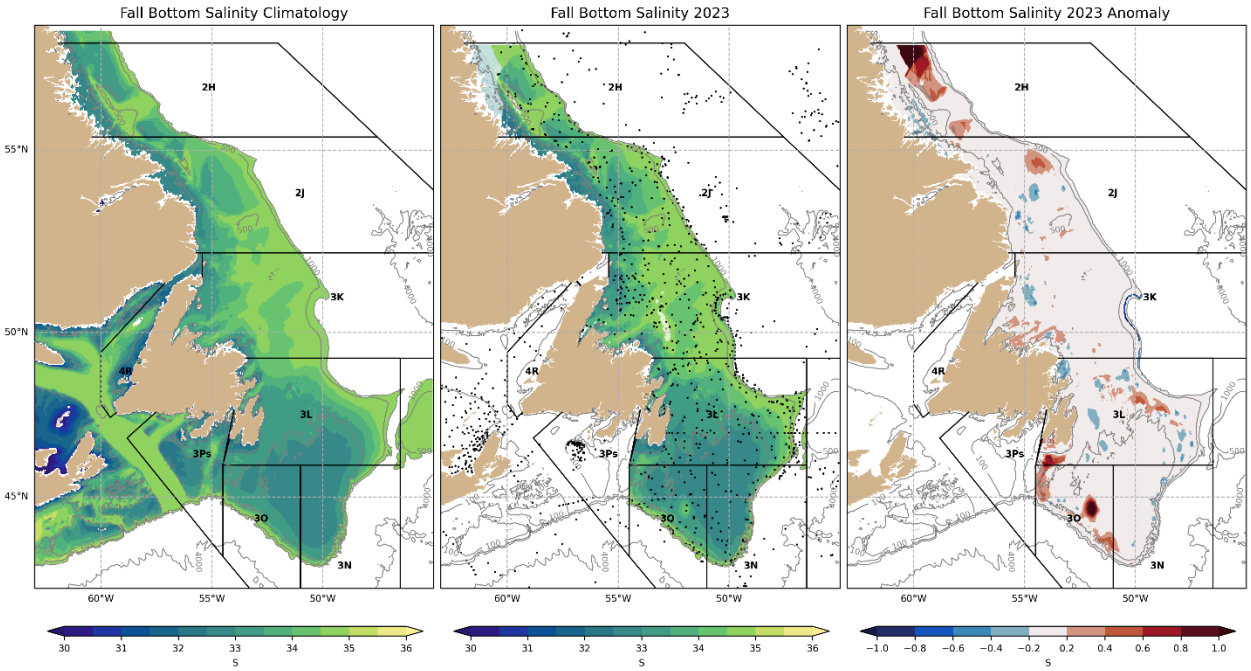

Figure 34: Maps of the climatological (1991–2020) mean fall bottom salinity (left), and fall 2023 bottom salinity (center) and anomalies (right) for NAFO Divisions 2HJ3KLNO only. The location of observations used to derive the salinity field is shown as black dots in the center panel. When applicable, the portions of the shelf where missing bottom salinities were filled with the climatology (see methodology) are left semi-transparent.

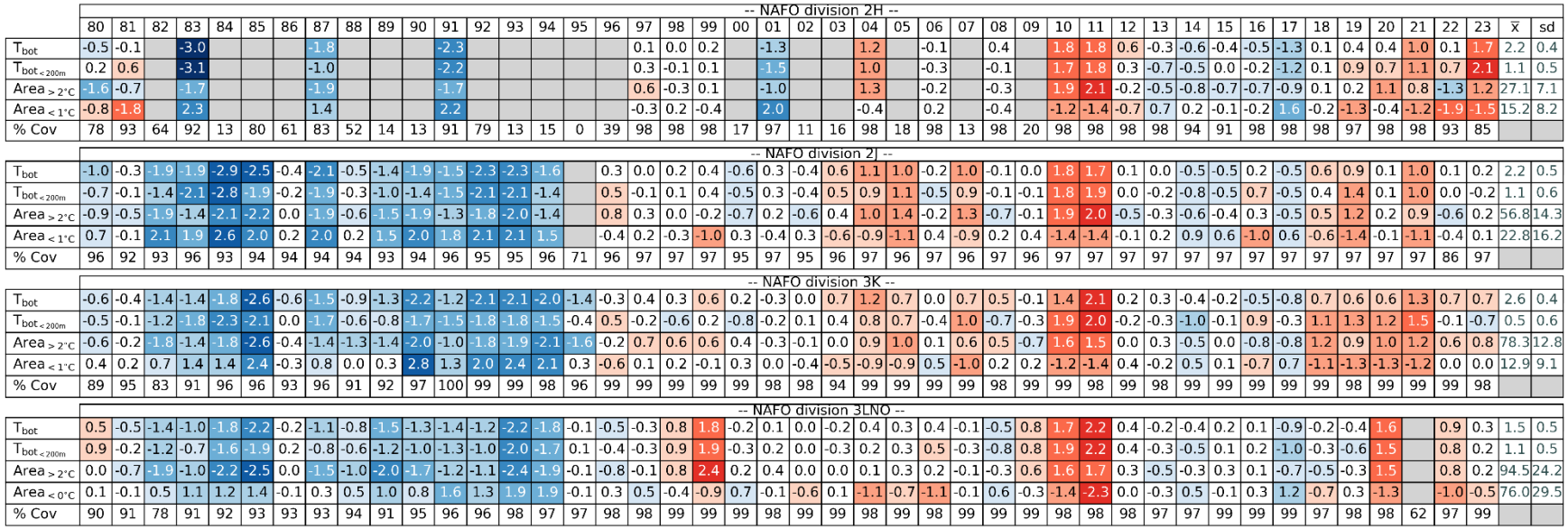

Figure 35: Scorecards of normalized fall bottom temperature anomalies (mean temperature, mean temperature for area shallower than 200 m, and area of sea floor covered by water above 2°C and below 0°C, respectively) for 2H, 2J, 3K and 3LNO.

6.3.3 Summary of bottom temperatures

When standardized anomalies of spring and fall bottom temperatures (first row of all scorecards in Figure 32 and Figure 35) are combined in a bar plot, the low frequency patterns of the bottom temperature on the NL shelf become apparent (Figure 36). The coldest period encompasses the mid-1980s to the mid-1990s. Such cold anomalies are not observed later in the time series. For example, despite a winter NAO index leading to colder conditions between about 2012 to 2017 (see section on meteorological conditions), the bottom temperature during these years was just back to normal, following the rather warm period of the mid-1990s to the mid-2010s. While 2021 is the warmest year on record for the bottom temperature (+2.5 SD) and 2022 the third warmest (+1.2 SD), 2023 was normal at +0.2 SD.

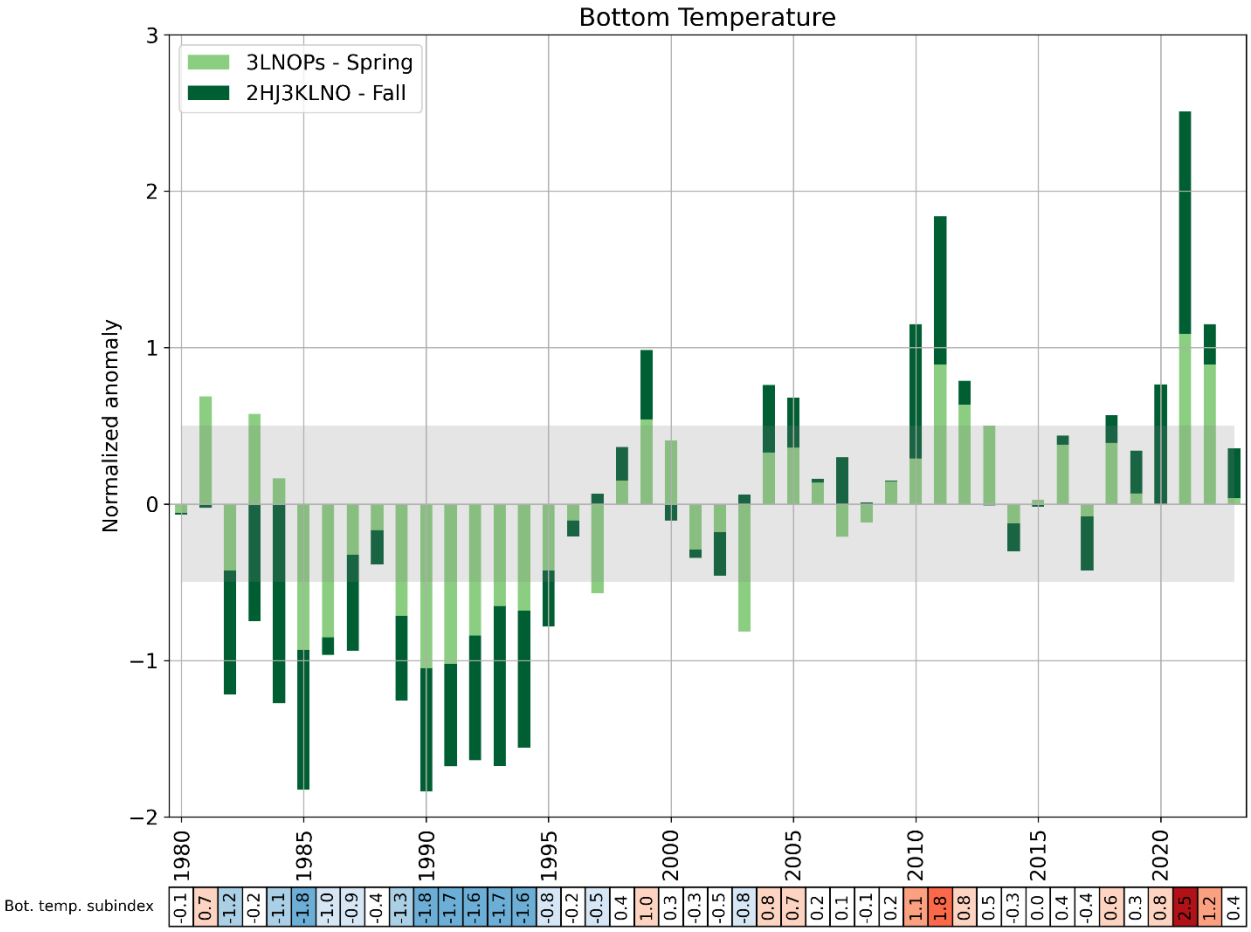

Figure 36: Normalized anomalies of bottom temperature in NAFO Divisions 3LNOPs (spring) and 2HJ3KLNO (fall). This time series corresponds to the average of the two seasons, in which each contribution is represented. The shaded area corresponds to the 1991–2020 average ±0.5 SD, a range considered "normal". The numerical values of this time series are reported in a color-coded scorecard at the bottom of the figure. This time series is one component of the NL climate index (Figure 39).

7 Labrador Current transport

The circulation in the NL region is dominated by the south-eastward flowing Labrador Current system, which floods the eastern shelf areas with cold and relatively fresh subpolar waters (Figure 37). This flow can significantly affect physical and biological environments off Atlantic Canada on seasonal and interannual time scales. On the shelf, the Coastal Labrador Current (Florindo-López et al., 2020) originates near the northern tip of Labrador where the outflow from the Hudson Strait combines with the eastern Baffin Island Current and flows southeastward along the Labrador coast. During its southward journey on the Labrador shelf, it is strongly influenced by the seabed topography, following the various cross shelf saddles and inshore troughs. A separate offshore branch of the Labrador Current flows southeastward along the western boundary of the Labrador Sea. This current is part of the large-scale Northwest Atlantic circulation consisting of the West Greenland Current that flows northward along the West Coast of Greenland, a branch of which turns westward and crosses the northern Labrador Sea forming the northern section of the Northwest Atlantic subpolar gyre.

Further south, near the northern Grand Banks, the Coastal Labrador Current becomes broader and less defined. In this region, most of the inshore flow combines with the offshore branch and flows eastward, with a portion of the combined flow following the bathymetry southward around the southeast Grand Bank, and the remainder continuing east and southward around the Flemish Cap (Figure 37). A smaller inshore component flows through the Avalon Channel and around the Avalon Peninsula, and then westward along the Newfoundland south coast. Off the southern Grand Bank the offshore branch flows westward along the continental slope, some of which flows into the Laurentian Channel and eventually onto the Scotian shelf. This extension of the Labrador Current on the Scotian shelf is referred to as the Scotian shelf break current. Additionally, there are strong interactions between the offshore branch of the Labrador Current and large-scale circulation. A significant portion of the offshore branch combines with the North Atlantic Current and forms the southern section of the subpolar gyre. Further east, the Flemish Cap is located in the confluence zone of subpolar and subtropical western boundary currents of the North Atlantic. Labrador Current water flows to the east along the northern slopes of the Cap and south around the eastern slopes of the Cap. In the eastern Flemish Pass, warmer high salinity North Atlantic Current water flows northward contributing to a topographically induced anticyclonic gyre over the central portion of the Cap.

Satellite altimetry data are used over a large spatial area to calculate the annual-mean anomalies of the Labrador Current transport (Han et al., 2014). A total of nine cross-slope satellite altimetry tracks are used to cover the Labrador Current on the NL shelf break from approximately 47°N to 58°N latitude (Figure 37). Similarly, five tracks from approximately 55°W to 65°W longitude are used for the Scotian shelf=break current. The nominal cross-slope depth ranges used for calculating the transport are from 200 to 3,000 m isobaths over the NL shelf break and from 200 to 2,000 m isobaths over the Scotian shelf break.

An empirical orthogonal function (EOF) analysis of the annual-mean transport anomalies was carried out. An index was developed from the time series of the first EOF mode and normalized by dividing the time series by its SD. The mean transport values are provided based on ocean circulation model output along the NL shelf break (Han et al., 2008) and over the Scotian shelf break (Han et al., 1997). The mean transport of the Labrador Current along the NL shelf break is 13 Sv (1 Sv = 10^6 m^3 s^{-1}) with a SD of 1.4 Sv, and the mean transport of the Scotian shelf break current is 0.6 Sv with a SD of 0.3 Sv. The mean transport values will be updated as new model output becomes available. The SD values will be updated as knowledge on nominal depth improves.

The Labrador Current transport along the NL shelf break was out of phase with that of the Scotian shelf break current for most of the years over 1993–2023 (Figure 38). The transport over the NL shelf break was strong in the early- and mid-1990s, weak in the mid-2000s and early-2010s, and became strong again in late 2010s. In contrast, the transport over the Scotian shelf break fluctuated in a nearly opposite way. The Labrador Current transport index was positively and negatively correlated with the winter NAO index over the NL and Scotian shelves breaks, respectively.

In 2023 the annual-mean transport of the Labrador Current over the Labrador and northeastern Newfoundland Slope was above normal at +1.1 SD. It has been positive for 7 of the last 8 years. The transport on the Scotian Slope in 2023 was above normal for the first time in 10 years at +1.4 SD. The last time the transport in both regions was more than 1 SD above normal was in 1996. A positive transport on the Scotian slope indicates that fresher and colder Labrador Slope water may reach the Scotian shelf and the mouth of the Laurentian Channel.

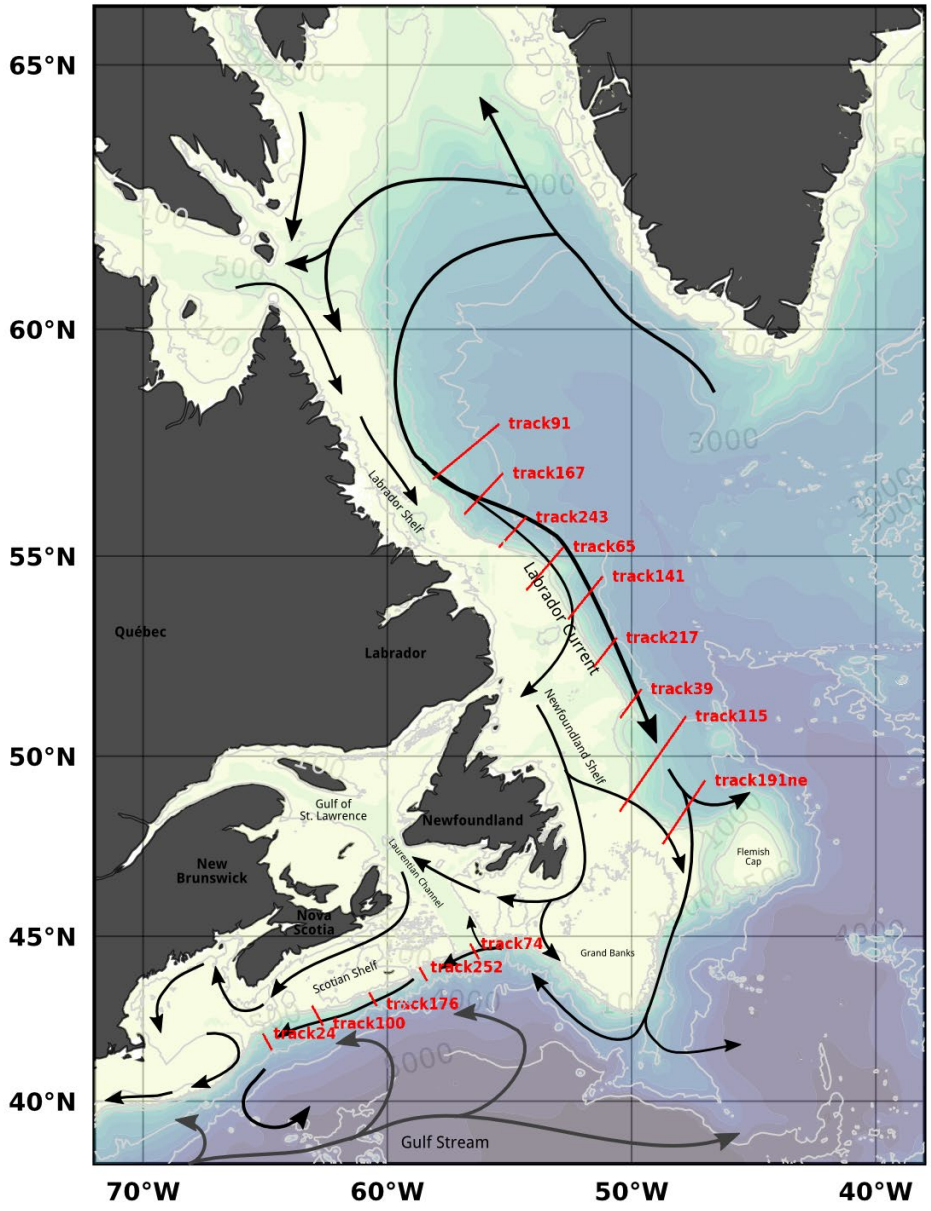

Figure 37: Map showing the Northwest Atlantic bottom topography (depth contour values in light gray) and schematic flow patterns (arrows). The transport is calculated across the cross-slope sections (red lines) identified by their satellite ground tracks numbers. The series of northern tracks are used for the Labrador Current calculation on the NL shelf, while the series of tracks in the south are used for the Scotian shelf break current transport.

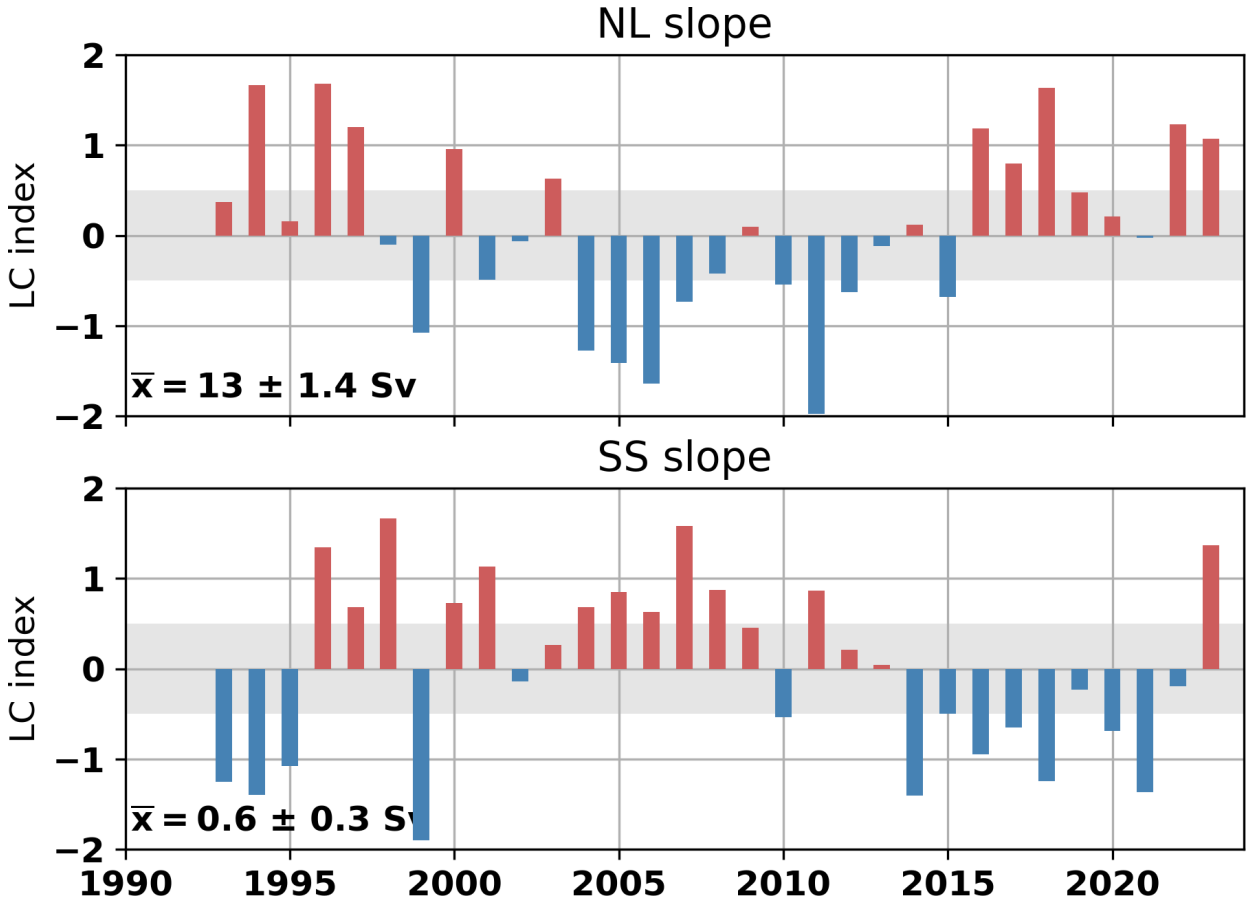

Figure 38: Normalized index of the annual-mean transport of the Labrador Current on the NL shelf break (top) and Scotian shelf break (bottom). Long-term averages over 1993–2023 (with standard deviation) are 13.0±1.4 Sv for the Labrador Current and 0.6±0.3 Sv for the Scotian shelf break current. Shaded gray areas represent the ±0.5 SD range considered "normal".

8 Summary

The NL climate index (NLCI; Cyr & Galbraith, 2021), summarizes selected time series discussed throughout this report (Figure 39). The NLCI runs between 1951 to present and is updated annually. This index is presented here in the form of a scorecard followed by a stacked bar plot of 10 equally weighted time series:

- Winter NAO index (starts in 1951; see Figure 3);
- Air temperatures at five sites (starts in 1950; see Figure 6);
- Sea ice season duration and maximum area for the northern Labrador, southern Labrador and Newfoundland shelves (starts in 1969; see Figure 12)
- Number of icebergs crossing 48°N (starts in 1950; see Figure 13);
- SSTs in NAFO Division 2GHJ3KLNOP (starts in 1982; see Figure 15);
- Vertically averaged temperature at Station 27 (starts in 1951; see Figure 18);
- Vertically averaged salinity at Station 27 (starts in 1951; see Figure 18);
- CIL core temperature at Station 27 (starts in 1951; see Figure 20);
- Summer CIL areas on the hydrographic sections Seal Island, Bonavista Bay and Flemish Cap (starts in 1950; see Figure 29); and
- Spring and fall bottom temperature in NAFO Divisions 3LNOPs and 2HJ3KLNO, respectively (starts in 1980; see Figure 36).

The NLCI can be interpreted as a measure of the overall state of the climate system with positive values representing warm and fresh conditions with less sea ice and conversely negative values representing cold and salty conditions.

The NLCI highlights the different climate regimes prevailing since the early 1950s. For example, the relatively warm 1960s were followed by cold conditions in the early 1970s and most importantly from the mid-1980s to the mid-1990s which was the coldest decade on record. The warming trend from the early 1990s that peaked in 2010 was followed by recent cooling that culminated in 2015. While the NLCI for years 2016 to 2019 were normal (with a certain spread between positive and negative subindices within those years), the NLCI has been positive since 2020, including the warmest year on record in 2021 (+1.4). In 2023, the NLCI was at +0.7. The NLCI and its subindices are available at https://doi.org/10.20383/101.0301 [consulted 2024-05-34] (Cyr & Galbraith, 2020).

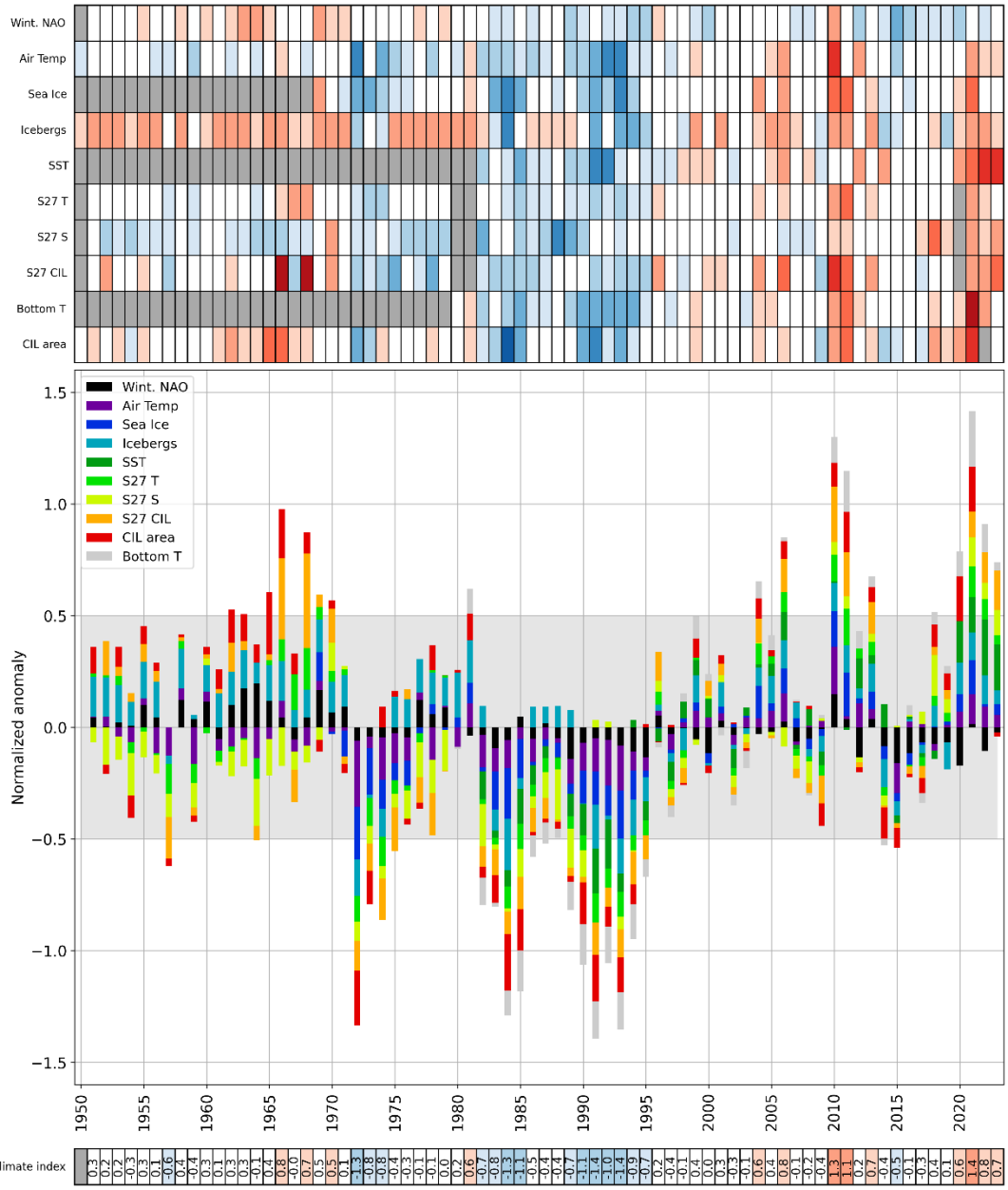

Figure 39: Newfoundland and Labrador climate index derived by averaging the normalized anomalies of various time series presented in this report. The scorecard in the top panel represents the 10 subindices used to construct the climate index, color-coded according to their value (blue negative, red positive, white neutral). The sign of some indices (NAO, ice, icebergs, salinity and CIL area) has been reversed when positive anomalies are generally indicative of colder conditions. Grey cells in the scorecards indicate the absence of data. The central panel represents the climate index in a stacked-bar fashion, in which the total length of the bar is the average of the respective subindices and in which their relative contribution to the average is adjusted proportionally. The scorecard at the bottom of the figure shows the color-coded numerical values of the climate index.

8.1 Highlights of 2023

- Based on the NL climate index, 2023 was overall warm at +0.7 (tied at the 7th warmest rank with 1968 and 2013).
- While the winter NAO, sea ice, Station 27 temperature, bottom temperature and CIL area were normal, all other sub-indices of the NLCI showed warm anomalies.
- Sea surface temperatures were at their second warmest on record (after 2022), and established new monthly and seasonal records across different NAFO divisions. The last three years were the warmest three on record.
- The transport on the Scotian Slope was positive for the first time in a decade.

9 Acknowledgements

This work is a contribution to the scientific program of the Atlantic Zone Monitoring Program. We thank the many scientists and technicians at the Northwest Atlantic Fisheries Centre for collecting and providing much of the data contained in this analysis and the Marine Environment Data Section of Fisheries and Oceans Canada in Ottawa for providing most of the historical data. We also thank the captain and crew of the CCGS Capt. Jacques Cartier, CCGS John Cabot, and RRS Discovery CCGS Cartier and RRS Discovery for oceanographic data collection during the spring, summer and fall of 2023, respectively. We thank Heather Andres and Jared Penney for reviewing the document.

References

Colbourne, E., Holden, J., Craig, J., Senciall, D., Bailey, W., Stead, P., & Fitzpatrick, C. (2015). Physical Oceanographic Conditions on the Newfoundland and Labrador Shelf During 2014. *DFO Can. Sci. Advis. Sec. Res. Doc.*, *2015/053*, v + 37 p.

Colbourne, E., Narayanan, S., & Prinsenberg, S. (1994). Climatic changes and environmental conditions in the Northwest Atlantic, 1970-1993. *ICES Journal of Marine Science Symposia*, *198*, 311–322.

Coyne, J., & Cyr, F. (2024). Canadian Atlantic Bottom Observations of Temperature and Salinity (CABOTS). *Federated Research Data Repository*. https://doi.org/10.20383/103.0969

Coyne, J., Cyr, F., Donnet, S., Galbraith, P. S., Geoffroy, M., Hebert, D., Layton, C., Ratsimandresey, A., Snook, S., Soontiens, N., & Walkusz, W. (2023). Canadian Atlantic Shelf Temperature-Salinity (CASTS). *Federated Research Data Repository*. https://doi.org/10.20383/102.0739

Cyr, F., Colbourne, E., Holden, J., Snook, S., Han, G., Chen, N., Bailey, W., Higdon, J., Lewis, S., Pye, B., & Senciall, D. (2019). Physical Oceanographic Conditions on the Newfoundland and Labrador Shelf during 2017. *DFO Can.Sci. Advis. Sec. Res. Doc.*, *2019/051*, iv + 58 pp. http://waves-vagues.dfo-mpo.gc.ca/Library/362068.pdf

Cyr, F., Coyne, J., Snook, S., Bishop, C., Galbraith, P. S., Chen, N., & Han, G. (2024). Physical Oceanographic Conditions on the Newfoundland and Labrador Shelf during 2022. *Canadian Technical Report of Hydrography and Ocean Sciences*, *377*, iv + 53 p.

Cyr, F., & Galbraith, P. S. (2020). Newfoundland and Labrador climate index. In *Federated Research Data Repository*. https://doi.org/10.20383/101.0301

Cyr, F., & Galbraith, P. S. (2021). A climate index for the Newfoundland and Labrador shelf. *Earth System Science Data*, *13*(5), 1807–1828. https://doi.org/10.5194/essd-13-1807-2021

Cyr, F., & Galbraith, P. S. (2023). Newfoundland-Labrador Shelf. Ch. 4.3. In C. González-Pola, K. M. H. Larsen, P. Fratantoni, & A. Beszczynska-Möller (Eds.), *ICES Report on Ocean Climate 2021* (p. 123 p.). ICES Cooperative Research Reports No. 358. https://doi.org/10.17895/ices.pub.24755574

Cyr, F., Snook, S., Bishop, C., Galbraith, P. S., Chen, N., & Han, G. (2022). Physical Oceanographic Conditions on the Newfoundland and Labrador Shelf during 2021. *DFO Can. Sci. Advis. Sec. Res. Doc*, *2022/040*, iv + 48 p. http://www.dfo-mpo.gc.ca/csas-sccs/Publications/ResDocs-DocRech/2016/2016_079-eng.html

Dickson, R. R., Meincke, J., Malmberg, S. A., & Lee, A. J. (1988). The “great salinity anomaly” in the northern North Atlantic 1968–1982. *Progress in Oceanography1*, *20*(2), 103–151.

Doubleday, W. G. (1981). Manual on groundfish surveys in the Northwest Atlantic. In *NAFC*

Sco. Coun. Studies 2 (p. 56 p.).

Drinkwater, K. F., Myers, R. A., Pettipas, R. G., & Wright, T. L. (1994). Climatic data for the Northwest Atlantic: the position of the shelf/slope front and the northern boundary of the Gulf Stream between. 50°W and 75°W, 1973-1992. *Canadian Data Report of Fisheries and Ocean Sciences*, *125*, iv +103 p.

Florindo-López, C., Bacon, S., Aksenov, Y., Chafik, L., Colbourne, E., & Penny Holliday, N. (2020). Arctic ocean and hudson bay freshwater exports: New estimates from seven decades of hydrographic surveys on the Labrador shelf. *Journal of Climate*, *33*(20), 8849–8868. https://doi.org/10.1175/JCLI-D-19-0083.1

Galbraith, P. S., Chassé, J., Shaw, J.-L., Dumas, J., & Bourassa, M.-N. (2024). Physical Oceanographic Conditions in the Gulf of St. Lawrence during 2023. *Canadian Technical Report of Hydrography and Ocean Sciences*, *378*, v + 91 p.

Galbraith, P. S., Chassé, J., Shaw, J., Dumas, J., Lefaivre, D., & Bourassa, M. (2023). Physical Oceanographic Conditions in the Gulf of St . Lawrence during 2022. *Canadian Technical Report of Hydrography and Ocean Sciences*, *354*, v+88p.

Galbraith, P. S., Larouche, P., Caverhill, C., Galbraith, P. S., Larouche, P., & Sea-surface, C. C. A. (2021). A Sea-Surface Temperature Homogenization Blend for the Northwest Atlantic A Sea-Surface Temperature Homogenization Blend for the. *Canadian Journal of Remote Sensing*, *47*(4), 554–568. https://doi.org/10.1080/07038992.2021.1924645

GEBCO Compilation Group. (2023). *GEBCO 2023 Grid*. https://doi.org/10.5285/f98b053b-0cbc-6c23-e053-6c86abc0af7b

Han, G., Chen, N., & Ma, Z. (2014). Is there a north-south phase shift in the surface Labrador Current transport on the interannual-to-decadal scale? *Journal of Geophysical Research: Oceans*, *119*(1), 276–287. https://doi.org/10.1002/2013JC009102

Han, G., Hannah, C. G., Loder, J. W., & Smith, P. C. (1997). Seasonal variation of the three-dimensional mean circulation over the Scotian Shelf. *Journal of Geophysical Research: Oceans*, *102*(1), 1011–1025. https://doi.org/10.1029/96jc03285

Han, G., Lu, Z., Wang, Z., Helbig, J., Chen, N., & de Young, B. (2008). Seasonal variability of the Labrador Current and shelf circulation off Newfoundland. *Journal of Geophysical Research*, *113*(C10), C10013. https://doi.org/10.1029/2007JC004376

Hebert, D., Layton, C., Brickman, D., & Galbraith, P. S. (2024). Physical Oceanographic Conditions on the Scotian Shelf and in the Gulf of Maine during 2023. *Canadian Technical Report of Hydrography and Ocean Sciences*, *IN PRESS*, vi + 71 p.

ICNAF. (1978). List of ICNAF Standard Oceanographic Sections and Stations. *ICNAF Selected Papers Number 3*, 109–117. https://doi.org/10.1111/j.1949-8594.1914.tb16026.x

International Ice Patrol. (2020). *International Ice Patrol Annual Count of Icebergs South of 48 Degrees North, 1900 to Present, Version 1*. https://doi.org/10.7265/z6e8-3027

Kerr, R. A. (2000). A North Atlantic Climate Pacemaker for the Centuries. *Science*, *288*(5473), 1984–1985.

Lu, G. Y., & Wong, D. W. (2008). An adaptive inverse-distance weighting spatial interpolation technique. *Computers and Geosciences*, *34*(9), 1044–1055. https://doi.org/10.1016/j.cageo.2007.07.010

McDougall, T. J., & Barker, P. M. (2011). *Getting started with TEOS-10 and the Gibbs Seawater (GSW) Oceanographic Toolbox* (Issue May). SCOR/IAPSO WG127.

Petrie, B., Akenhead, S. A., Lazier, S. A., & Loder, J. (1988). The cold intermediate layer on the Labrador and Northeast Newfoundland Shelves, 1978–86. *NAFO Science Council Studies*, *12*, 57–69.

Petrie, B., Pettipas, R. G., & Petrie, W. M. (2007). An Overview of Meteorological, Sea Ice and Sea-Surface Temperature Conditions off Eastern Canada during 2006. *Canadian Science Advisory Secretariat*, *2007/022*, iv + 38pp.

Therriault, J. C., Petrie, B., Pepin, P., Gagnon, J., Gregory, D., Helbig, J., Herman, A., Lefaivre, D., Mitchell, M., Pelchat, B., Runge, J., & Sameoto, D. (1998). Proposal for a northwest zonal monitoring program. *Canadian Technical Report of Hydrographic and Ocean Sciences*, *194*, vii + 57 p.

Thyng, K. M., Greene, C. A., Hetland, R. D., Zimmerle, H. M., & DiMarco, S. F. (2016). True colors of oceanography: Guidelines for effective and accurate colormap selection. *Oceanography*, *29*(3), 9–13. https://doi.org/10.5670/oceanog.2016.66

Vincent, L. A., Wang, X. L., Milewska, E. J., Wan, H., Yang, F., & Swail, V. (2012). A second generation of homogenized Canadian monthly surface air temperature for climate trend analysis. *Journal of Geophysical Research*, *117*(D18110). https://doi.org/10.1029/2012JD017859